Naval Research Laboratory

Washington, DC 20375-5320

NRL/MR/7220--07-9086

Study of the Implications of Whitecap Intermittency on the Uniform Sea-salt Aerosol Source Approximation and Deposition Velocity

WILLIAM A. HOPPEL

Computational Physics, Inc.
Springfield, Virginia

PETER F. CAFFREY

Remote Sensing Physics Branch
Remote Sensing Division

October 29, 2007

REPORT DOCUMENTATION PAGE

Form Approved
OMB No. 0704-0188

1. REPORT DATE *(DD-MM-YYYY)*	**2. REPORT TYPE**	**3. DATES COVERED** *(From - To)*
29-10-2007	Memorandum Report	April 2006 – August 2007

4. TITLE AND SUBTITLE

Study of the Implications of Whitecap Intermittency on the Uniform Sea-salt Aerosol Source Approximation and Deposition Velocity

5a. CONTRACT NUMBER

5b. GRANT NUMBER

5c. PROGRAM ELEMENT NUMBER

6. AUTHOR(S)

William A. Hoppel* and Peter F. Caffrey

5d. PROJECT NUMBER

5e. TASK NUMBER

5f. WORK UNIT NUMBER

7. PERFORMING ORGANIZATION NAME(S) AND ADDRESS(ES)

Naval Research Laboratory
4555 Overlook Avenue, SW
Washington, DC 20375-5320

8. PERFORMING ORGANIZATION REPORT NUMBER

NRL/MR/7220--07-9086

9. SPONSORING / MONITORING AGENCY NAME(S) AND ADDRESS(ES)

10. SPONSOR / MONITOR'S ACRONYM(S)

11. SPONSOR / MONITOR'S REPORT NUMBER(S)

12. DISTRIBUTION / AVAILABILITY STATEMENT

Approved for public release; distribution is unlimited.

13. SUPPLEMENTARY NOTES

*Computational Physics, Inc., Suite 210, 8001 Braddock Road, Springfield, VA 22151

14. ABSTRACT

The source function and deposition velocity of sea-salt particles used in large-scale models assumes that the source and deposition is uniform over areas large compared to the horizontal grid spacing of the model, whereas sea-salt aerosol is overwhelmingly generated by white caps whose surface distribution is usually sparse and sporadic. The analysis presented here uses several puff plume models to study the validity of the underlying assumptions of the horizontally uniform surface source and deposition, and a time series of puff plumes is averaged to obtain the large-scale source and deposition flux. The analysis demonstrates the remarkable difference between (i) the case where deposition results exclusively from non-gravitational deposition processes at the surface (i.e., small particles) and (ii) the case where deposition is solely from gravitational settling (i.e., large particles). For Case (i), the magnitude of the gradient (eddy correlation) flux, initially equal to the source flux, will evolve to an equilibrium state where there is no gradient flux. This can be contrasted to Case (ii) where the upward gradient flux is always equal to the source flux (at a given height) and the transient behavior is governed by the increase of the gravitational flux during the transition to equilibrium (upward gradient (source) flux equals the downward deposition flux). The intermediate case where both the gravitational and deposition fluxes are important is a mixture of the above two cases.

15. SUBJECT TERMS

16. SECURITY CLASSIFICATION OF:			**17. LIMITATION OF ABSTRACT**	**18. NUMBER OF PAGES**	**19a. NAME OF RESPONSIBLE PERSON**
					Peter F. Caffrey
a. REPORT	**b. ABSTRACT**	**c. THIS PAGE**	UL	88	**19b. TELEPHONE NUMBER** *(include area code)*
Unclassified	Unclassified	Unclassified			(202) 767-8474

Standard Form 298 (Rev. 8-98)
Prescribed by ANSI Std. Z39.18

Table of Contents

Executive Summary

The sea-salt aerosol source function (SSASF) and deposition velocity of sea-salt particles used in large-scale models assumes that the source and deposition is uniform over areas large compared to the horizontal grid spacing of the model. This horizontal grid spacing is typically one to 100 km in length. Sea-salt aerosol is overwhelmingly generated by white caps whose surface distribution is usually sparse and sporadic with spots of intense particle generation separated by large areas with no white cap coverage. Most deposition occurs in the regions free of white caps. The analysis presented here uses (several) puff plume models to study the validity of the underlying assumptions of the horizontally uniform surface source and deposition. The puff plume solutions are based on the same turbulent diffusion equation as used in the large-scale models but have high resolution (in all cases an analytical solution). A time series of puff plumes is averaged to obtain the large-scale source and deposition flux. *The process of going from the flux of particles generated by the individual small-scale events to a meaningful large-scale average is the subject of this study.* A similar problem is encountered in bridging the gap between the transient deposition flux from a whitecap plume and a meaningful large-scale deposition velocity appropriate for larger scale models. *One of the advantages of considering a series of puffs is that the transient behavior of the system as it evolves can be studied*. Prior studies have relied on solutions to the steady-state differential equation.

The analysis demonstrates the remarkable difference between (i) the case where deposition results exclusively from non-gravitational deposition processes at the surface (such as impaction and Brownian diffusion) and (ii) the case where deposition is solely from gravitational settling. For the case (i) when deposition is from non-gravitational processes, the effect of deposition is carried to the interior of the MBL by the gradient (eddy-correlation) flux. Assuming a MBL is initially free of aerosol with transition to a terminal equilibrium where deposition is balanced by the source, the magnitude of the gradient flux, which initially will be equal to the source flux, will evolve to an equilibrium state where there is no gradient flux. This can be contrasted to the case (ii) where gravitational settling is dominant (larger particles). Here the upward gradient flux is always equal to the source flux (at a given height) and the transient behavior is governed by the increase of the gravitational flux during the transition to equilibrium - where the upward gradient (source) flux is equal to the downward deposition flux. The intermediate case where both the gravitational flux and deposition flux are important is a mixture of the above two cases.

In Sections IV and V1, the process of going from the results of a series of puffs to a large scale average source (SSASF) is discussed in detail together with the implication of the process to both (i) the inclusion of a source and deposition velocity in large scale numerical models and (ii) the various measurement techniques from which the SSASF are derived. The relationship between the puff plume analysis and empirical methods used to determine the SSASF is discussed in Section IV.

Finally an analysis, which assumes large-scale homogeneous conditions but also treats the transient conditions under the valid assumption that a quasi steady state exists during the transition, is presented.

Study of the implications of whitecap intermittency on the uniform sea-salt aerosol source approximation and deposition velocity

I. Introduction

The primary mechanism for sea-salt aerosol generation is through bubble bursting at the ocean surface. Air entrained through wave action form bubbles that rise to the surface and burst. As the bubble penetrates the ocean surface a liquid film is produced, which breaks forming a number of liquid droplets that partially evaporate to form sea-salt solution or salt crystal aerosol depending on the relative humidity. As the bubble collapses a water jet emanates from its center. As this jet breaks up, larger droplets are formed and evaporate to produce additional coarse-size aerosol. The number of film and jet droplets formed per breaking bubble is a function of the bubble size (see for example, *Wu* [1992]). As the wind speed and sea-state increase, the wind tears sheets of water off the breaking waves. The breakup of these sheets form (spume) aerosol of diverse sizes including very large particles. These various formation mechanisms have been studied for decades and the interested reader is referred to *Andreas* [2002] and the recent review by *Lewis and Schwartz* [2004] and references therein for additional background.

The entrainment of air by breaking wave action and subsequent bubble bursting is associated primarily with the occurrence of white caps, so it is natural to associate the amount of marine aerosol generation with the frequency of breaking waves or the factional white cap coverage. Current expressions for the flux of sea-salt aerosol from the ocean surface is given as a function of the fractional white cap coverage, which in turn is expressed as a function of wind speed. Figure 1 shows the percentage of the sea surface covered by white caps as a function of wind speed for four different expressions (*Monahan* [1986], *Wu* [1992] for warm and cold water and *Hanson and Phillips* [1999]). It is seen, that while there is wide scatter in the data, less than 0.1% of the sea-surface is covered with white caps at wind speeds of 5 m s^{-1}, less than 1% at 10 m s^{-1} and about 10 % at wind speeds at 20 m s^{-1}. The distribution of the coverage is sporadic with spots of intense particle formation and large areas where there are no whitecaps. A parcel of air passing over a white cap will experience a pulse of particles at the surface with upward flux of particles as turbulence disperses the particles upward. Down wind of the puff, particles will be deposited back to the surface. The parcel will then encounter additional puffs at a frequency depending on the fractional white cap coverage. If we consider the puff to be from a 1 m^2 area of the surface, and the fractional coverage is 1% (value appropriate for a 10 m s^{-1} wind speed), then a column of air with 1 m^2 base will see, on average, one puff every 10 seconds, or one puff every 100 m).

In aerosol models whose purpose is to simulate (average) concentrations of aerosol with resolution on the scale of a km or greater, the average effect of many whitecaps is formulated in terms of a uniform surface generation function, and the loss to the surface in terms of some uniform deposition velocity. The goal of these models is to predict the average aerosol concentration in the MBL at a given point in time so that aerosol effect on other atmospheric processes, such as EM propagation or cloud microphysics, can be predicted. However there are other applications, such as moisture and heat transfer and some chemical reaction studies, where

Manuscript approved September 5, 2007.

the average concentration is less important than the total aerosol mass processed through the MBL.

To illustrate some of the potential problems with the uniform-source assumption consider the white caps to be puff plumes and consider two cases: (1) there is negligible loss resulting from surface deposition during the life time of the particle, and (2) there is significant surface deposition of particles between whitecap encounters. The first case is applicable to submicron particles, the second to super-micron particles. In the first case particles are conserved, each puff adds linearly to the concentration in the MBL, and a quasi steady state flux is established while the MBL concentration slowly builds up with loss occurring occasionally by precipitation scavenging events or dilution due to exchange with the FT. In this case, the net flux into the MBL is just the sum of the flux from all the puffs regardless of how infrequent the whitecaps. For large particles (i.e., Case (2)), the situation is much different. A single puff produces an initial upward flux that quickly reverses and all particles eventually get re-deposited at the surface. An instrument measuring net flux would indicate that the average flux is zero while a measurement of concentration would indicate some average concentration during the lifetime of the puff, even if no particles remain suspended at the end of the time. We then have a case where the average flux is zero but the average concentration is not zero. This latter case is an extreme example, as additional puffs would usually be encountered before all particles from a prior puff are removed. Nevertheless it illustrates an important concept – when there is significant surface deposition between whitecaps, the deposition diminishes the average effective source flux, i.e., the source flux below that calculated from the source strength without intervening deposition. This consideration has important consequences on calculating oceanic source function from laboratory data on breaking waves for super micron size particles.

In the following analysis various versions of the "puff" plume model will be used to study the validity of the underlying assumptions of the horizontally uniform, surface source formulation. The analytical solutions given below for the dispersion of puff plumes are solutions to the same differential equation used in numerical finite difference schemes in larger scale meteorological and boundary layer models. However, the grid and time scales used in the meteorological models are too coarse to capture individual plumes. In fact, the whitecap density within a single grid of the meteorological models will be sparse and the average number within a given grid may be large or small depending on the white cap coverage at the time. *The process of going from the flux of particles generated by the individual small-scale events to a meaningful large-scale average is the subject of this study.* A similar problem addressed here is that encountered in bridging the gap between the transient deposition flux from a whitecap plume to a meaningful large-scale deposition velocity appropriate for larger scale models.

We will begin the analysis (Section II) with the simple case of the Gaussian plume model with a delta function source at time zero (t=0) and zero concentration far from the source, considering both the case of a perfectly reflecting surface and the case of totally absorbing surface. We then extend these simple cases to consider the case of the partially absorbing surface, where the deposition velocity at the surface can be specified. In these cases it is assumed that the gravitational settling velocity is negligible and that deposition results from Brownian diffusion and impaction to the ocean surface – these results therefore apply only to submicron size particles. Section III then further extends the analysis to look at the case where

the gravitational settling velocity is included in the differential equation and dominates the aerosol surface deposition.

The questions to be addressed are as follows:

1. Is there a valid way to average the transient flux of particles from individual white caps which will supply a meaningful uniform surface source function appropriate for large scale modeling?
2. And if so, how is this average to be calculated? We have already pointed out that for large particles, the average net flux can be zero during the transient life of a puff while the average concentration over the same period is a positive definite number.
3. What is the relationship of various measurement methods of white cap particle flux to the average source function appropriate for meteorological scale models; i.e.; how do wave tank measurements, eddy correlation flux measurements, and equilibrium measurement methods relate to a source function required in larger-scale models.
4. How does the transient deposition velocity for a plume translate to a deposition velocity appropriate for numerical models.

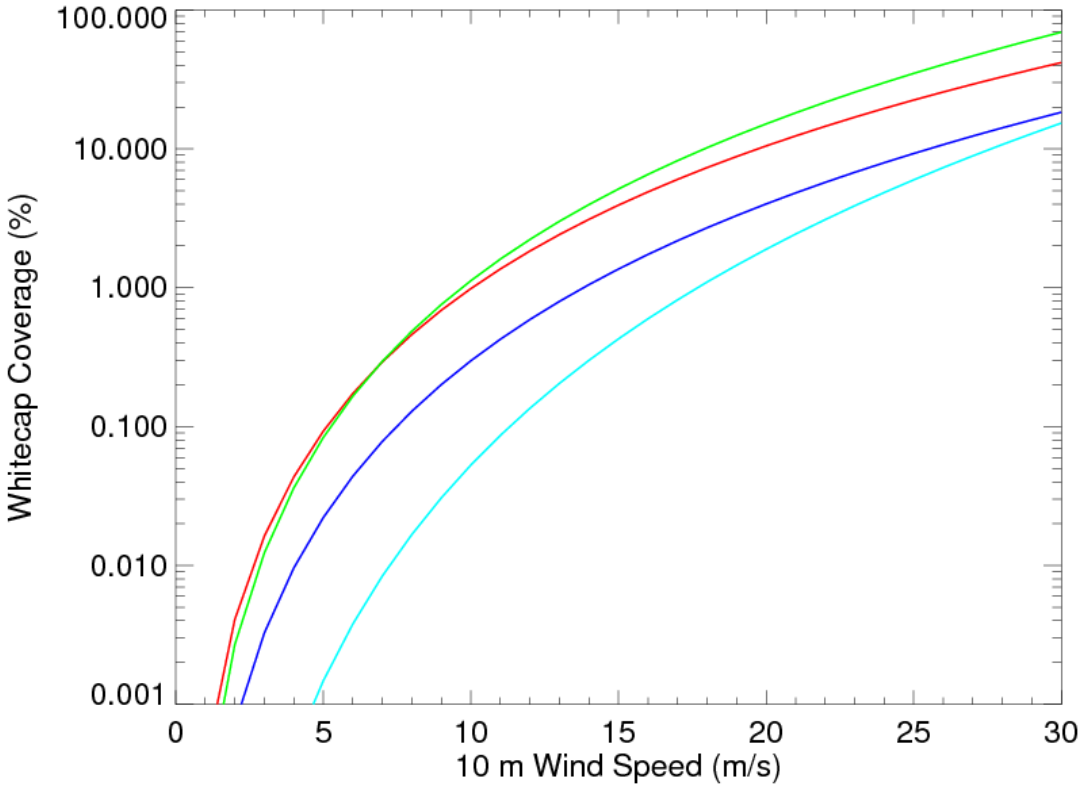

Figure 1. Percentage of whitecap coverage as a function of 10 m wind speed as given by several investigators: Monahan et al (1986) in red, Wu (1992) in green (warm) and blue (cold), and Hanson and Philips (1999) in cyan.

II. Puff plumes with *no* gravitational settling (Cases 1 to 4)

Case 1. Gaussian Plume with totally reflecting or totally absorbing surface: eddy diffusivity K=constant with height, no gravitational settling

The simplest case is that of a Gaussian plume with totally reflecting or absorbing surface and a constant turbulent diffusion coefficient with height. While these are unrealistic circumstances, it demonstrates the important physical principles involved in two extreme cases - one where there is no surface deposition (approximating the behavior of small particles; i.e. no negligible surface deposition over time periods comparable to the lifetime of the particle), and anther with a totally absorbing surface combined with a turbulent diffusion coefficient constant with height. This latter case, due to the constant eddy diffusivity extended all the way down to the surface, results in deposition at the surface comparable to very large particles (tens of μm), but is unrealistic in that the settling velocity term has not been included in the differential equation and therefore doesn't account for settling effects above the surface layer.

We can begin with the assumption that the number concentration *n(x,y,z,t)* of particles of a given size is given by the turbulent diffusion equation

$$\frac{\partial n}{\partial t} + u\frac{\partial n}{\partial x'} = K_x \frac{\partial^2 n}{\partial x'^2} + K_y \frac{\partial^2 n}{\partial y^2} + K_z \frac{\partial^2 n}{\partial z^2} \quad , \tag{1}$$

where x' is the coordinate along the direction of the wind velocity u (assumed to be constant with height), z is the vertical coordinate, and y the horizontal coordinate perpendicular to the wind velocity u. K_x, K_y, K_z are the eddy diffusion coefficients associated with the three directions. If we let x=x'-ut, then eq. (1) can be written as

$$\frac{\partial n}{\partial t} = K_x \frac{\partial^2 n}{\partial x^2} + K_y \frac{\partial^2 n}{\partial y^2} + K_z \frac{\partial^2 n}{\partial z^2} \tag{2}$$

and the solution interpreted as the concentration in a Lagrangian column moving with the mean wind speed u. The solution for an instantaneous source (puff) at *x=y=0*, and *z=h*, and zero concentration at $x = y = \pm\infty$ *and* $z = \infty$ at all time is well known (for example, see *Fuchs* [1964] or *Seinfeld* [1986]) and given by

$$n(x,y,z,t) = \frac{1}{4p\sqrt{K_x K_y}\,t} Exp\left\{\frac{-x^2}{4K_x t} - \frac{y^2}{4K_y t}\right\}\left[\frac{1}{\sqrt{4pK_z t}}\left\{Exp\left(\frac{-(z-h)^2}{4K_z t}\right) \pm Exp\left(\frac{-(z+h)^2}{4K_z t}\right)\right\}\right] \tag{3}$$

This solution is for a unit source. The plus sign is for totally reflective surface (z=0) and the minus sign for totally absorbing surface. It is convenient to eliminate the x and y dependence by integrating over the x and y coordinates, in which case the total number *N(z,t)* in a layer dz (i.e., particles per unit length) is obtained

$$N(z,t) = \frac{1}{\sqrt{4pK_z t}}\left\{ Exp\left(\frac{-(z-h)^2}{4K_z t} \right) \pm Exp\left(\frac{-(z+h)^2}{4K_z t} \right) \right\} \qquad (4)$$

(*N(z,t)* has units of inverse length).

The total flux (integrated over the x-y plane) at z resulting from a single puff at h is just

$$F_z(z,t) = -K_z \frac{\partial N}{\partial z} = \frac{2K_z}{(4K_z t)^{\frac{3}{2}} p^{\frac{1}{2}}}\left\{ (z-h) Exp\left(\frac{-(z-h)^2}{4K_z t} \right) \pm (z+h) Exp\left(\frac{-(z+h)^2}{4K_z t} \right) \right\} \qquad (5)$$

The integrated flux flowing through the z-plane at z, between time zero and time t is just

$$FI(z,t) = \int_0^t F_z dt = \frac{1}{2\sqrt{p}}\left[\Gamma\left(1/2, \frac{(z-h)^2}{4K_z t} \right) \pm \Gamma\left(1/2, \frac{(z+h)^2}{4K_z t} \right) \right] \qquad \text{for } z > h \qquad (6)$$

where *G(a,x)* is the incomplete gamma function. *FI(z,t)* can be viewed as the integrated number of particles passing through a surface at height z, over a time interval t, resulting from a single puff at time *t=0*. *FI(z,t)* is thus the number of particles above the *z*-plane at time *t*.

The integrated flux through any surface z over all time is just

$$FI(z,\infty) = \int_0^\infty F_z dt = \frac{1 \pm 1}{2} = 1,0 \qquad \text{for } z > h \qquad (7)$$

For a reflective surface the integrated flux from a unit source through any surface is just unity – given enough time everything flows out the "top" of the domain. For a totally absorbing surface the integrated flux is zero at $t = \infty$; that which flows upward initially must eventually flow back down and be removed at the surface.

The total normalized concentration given by Eq. (4) and the flux given by Eq. (5) are shown in Figures 2 and 4 for reflecting surface. For a reflecting surface the concentration at the surface is finite, but the flux is zero at the surface as shown in Figure 4. For a totally absorbing surface the opposite is true, the concentration at the surface is zero as shown in Figure 3 and the flux at the surface has some value (Figure 5). The flux at the surface for a source at height h requires that the flux at the surface is always downward. But at any point above the source where will be an initial upward flux followed by a downward flux at some point after passage of the initial puff. In the Figures, the value of K_z is taken to be 1 m s^{-1} and the source height is 0.2 m (h=0.2 m).

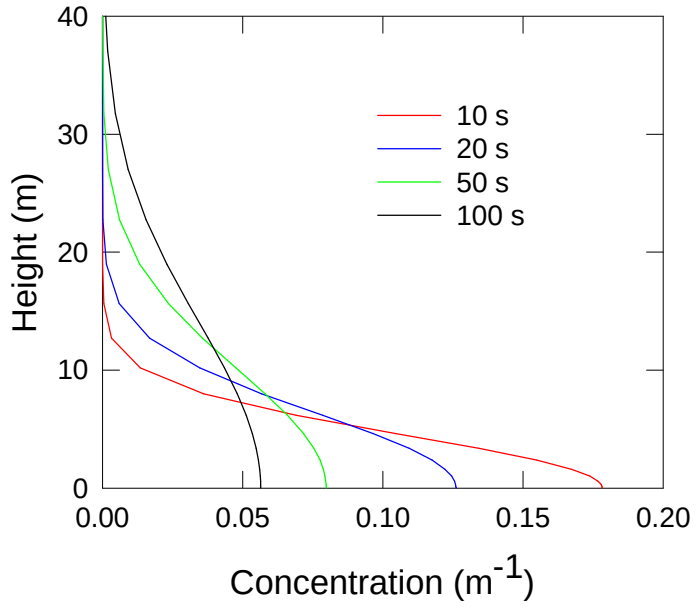

Figure 2. Normalized concentration, *N(z,t),* as function of height for a reflecting surface for times of 10, 20, 50 and 100 s. No particles are lost at the surface during upward dispersion. The gradient is zero at the surface and K_z= 1 m^2 s^{-1}.

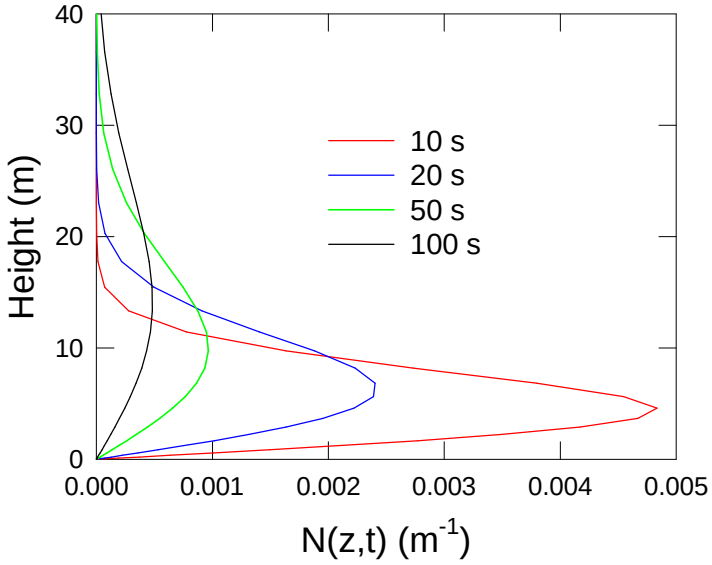

Figure 3. Normalized concentration, *N(z,t),* vs. height for a totally absorbing surface. Particle concentration at the surface is zero and particles are removed at the surface at a rate given by the product of the gradient at the surface and the eddy diffusion coefficient. Times of the profiles shown are 10, 20, 50, and 100 seconds.

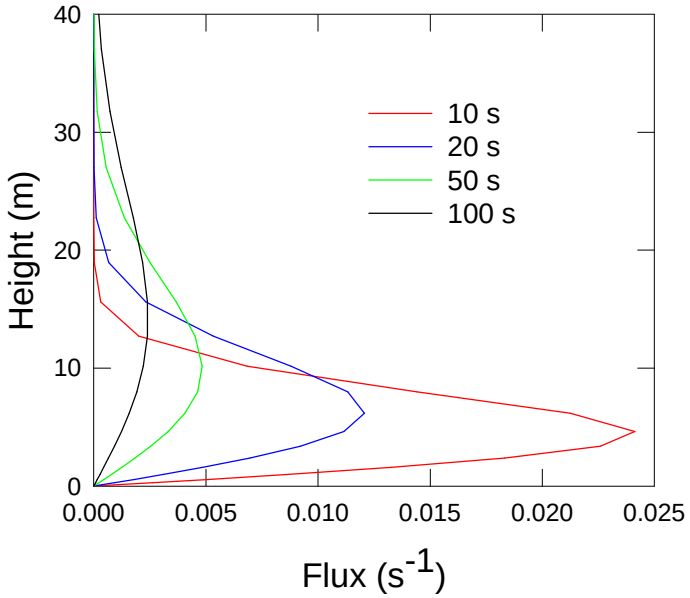

Figure 4. Flux of particles, *F(z,t)*, through a plane at height z at 10, 20, 50, and 100 s for a reflecting surface (case shown in Figure 2). The flux is everywhere positive indicating upward flux at all heights.

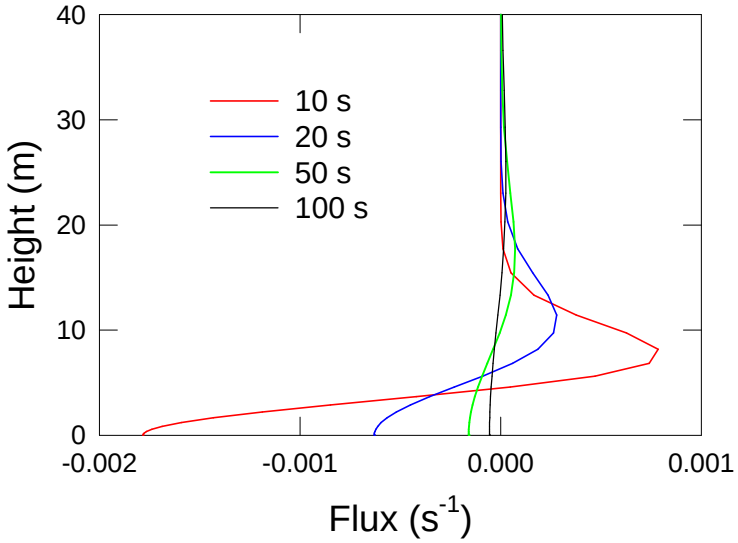

Figure 5. Flux of particles, *F(z,t)*, through a plane at height z and for times 10, 20, 50, and 100 s for an absorbing surface (case shown in Figure 3). Negative values of flux indicate downward flow. There is a downward flux near the surface at all times as particles diffuse back to the surface. There is an initial strong upward flux – the upward flux diminishes with time and eventually the particles which have been dispersed upward return to the surface as indicated by the downward flux at all heights at 50 seconds. The critical height where the flux changes sign is $z_c \approx \sqrt{2K_z t}$ (assumes $z_c > h$).

For the absorbing case we can calculate a deposition velocity as a function of time. The conventional definition of the deposition velocity is the ratio of the downward flux at the surface to the concentration at some reference height.

$$v_d(z_{ref},t)=\frac{-F(0,t)}{N(z_{ref},t)} \tag{8}$$

If the reference height is at the surface, then v_d is infinite because *N(0,t)=0* for a totally absorbing surface. The deposition velocity for a reference height of 10 m calculated from the above equations is shown in Figure 6. At long times the deposition velocity is approximately K_z/Z_{ref} (=0.1 m s^{-1}). This asymptotic behavior for constant K_z is discussed in *Hoppel et al.* [2005] and occurs when the reference height is well within the diffusion layer as depicted in Figure 3. The height of 10 m is not in the diffusion boundary layer (region of constant slope) until well after 100 seconds.

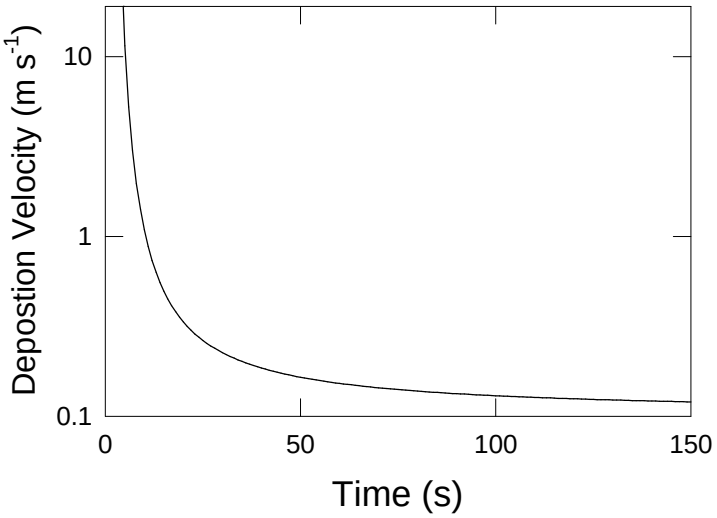

Figure 6. Deposition velocity for a single puff as a function of time for a reference height of 10 m (absorbing surface).

The integrated flux from formation (t=0) to time t as given by Equation (6) for a single puff is shown in Figure 7 for a height of 3 m for both the case of reflecting and the totally absorbing surface.

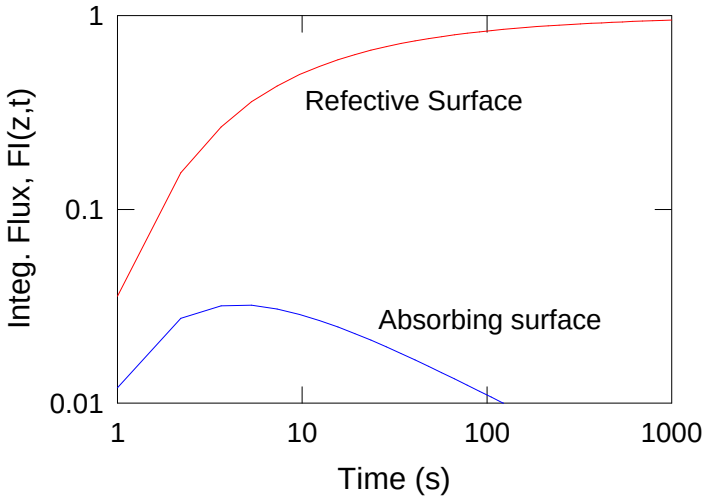

Figure 7. The integrated flux, *FI(z,t)*, for the reflecting case is shown in red and the absorbing case in blue. The height for the curves shown is 3 m. For the reflecting surface no particles are lost and the integrated flux goes to unity indicating that essentially all particles produced by the puff are above 3 m. For the absorbing surface some particles are initially dispersed above 3 meters, but after about 5 seconds, the flux has reversed at 3 meters.

The behavior shown in Figure 7 for the integrated flux in the two extreme cases is important to understanding the subsequent results. For a reflecting surface all the particles from a puff stay airborne and the flux from each puff is additive, whereas for the absorbing surface the integrated flux from a single puff reverses after some time, so that the time between puffs becomes very important in determining the cumulative number of particles which are airborne at any given time. As discussed later, this behavior is related to whether or not a steady state exists for a continuous series of puffs (i.e. continuous source).

1.a. Series of puffs for a Reflecting surface

Whitecaps occur randomly on the sea surface, and to simulate the effect of a series of Gaussian plumes resulting from whitecaps, a series of equally spaced whitecaps entering the bottom of an advecting Lagrangian column is considered next. Equation (5) can be summed to give the instantaneous flux for a number of puffs separated by some time interval Δt. Figure 8 shows the instantaneous flux at a height of 3 m from a series of 10 puffs separated by 10 s and introduced at 0.2 meters. The individual puffs dominate the signal, the flux is always positive, and the average flux, after some time, appears to be almost constant. This average flux disperses particles upward, causing a slow build-up of particles in the atmosphere.

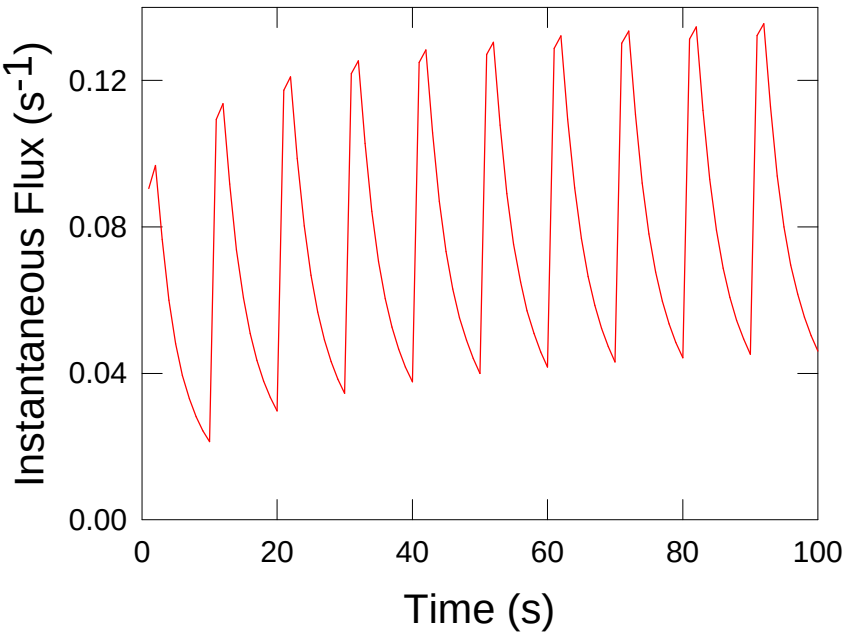

Figure 8. Instantaneous flux, *FS(z,t)*, as function of time at 3 meter for 10 puffs separated by 10 seconds for a reflecting surface. $K(z)=1\ m^{-1}\ s^{-1}$.

The integrated flux from a number of puffs can be obtained by summing Equation (6) over a number of puffs entering the column at different times denoted by t_m.

$$FIS(z,t_M)=\left(\frac{1}{2\sqrt{p}}\right)\sum_{m=1}^{M}\left[\Gamma\left(1/2,\frac{(z-h)^2}{4K_z t_m}\right)\pm\Gamma\left(1/2,\frac{(z+h)^2}{4K_z t_m}\right)\right] \qquad \text{for } z>h \qquad (9)$$

$FIS(z,t_M)$ is the integrated flux resulting from M puffs of unit strength introduced at times t_m. The plus sign is for reflecting surface and the minus sign for a totally absorbing surface. Figure 9 shows the integrated flux for 50 puffs introduced at equal time intervals of 10 (red), 20, 50, and 100 (black) seconds for a reflecting surface at a height of 3 meters. For the reflective surface all flux is upward at all heights and is the same for the same number of puffs (or nearly the same – the small increase for longer puff intervals seen in Figure 9 is due to the fact that the upward current from a single puff continues at a greatly diminished rate with increasing time.) The solid red line at time 100 seconds corresponds to the integration of the instantaneous flux shown in Figure 8 over the first 10 puffs.

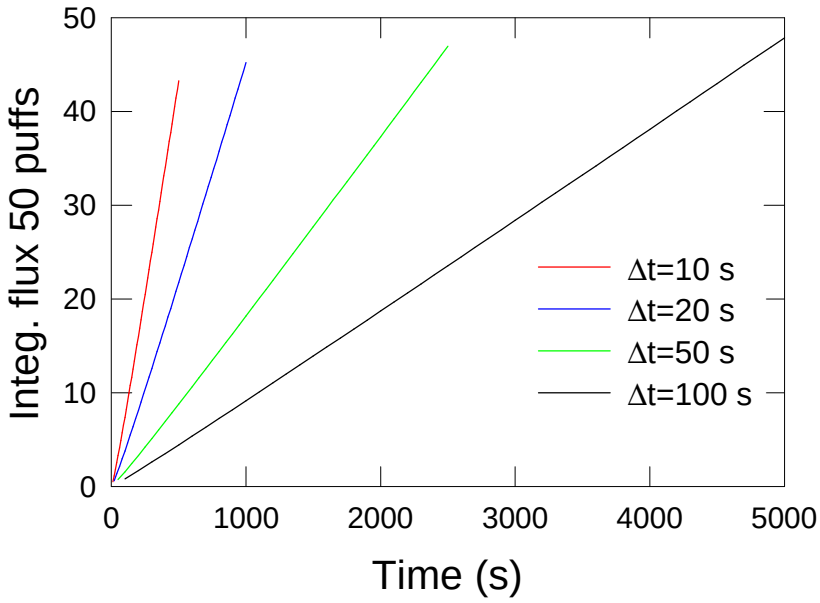

Figure 9. Integrated flux *FIS(z,t)* due to 50 puffs introduced at time intervals of 10 (red), 20 (blue), 30, and 50 seconds for a height of 3 meters and a reflecting surface.

The average upward diffusion (source) flux *SI(z, MDt)* at time *MDt* is just the slope of the curves in Figure 9,

$$SI(z, M\Delta t) = \frac{FIS[z, M\Delta t] - FIS[z, (M-1)\Delta t]}{\Delta t} = \frac{FI(z, M\Delta t)}{\Delta t} \qquad (10)$$

SI is shown in Figure 10 as a function of the number of puffs encountered as opposed to time as in Figure 9. The solid curves are for puff intervals of 10, 20, 50 and 100 seconds at a height of 2 m. After an initial transient the (average) source is constant. The constancy after an initial transient indicates the flux is in a quasi steady-state during the filling process as discussed by *Hoppel et al*. [*2005*]. The dashed lines give the source flux at 1 and 5 m for the case of puffs every 20 seconds. The small asymptotic difference is due to the difference in the quasi steady-state gradient at the different heights. The steady state source flux is just 1/Δt for a unit puff.

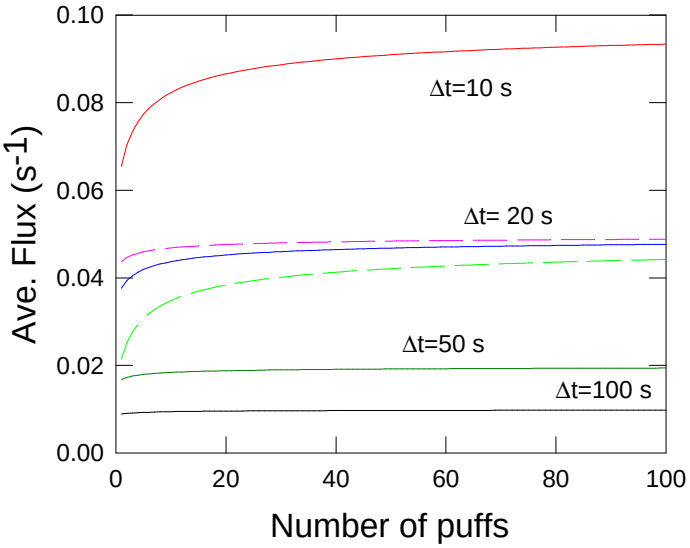

Figure 10. The time average flux *SI(z,MDx)* as function the number of puffs for puff intervals of 10, 20, 50, and 100 seconds at 2 meters and a reflecting surface. Dashed lines show the small difference in flux at 1 m (pink) and 5 m (green) as compared to that at 2 meters.

Even though the (source) flux is nearly constant with time as shown in Figure 10, the concentration in the atmosphere above is steadily increasing. The vertical concentration profile at various times for puff interval of 20 seconds is shown for (50 puffs) 1000 s, 2000 s, 4000 s and 8000 s (400 puffs) in Figure 11.

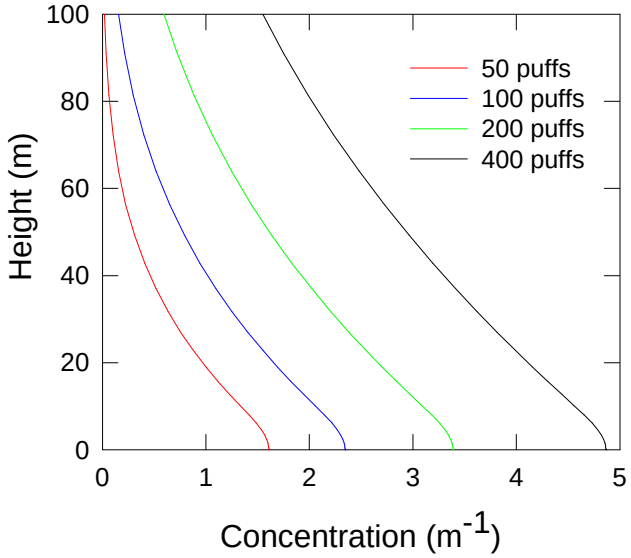

Figure 11. Vertical profile of concentration due to 50, 100, 200, and 400 puffs where the puffs are separated by 20 seconds, for a reflecting surface. $K(z)=1\ m^{-1}\ s^{-1}$.

The above illustration indicates that, in the case of no surface deposition, a discontinuous source of particles in the form of Gaussian puffs can be viewed as a constant average source. Even though the concentration is increasing, the quasi steady-state is reached where the average flux, just above the source, is constant even though the concentration in the MBL is steadily increasing. This conclusion is not surprising and may have been anticipated, just based on conservation of particles. However, the above example is now contrasted to the case where there is total absorption at the surface, and the results are not as trivial. Also, please note that the vertical profiles in this illustration are **not realistic** because, unlike the MBL, the vertical domain is unbounded.

1.b. Series of puffs – totally absorbing surface

The contrasting behavior shown in Figure 7 for the total integrated flux from a single puff for the cases of total absorption vs. total reflection indicate that the behavior for absorption at the surface will be remarkably different than that shown above for a reflecting surface. The loss of particles between puffs influences the total concentration and source flux, and therefore the puff frequency will play a more complicated role. The instantaneous flux at 2 m, from 10 puffs separated by 10 seconds, is shown in Figure 12 [calculated from Eq. (5) for a series of puffs]. This can be contrasted to Figure 8, where the flux is always positive and increasing. For absorption, there is an initial upward pulse near the puff and then a downward flux more distance from the puff with diminishing negative flux with time as the plume dissipates.

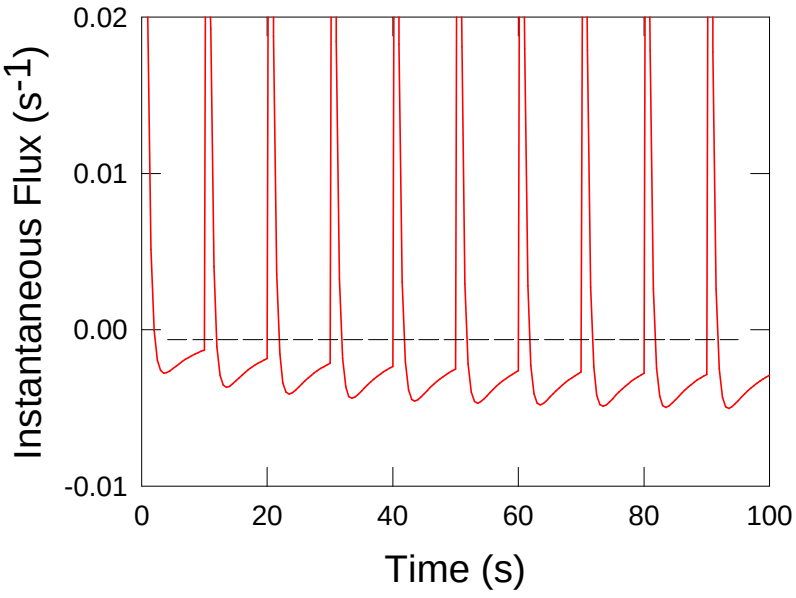

Figure 12. Instantaneous flux, *FS(z,t)*, at 2 m as function of time during the encounter of the first 10 puffs separated by 10 seconds for a totally absorbing surface.

The integrated flux, *FIS(z,t)*, is given by Eq. (9) and shown in Figure 13 for 50 puffs where the four curves are for puff intervals of 10, 20, 50, and 100 seconds. Even though the

instantaneous flux shown in Figure 12 spend more time as a downward flux the net (average) flux is upward. The negative flux increases (in magnitude) until the concentration at the surface reaches an average steady-state value (seen later in Figure 15 near the surface); i.e., the downward fluxes from the most distant puffs are negligible. Compared to the reflecting case the average fluxes are much smaller since most particles do not stay airborne but are re-deposited on the surface.

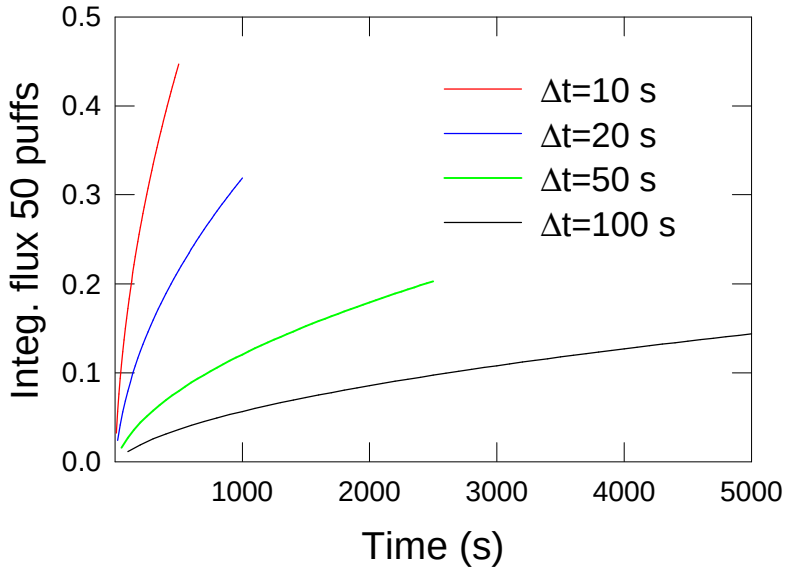

Figure 13. Integrated total flux through the plane at 2 m as a function of time for puff separations of 10, 20, 50, and 100 seconds, 50 total puffs, and totally absorbing surface.

Again we will define the average upward (source) flux (at the time of puff M) at 2 m as the slope of the integrated flux between puffs M and M+1 [Eq. (10)]. The average upward flux (effective source) as a function of the number of puffs is shown in Figure 14, where the curves are for puff separations of 10, 20, 50, and 100 seconds. The time coordinate for each curve can be obtained by multiplying the number of puffs by the puff separation. The curvature of the curves in Figure 14 is opposite that of Figure 10 for a reflective surface because the loss at the surface, unlike that of a reflecting surface, increases as the average concentration above the surface increases. The curves in Figure 14 continue to decrease and go to zero as time goes to infinity, at which time there would be an equilibrium; i.e., the gradient flux above the source would go to zero with a strong gradient below the source driving all newly injected particles back to the surface. However, because in this example the vertical domain extends to infinity, equilibrium is never truly achieved. The lifetime of particles of the size implied by the assumption of an absorbing surface with constant eddy diffusion all the way down to the surface is short, and therefore ignoring the gravitational settling velocity in the differential equation (as we have done here) is not realistic, as mentioned previously and as we will see in the next Section III.

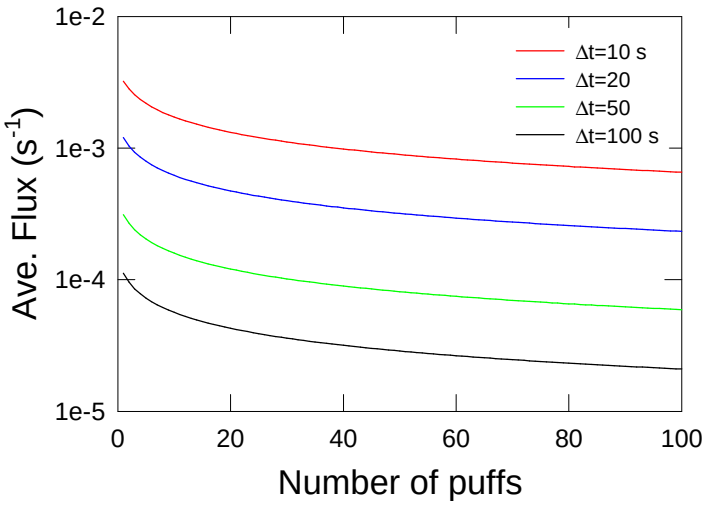

Figure 14. Upward average flux, *SI(z,MDx)*, at 2 m for puff separations of 10, 20, 50, and 100 seconds as a function of the total number of puffs for an absorbing surface.

The 'filling' process (i.e., the filling of the MBL by sea salt particles injected at the surface) is shown in Figure 15, where the concentration profile for puff separation of 20 s is shown for (25 puffs) 500 s, 1000 s, 2000 s and 10000 s (500 puffs). The totally absorbing surface requires that the concentration at the surface must be zero. The nearly constant concentration gradient over the lowest 5 m indicates that the source flux is nearly the same over the lowest five meters and changes very slowly as the upper atmosphere fills.

Now, even though we have an absorbing surface and have previously discussed the equivalent deposition velocity for this case, the concept of deposition velocity actually has little meaning here for several reasons. When the surface concentration is zero, as in the case of perfect absorption, the deposition velocity is infinite when referenced to the surface concentration. The deposition velocity is changing with time as the gradient at the surface is changing. In the limit as time goes to infinity, the concentration gradient above the source vanishes requiring the gradient below the source to be large enough so that the flux of new particles ($1/\Delta t$) is equal to the deposition flux

$$K\frac{N(h)}{h} \approx \frac{1}{\Delta t} \qquad (11)$$

thus

$$v_d\left(t=\infty\right) \approx \frac{K}{h} \qquad \text{for z>h} \qquad (12)$$

Making the deposition velocity for all reference heights with $z_{ref} > h$ a function of the source height.

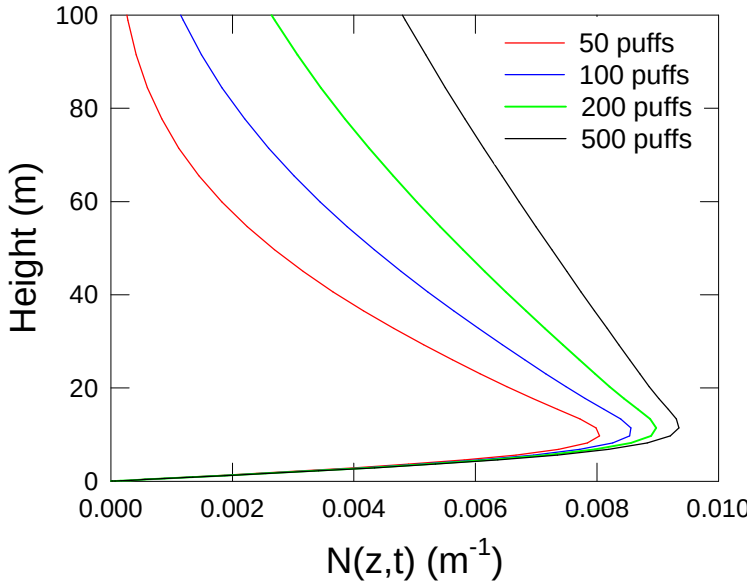

Figure 15. Vertical concentration profiles after 25, 50, 100, and 500 puffs for puff separation of 20 seconds for totally absorbing surface.

The case of total absorption at the surface is also unrealistic in the sense that the turbulent diffusion coefficient of 1 m^2 s^{-1} is unrealistically large as it extends down to the surface and gives rise to very high deposition rates. The deposition velocity downwind of a single puff referenced to 10 m was seen to be greater than 10 cm s^{-1} (Figure 6). This corresponds to a fall velocity for particles greater than 30 μm radius and explains the rapid loss of particles shown in Figure 12.

For the case of a reflecting surface we see that the integrated flux (number of particles suspended) increases linearly with the frequency of the puffs (Figures 9 and 10). That is not the case for a totally absorbing surface where the time between puffs is an important factor in determining the upward flux (effective source). This difference is clearly illustrated by letting the puff separation be infinitely long. The integrated flux from a single puff (of unit strength) goes to unity for a reflecting surface, whereas the integrated flux for the absorbing surface goes to zero. This has important implications when deriving the surface source function from measurements of aerosol production from a single breaking wave, as in a wave tank, and extrapolating the result to source flux for the ocean surface made up of many whitecaps.

Before proceeding to analyzing more complete scenarios, we summarize the various flux variables defined above. This notation is used in the 6 cases that follow.

Table 1. Definitions of various flux variables

Symbol	Description	Units
F(z,t)	Flux of particles from a single puff at time 0, through the plane at height *z*	s^{-1}
FI(z,t)	Flux from a single puff through a plane at height z integrated from time *t=0* to *t=t* $$FI(z,t) = \int_0^t F(z,t)dt$$ *Interpretation*: Number of particles above the z-plane resulting from a puff at time *t=0.*	Dimensionless
FS(z,MDt)	Flux through a plane at height z at discrete times from a series of *M* puffs separated by *Dt* $$FS(z, M\Delta t) = \sum_{m=1}^{m=M} F(z, m\Delta t)$$	s^{-1}
FIS(z,MDt)	Flux from a series of puffs separated by Δt, integrated over a time period *MDt* $$FIS(z, M\Delta t) = \sum_{m=1}^{m=M} FI(z, m\Delta t) = \sum_{m=0}^{M} \int_0^{mt} F(z,t)dt$$ *Interpretation*: Total number of particles above the z-plane at time *MDt* resulting from *M* puffs.	Dimensionless
SI(z,MDt)	Average flux over time *Dt* at time *MDt* resulting from a series of *M* puffs $$SI(z, M\Delta t) = \frac{FIS[z, M\Delta t] - FIS[z, (M-1)\Delta t]}{\Delta t} = \frac{FI(z, M\Delta t)}{\Delta t}$$ *Interpretation*: The (upward) gradient flux of particles integrated over the horizontal plane at *z* and at time *MDt* resulting from *M* prior puffs.	s^{-1}

To get the average flux per unit area the flux SI must be associated with the appropriate area of the ocean surface. This will depend upon the white cap frequency, the area of white water coverage, and the strength assigned to our (unit) puff. This will be treated in Section IV. Also, while SI is the puff source flux at the source for a reflecting surface that is not the case for an absorbing surface.

To help understand the physical interpretation of the equation for the $SI(z, t_M)$ [Eq. (10)], *FI(z,MDt)* is plotted for seven puff plumes offset by 10 s for the case of perfect reflection in Figure 10. At any time, *FIS(z,MDt)* is the sum or the magnitude of all curves and $SI(z, t_M)$ is the difference in *FIS* over a time interval *Dt*. The sum at time *MDt* differs from that at *(M-1)Dt* by the value of the curve from the first puff, *FI(z,MDt)*. For the case of reflection, if you wait long enough, this just means that every puff adds the value of one (for unit puff) so that $SI(z, t_M)$ is just $(\Delta t)^{-1}$. For the case of absorption as shown in Figure 7, *FI(z,8)*, becomes zero and the earliest puffs no longer contribute, FIS no longer change with time and $SI(z, t_M)$ is therefore zero.

A steady state can exist only if the memory of the earliest puffs is lost. For cases that do not contain the fall velocity this means that eventually the gradient above the surface must go to zero and all new particles are re-deposited on the ground at the same rate at which they are formed.

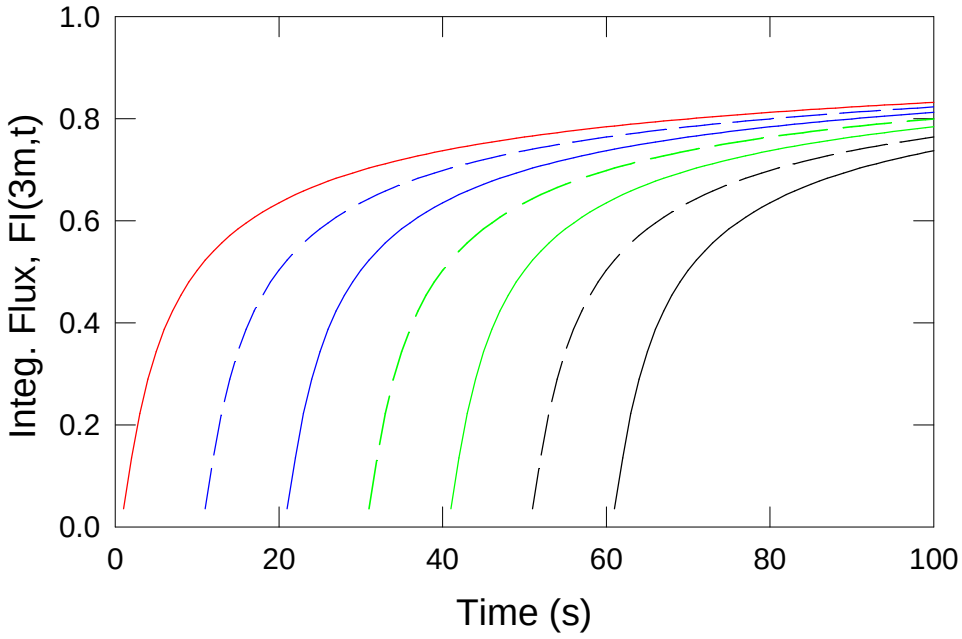

t=MΔt

Figure 16. *FI(3m,t)* for 7 puffs offset by 10 seconds for the perfectly reflecting case. At 70 seconds the sum of the puffs is the same as the sum of the puffs at 60 seconds plus the contribution of the first puff at 70 seconds.

We now extend the analysis by first looking at two more reflecting surface cases, but first with the eddy diffusivity set to zero at the surface and increasing linearly with height (Case 2), and then with the domain capped by letting the eddy diffusivity go to zero at the top of the MBL (Case 3).

Case 2. Gaussian Plume with K(z)=kz for totally reflecting surface, no gravitational settling

The general solution for a plume downwind of a line source with perfectly reflecting surface has been given by *Huang* [1979] for the case when the wind and eddy diffusion coefficient are given by the following power laws

$$u(z) = \bar{u} z^{p} \quad \text{and} \quad K(z) = kz^{n} \tag{13}$$

where the wind is taken along the x-direction. By using arguments similar to those discussed in connection with Case 1, we can adapt the Huang solution for a line source to a puff plume by letting, $x = \bar{u}t$ and $p=0$ (no wind shear), and by normalizing the source to unity ($Q/\bar{u} = 1$). The solution then becomes

$$N(t,z) = \frac{(zh)^{\frac{1-n}{2}}}{kt} Exp[\frac{-\left(z^a + h^a\right)}{4kt}] I_n(\frac{2(zh)^{\frac{a}{2}}}{4kt}) \quad (14)$$

where $a = 2 + p - n$, $n = (1-n)/a$, z=h is the height of the source and I_ν is the modified Bessel function of order ν.

Here we are interested in the linear *(n=1)* eddy diffusion coefficient, *K(z)=kz***,** which is generally believed to be the profile which best describes the turbulent mixing in the surface layer during periods of neutral stability. But before proceeding, we point out that Equation (14) is the same as Eq. (4) for a constant K (*n=0*). This can be seen using the following identity

$$I_{\frac{1}{-\frac{1}{2}}}(y) = \sqrt{\frac{2}{p\ y}} \frac{(e^y + e^{-y})}{2} \quad (15)$$

and completing the squares in the exponents of Eq. (14).

For the case of a linear diffusion profile, *n=1*, the solution becomes

$$N(t,z) = \frac{1}{kt} Exp\left[\frac{-(z+h)}{kt}\right] I_0\left(\frac{2\sqrt{zh}}{kt}\right) \quad (16)$$

The gradient can be expressed as

$$\frac{\partial N(t,z)}{\partial z} = \frac{1}{(kt)^2} Exp\left(\frac{-(z+h)}{kt}\right)\left[\sqrt{\frac{h}{z}}\ I_1\left(\frac{2\sqrt{zh}}{kt}\right) - I_0\left(\frac{2\sqrt{zh}}{kt}\right)\right] \quad (17)$$

The flux at any time t, passing through a plane at height z is then given by

$$F(z,t) = -kz\left(\frac{\partial N(t,z)}{\partial z}\right) \quad (18)$$

The integrated flux passing through a plane at height z between *t=0* and *t= t* is just

$$FI(t\ ,z) = \int_0^t F(t,z)dt \quad (19)$$

The integrated flux at 1 and 3 m for a single puff is shown in Figure 17 by the red and black solid lines where the integrated flux for k =0.16 m s^{-1} corresponds to that of a 10 m s^{-1} wind speed (and neutral stability). The dotted lines are the fluxes at 1 and 3 m for a constant K of 1 m^2 s^{-1} as given by Eq. (6) and shown in Figure 7. In both cases the source is at h=0.2 m. Because of the small value of mixing near the surface in the linear case it takes longer for the particles to move

upward through the plane at z=3 m. However it is important to realize that in either case the flux for the reflecting surface approaches unity after about 100s, so that the form of the turbulent mixing profile is not very important for small particles where surface deposition is small (i.e., the well-mixed case). For an absorbing surface we would expect the form of the mixing profile to be important since a low mixing coefficient near the surface inhibits upward mixing; however, for a linear profile the only transport mechanism is gradient transport, and there is no mechanism by which particles can be deposited right at the surface (since K goes to zero). In a subsequent section gravitational flux will be added to governing equation.

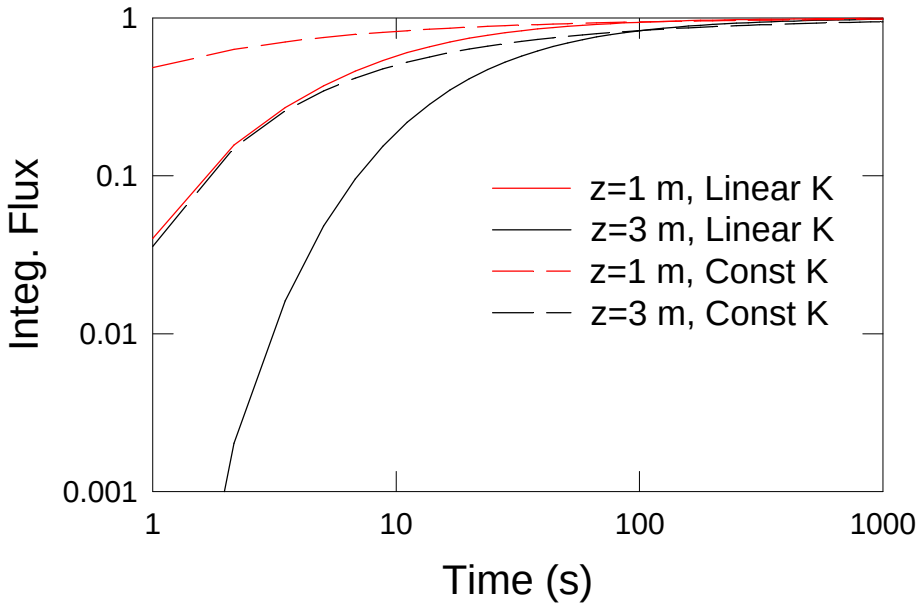

Fgure 17. The integrated flux at time τ at 1m (red) and 3 m (black) from a single puff at z=0.2 m for a perfectly reflecting surface. The solid lines are for linearly increasing diffusion coefficient (K=0.16z) and the dashed lines for constant K=1 m^2 s^{-1}.

So, these results show that *for a reflecting surface (i.e., no surface deposition – small particles) the shape of the eddy diffusivity in the surface layer of the MBL has little effect on the cumulative integrated flux from a series of puffs*. However, the next section will show that capping the MBL has an important effect.

Case 3. Plumes in a capped boundary layer, with a reflecting surface and no gravitational settling

In all the prior cases the vertical domain is unbounded and particles continue to flow upward indefinitely. However, the MBL is usually capped by a potential temperature inversion that effectively traps the sea-salt particles in the MBL. A more realistic profile for the mixing coefficient, K(z), which caps the MBL at a height H is given by

$$K(z) = ku_* z(1-\frac{z}{H}) \qquad (20)$$

κ and u_* are the von Karman constant and the friction velocity, respectively. This form of the diffusion coefficient retains the linear increase in the surface layer, is a maximum in the center of the MBL, and goes to zero at the top of the MBL. The solution for this form of the eddy diffusion coefficient is given by *Nieuwstadt* (1980) in terms of Legendre polynomials, $P_n(z)$, where n is the order of the polynomial:

$$N(z,t)=\frac{Q}{H}\left[1+\sum_{n=1}^{\infty}(2n+1)P_n\left(\frac{2h}{H}-1\right)P_n\left(\frac{2z}{H}-1\right)Exp\left\{-n(n+1)\frac{kt}{H}\right\}\right] \tag{21}$$

where Q=1 for a unit puff and $k=ku_*$. The flux is found by term-by-term differentiation

$$F(z,t)=-kz\left(1-\frac{z}{H}\right)\frac{dN(z,t)}{dz} \tag{22}$$

Likewise term by term integration from t=0 to t=τ gives the integrated flux, FI(z,t), at height z and time τ for a single puff. Explicitly,

$$FI(z,t)=-z(1-\frac{z}{H})\sum_{n=1}^{\infty}(2n+1)P_n\left(\frac{2h}{H}-1\right)\frac{dP_n(x)}{dz}\frac{\left\{1-Exp\left[-n(n+1)\frac{kt}{H}\right]\right\}}{n(n+1)} \tag{23}$$

where $x=\frac{2z}{H}-1$, and

$$\frac{dP_n}{dz}=\frac{dx}{dz}\frac{dP_n}{dx}=\frac{2}{H}\left[\frac{n\{xP_n(x)-P_{n-1}(x)\}}{x^2-1}\right] \tag{24}$$

The expression used here for the derivative of the Legendre polynomial can be found in *Abramowitz and Stegun* (1964).

The concentration, as a function of height, from a single puff in a MBL capped at 100 m is shown for times of 50, 100, 500 and 1000 seconds in Figure 18. The curve at 1000 seconds indicates the particles are well mixed over a height of 100 m. For unit puff, the final result should be a uniform concentration of $0.01 m^{-1}$.

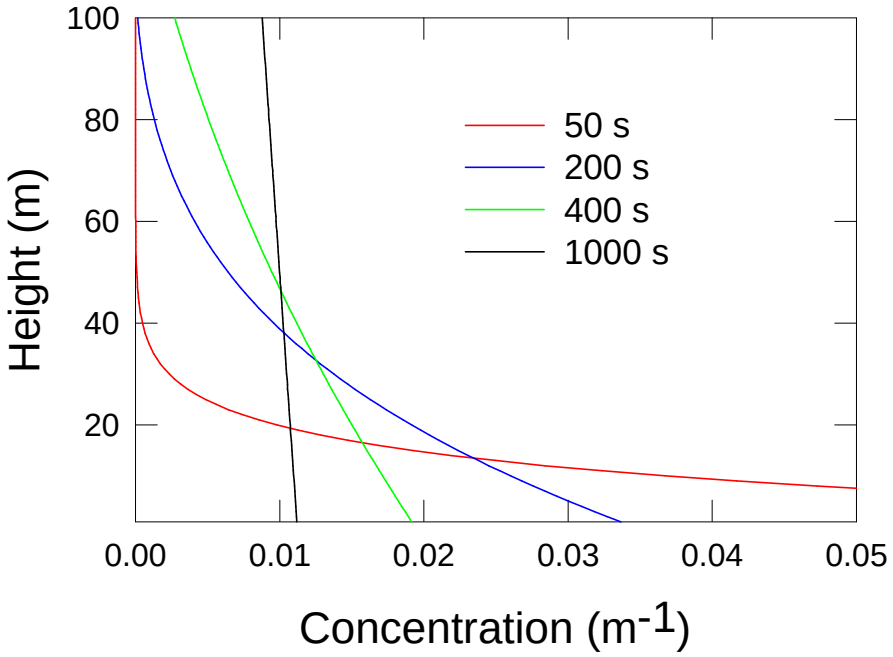

Fgure 18. Concentration as function of height at 50, 200, 500, and 1000 seconds for capped MBL and reflecting surface.

Figure 19 plots *SI(z,t)* for 1 to 100 puffs separated by 20 seconds at heights of 2, 10 and 50 meters. At 2 m the upward flux approaches 0.05 (asymptotic limit would be (0.98)(.05)=.049). Since only half the particles are found above 50 meters the source flux at 50 m would be only .025. The flux at 50 m is much different in the capped case than in the unbounded case (Case 2). Therefore the height at which you measure the flux and the height of the MBL will affect the measured flux.

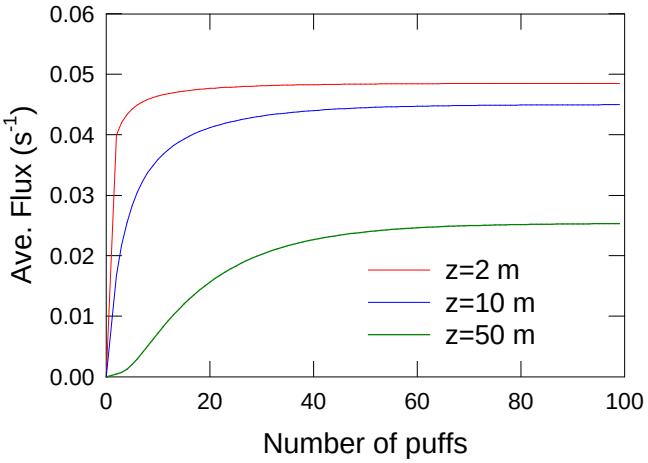

Figure 19. *SI(z,t)* for the capped case at 2, 10 and 50 meters. Puff interval is 20 seconds.

Twenty terms of the series in equation (21) are more than adequate to evaluate *N(z,t)* and *F(x,t)*. However, the series for *FI(z,t)* exhibited an oscillation around the mean profile when plotted as a function of z. The amplitude of the oscillation decreased and the frequency increased as the number of terms in the series increased. We carried out the calculation for *FI(z,t)* [and *SI(z,t)*] using up to 120 terms, at which point the amplitude was very small but still visible when plotted as a function of z. The oscillations do not affect Figure 19 because the plot is a function of time at fixed z. A similar but less predicable behavior was observed with the series solution to be described in the next case where we also have an infinite series.

Case 4. Gaussian Plumes with specified surface deposition, capped boundary layer, K=constant and no gravitational settling.

In the prior cases we have assumed that the earth's surface was either a perfect reflector or a perfect absorber (with a very unrealistic constant *K(z)* all the way to the surface). We now consider the more realistic case where there is partial absorption at the surface determined by specifying a deposition velocity for surface deposition. Note that this is not equivalent to including gravitational settling; this is only a boundary condition and includes only the effects of deposition at the surface via impaction, Brownian diffusion, etc. Also, as in Case 3, the boundary layer is now capped by a reflecting surface at height H to simulate the finite depth of the MBL. The solution to the diffusion equation (Eq. 1) for these boundary conditions is given by *Seinfeld* [1986] and *Seinfeld and Pandis* [1998]. Following the same procedure as before, the horizontal dispersion can be separated from the vertical dispersion by separation of variables. The solution in the x-y plane is the same as in the last section and the solution of the vertical dispersion of the concentration, *N(z,t),* from a puff at height h and at time t=0 is given by *Seinfeld* [1986] as

$$N(z,t) = 2\sum_{n=1}^{n=\infty} \frac{\left(l_n^2 + b^2\right)\cos[l_n(H-h)]\cos[l_n(H-z)]}{H(l_n^2 + b^2) + b} Exp\left(-l_n^2 K_z t\right) \qquad (25)$$

where h is the height at which the puff is introduced and λ_n are given by the roots of

$$l_n \tan(l_n H) = b \qquad (26)$$

and $b = \frac{v_d}{K_z}$.

The solution satisfies the surface boundary condition

$$K_z\left(\frac{dN(z,t)}{dz}\right)_{z=0} = v_d N(0,t) \qquad (27)$$

where v_d here is the deposition velocity referenced to the surface concentration. As the surface concentration changes so does the surface gradient, and both have the same time dependence at the surface, such that the deposition velocity remains constant with time. The surface deposition

resulting from all mechanisms included in the deposition velocity must be reflected in the surface gradient as required by the differential equation which *allows only for gradient transport*. At the top of the boundary layer the domain is capped by requiring the flux be zero (no concentration gradient).

In the calculations to be given here the value of K_z is set to 5 m^2 s^{-1}, the source is located at one-half meter (h=0.5 m), the boundary layer is capped at 100 m, and v_d is 0.0065 m s^{-1}, a deposition velocity roughly equal to that of a 5 μm radius particle at wind speeds of about 10 m s^{-1} [*Hoppel et al*., 2002]. The deposition velocity has both a gravitational settling component of about 0.004 m s^{-1} (sea-salt particles at 80% RH) and an impaction component of about 0.0025 m s^{-1}. We note here that since the gravitational component is large compared to the non-gravitational component the gravitational settling should be (but is not, as mentioned above) included in the differential equation. It will be included in the results presented in Section III. Particles smaller than 5 μm will generally have deposition velocities that are much smaller. The value of K_z is nominally that found at a height of about 30 m in the MBL for neutral conditions and wind speeds of about 10 m s^{-1}.

The solution for the vertical profile of concentration from a single puff at 20, 60, 100 and 500 seconds is shown in Figure 20. The number of terms in the sum used here is 50, but less than 10 is needed to capture the concentration profile. It is seen that the particles are nearly uniformly distributed after 500 seconds. Since particles cannot penetrate the upper boundary at H=100 m and loss at the surface is small on the time scales shown, a finite, nearly uniform concentration is obtained after about 500 seconds. There will be a further slow decay of the uniform concentration with time due to surface deposition. The nearly uniform profile during the decay is indicative of the quasi steady state.

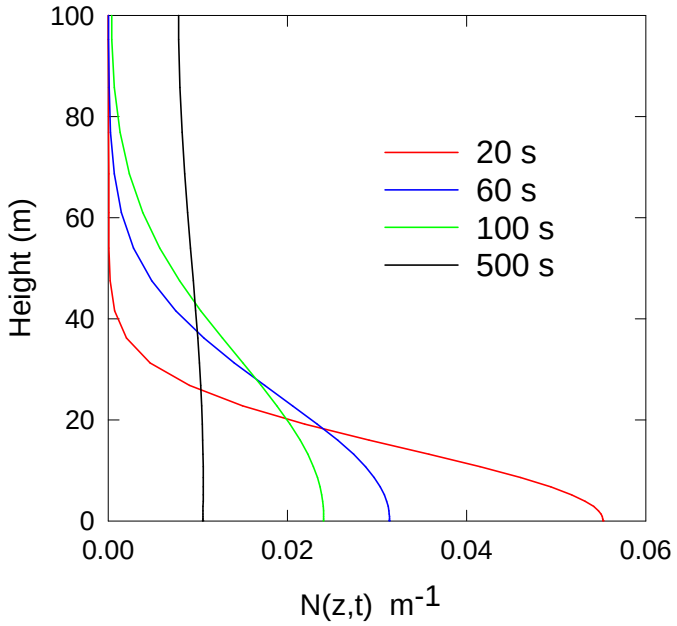

Figure 20. Concentration vs. height with K_z=5 m^2 s^{-1}, v_d=0.0065 m s^{-1} and H=100 m at times of 20, 60, 100 and 500 seconds.

Equation (25) can be differentiated term by term to give the gradient, as follows:

$$\frac{\partial N(z,t)}{\partial z} = 2\sum_{n=1}^{n=\infty} \frac{l_n\left(l_n^2 + b^2\right)\cos[l_n(H-h)]\sin[l_n(H-z)]}{H(l_n^2 + b^2) + b} Exp\left(-l_n^2 K_z t\right) \qquad (28)$$

The vertical profile of the gradient (negative of the flux, $-F/K_z$) resulting from a single puff is shown in Figure 21 at times of 20, 60, 100 and 500 seconds.

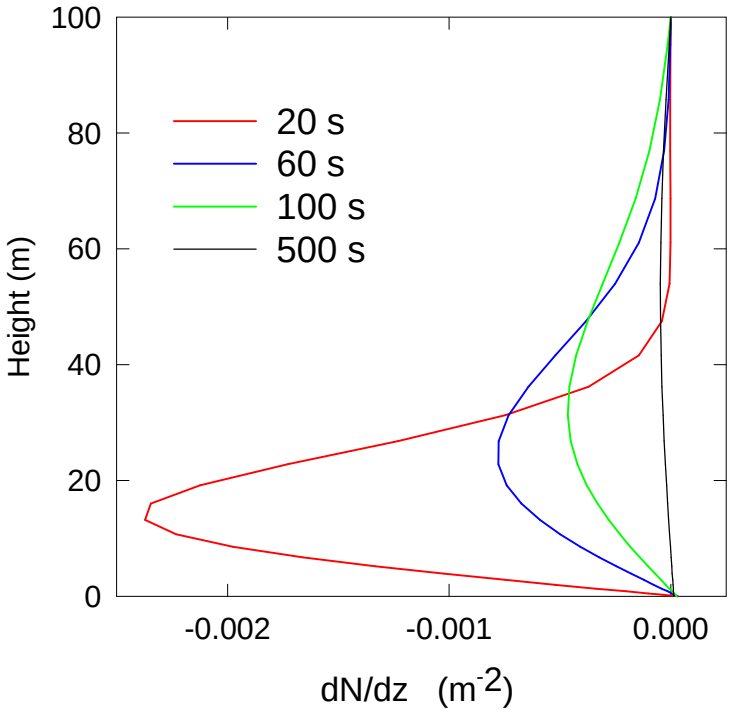

Figure 21. Concentration gradient vs. height for K_z=5 m^2 s^{-1}, v_d=0.0065 m s^{-1} and H=100 m at times of 20, 60, 100, and 500 seconds.

The downward flux (positive values of the gradient) near the surface is very small and difficult to detect in Figure 21 in comparison to the large upward flux during the first 100 seconds or so. The zero crossing (point where the flux changes direction) is slowly moving upward with time. The critical height where the flux changes direction is shown in Figure 22 and found numerically by locating the zeros in the concentration gradient, Eq. (28), as a function of time. The critical height does not reach 10 m until after 400 seconds. This is much slower than the upward propagation of the crossing point shown in Figure 5 for total absorption. For total reflection, $v_d=0$, the flux is always upward. Since the deposition flux is much smaller than that observed for the case of total absorption, the solutions here more closely resemble that of reflection than that of total absorption over short time periods. However over longer time periods the loss to surface deposition is significant.

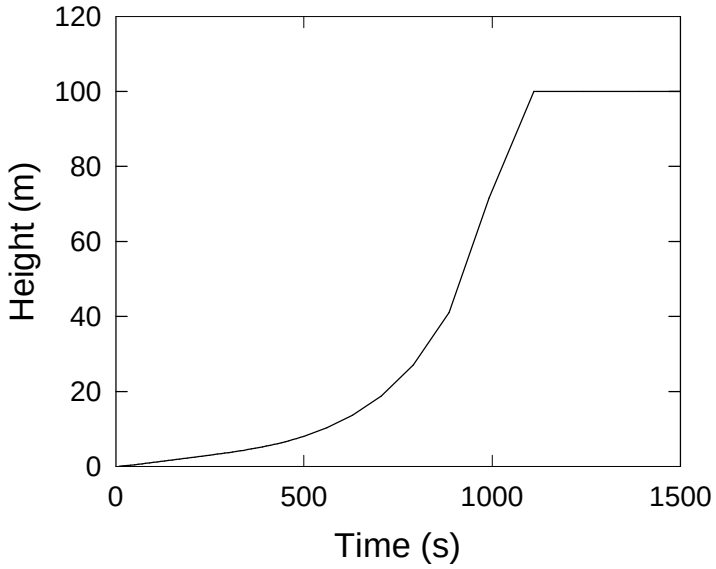

Figure 22. The height at which the gradient changes sign (the flux changes direction) vs. time for Case 4.

As demonstrated in the last section, the instantaneous value of the flux (as demonstrated in Figures 8 and 12 for total reflection and total absorption) is of little interest since measurements and parameterizations in numerical models deal only with average values over a large number of whitecaps. And as also discussed earlier, the total integrated flux per puff, *FI(z,t),* is an important function which indicates the length of time for equilibrium to be reached. For a perfectly reflecting surface we saw that equilibrium is never achieved and the particle concentration increases indefinitely. *FI(z,t)* is found for this case by integrating Equation (28) from time zero to time t. Term by term integration of Equation (28) over a time interval from t=0 to time t is equivalent to replacing the exponential factor for the time dependence by a new factor equal to

$$-\frac{1}{l_n^2 K_z}\left[\left(Exp(-l_n^2 K_z t\right)-1\right] \tag{29}$$

For the integrated flux, *FI(z,t)* (a measure of the number of particles above height z), the series solution converges very slowly and 100 terms in the sum were used. The total integrated flux from a single puff is shown in Figure 23 over a time period of 3.3 hours at heights of 2, 4, and 10.7 meters. Near the surface nearly all particles are dispersed upward, about 90% cross the 2 meters level at times less then 500 s; less at higher altitudes, as expected because the domain is capped. At longer times there will be a slow decrease in the integrated flux as particles dispersed above make their way back downward and are re-deposited on the surface at a rate dictated by the specified deposition velocity. After 3 hours more than half the particles have been re-deposited on the surface. This behavior can be compared, although on different scales, to that shown in Figure 7. For total reflection, the integrated flux goes to unity indicating that all particles are forever dispersed upward. For total absorption the particles dispersed upward,

rapidly resettle to the surface giving zero total flux after a short period of time (also demonstrated in Figure 7).

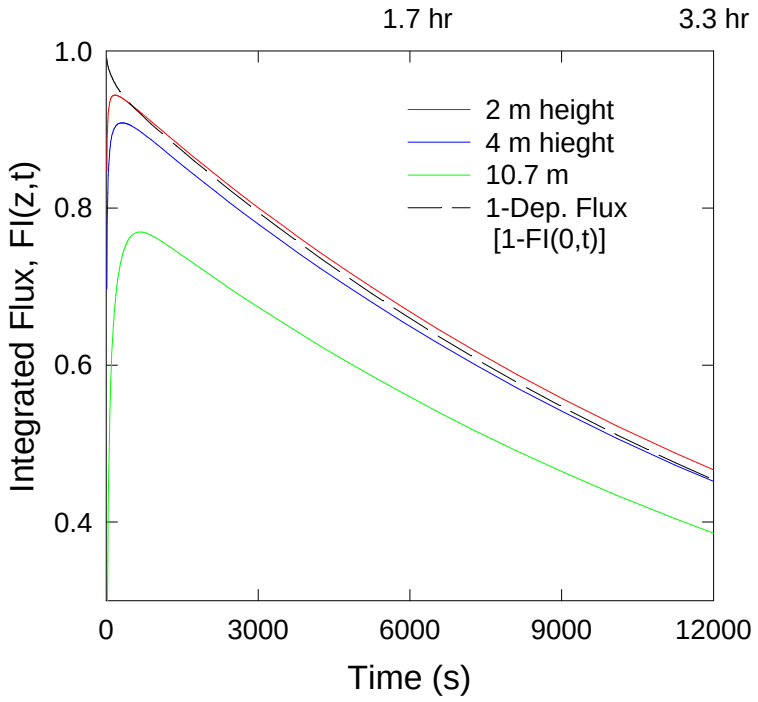

Figure 23. Total Case 4 integrated flux from t=0 to time t, for a single puff through planes at 2, 4 and 10 m. The dashed line is 1 minus the deposition flux.

Also shown by the dashed line in Figure 23 is the integrated deposition flux obtained from

$$FI_{dep}(0,t) = v_d \int_0^t N(0,t)dt \qquad (30)$$

where term-by-term integration of N(0,t) can be carried out and is similar to that indicated in Eq. (29) for the flux. $FI_{dep}(0,t)$ starts at zero and is unity when all particles are re-deposited. In Figure 23 we have plotted the quantity, $1.0 - FI_{dep}(0,t)$, by the black dashed line to demonstrate that the sum of the upward gradient flux measured close to the surface and deposition flux at the surface is unity - the total source for a unit puff plume. The same will hold for a series of puffs as will be shown below. While this is simply a statement of conservation of particles, it has important consequences in that it demonstrates that a measurement of these two quantities (i.e., the (upward) diffusion flux *near the ground* and the deposition flux via the concentration and the v_d near the ground) will provide a measure of the source strength. This assumes that the deposition velocity is known, which unfortunately is often not the case.

In calculating *FI(z,t)*, if too few terms are used in the sum the plot, as a function of height, exhibits unacceptable oscillations. As the number of terms increases, the amplitude of the oscillations decrease, but what looks like numerical instability develops near and just above the source. The latter may be due to the accuracy with which the eigenvalues and sum are calculated. Since the oscillations are seen to be in phase at all times at a given height, they do

not appear in the temporal plots shown in Figure 23, but as a result the accuracy of Figure 23 is somewhat limited by these small oscillations. For the parameters (and software) used in the calculations, the best accuracy was obtained using about 100 terms in the series.

We now consider this case with a series of puffs. Figure 24 shows particle concentration as a function of height, the result of summing Eq. (25) over a series of 100 and 200 puffs with puff separation of 20 seconds (total time of 2000 and 4000 s). If there were no loss of particles the average of the vertical profiles over 100 m would be 1 and 2 m^{-1}, respectively. The increase in concentration with time decreases as equilibrium is approached and the gradient decreases with time. (The calculations above were run out to 1000 puffs with 20 second puff separations and indeed the concentration was seen to approach equilibrium.) There must always be some gradient during the filling process. At steady state the filling is complete and the gradient must approach zero at all heights above the source (because of the upper boundary condition which requires the gradient to be zero). An average gradient below the source at $z=h$ (0.2 m in the example), sufficiently strong to direct all newly injected particles to the surface, is established.

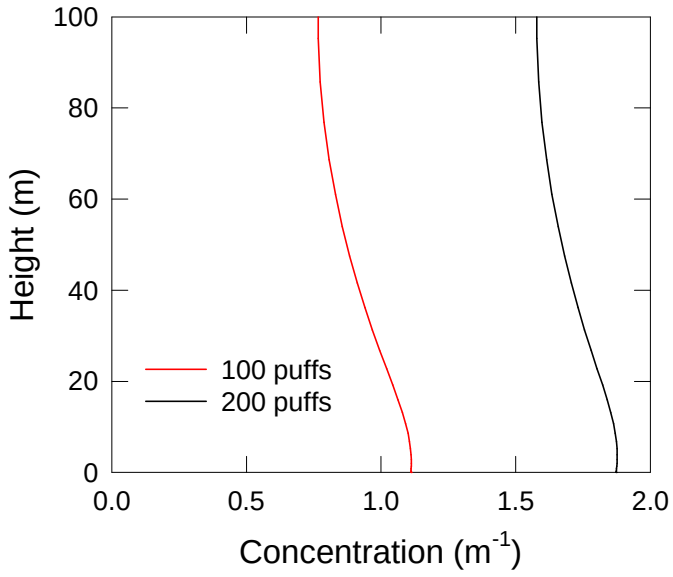

Figure 24. Concentration vs. height after a series of 100 and 200 puffs for 20 seconds puff separation.

The integrated total fluxes, *FIS(z,t)*, from a series of 250 puffs separated by 10, 20 50 and 100 seconds are shown in Figure 25, which can be compared to Figures 9 and 13 for total reflection and total absorption. At higher puff frequencies the curves in Figure 25 are nearly the same as the reflecting case because there is little depositional loss for the earlier puffs during the time required for 250 puffs to occur. For the longer puff separation (100 s), the earlier puffs are dissipating and contributing little to the time integrated flux. With increasing time the integrated flux approaches a constant value, indicating no (average) gradient flux. The straight dashed lines indicate the integrated puff source flux and the difference between the total time-integrated flux and the diffusion flux is the time-integrated deposition flux. The slopes of these lines are the average flux at that point in time.

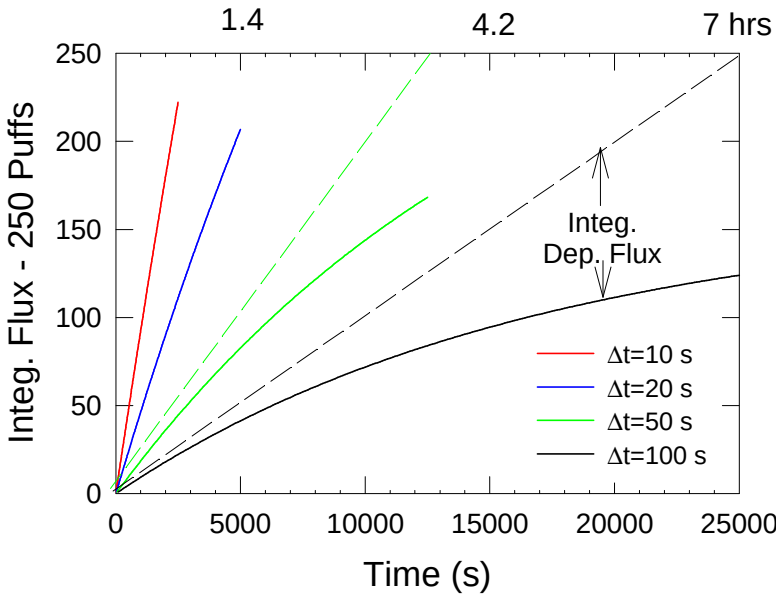

Figure 25. Integrated Case 4 total flux through the plane at 2 m as a *function of time* for puff separations of 10, 20, 50, and 100 seconds where the total number of puffs is 250.

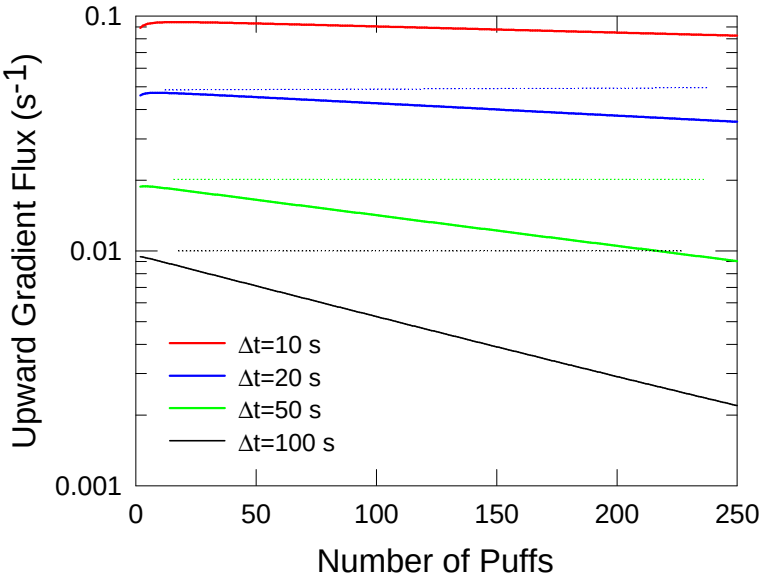

Figure 26. Upward Case 4 average diffusion flux at 2 m for puff separations of 10, 20, 50, and 100 seconds as a function of the *total number of puffs*.

The time averaged upward diffusion (gradient) flux *SI(z,t)* at the 2 m height for puff separations of 10, 20, 50, and 100 seconds as a function of the total number of puffs is shown in Figure 26. Over very long times the diffusion flux will continue to decrease and eventually *SI(z,t)* will go to zero at which time the concentration at the surface will be large enough to sink all new particles introduced at h, and the concentration gradient will be in accordance with the boundary condition given by Eq. (27). Above the source the gradient goes to zero. (If you are measuring the eddy correlation flux it will go to zero above the source!) The dashed horizontal

lines give the total puff source flux and the difference between the diffusion flux and the total source flux is the deposition flux (assuming that the diffusion flux is taken sufficiently near, and above, the source). ***The important point here is that, for the case where there is only diffusive flux allowed, a measurement of the average diffusive flux plus the deposition flux from a measurement of the concentration [Eq. (30)], the total puff source can be obtained***. Or from a modeling perspective the puff source can be the source from the surface into the lowest cell and the removal to the surface is the surface concentration times the deposition velocity. The above is for the case that there is no appreciable gradient in concentration across the lowest cell.

The time for a puff to decay is a strong function of particle size. Figure 27 shows the total integrated flux vs. time at 2 m from a single puff for particles of 1, 5 and 10 μm radius and indicates the difference in the time required to establish equilibrium. For a 1 μm size particle the deposition velocity is taken to be 0.0002 m s^{-1}. This deposition velocity is appropriate for a 10 m s^{-1} wind speed and is essentially the gravitational settling velocity - the impaction and Brownian contributions are negligible for 1μm particles at 10 m s^{-1} wind speed. The deposition velocity for a 5 μm particle is as given previously, and that of a 10 μm radius particle is taken to be 0.023 m s^{-1} (gravitational and impaction deposition contribute 0.015 and 0.008 m s^{-1} respectively). For the well-mixed case the filling time constant can also be estimated from the H/v_d. The estimated time constant for the above three cases are 6 days, 4.2 hr and 1.2 hr, respectively, which agrees roughly with the decay times shown in Figure 27. It should be remembered, that for ease of calculation, we have used an unrealistically low MBL height of 100 m. A more typical MBL height would be 500 to 1000 m and the time constants given above would increase by a factor of 5 to 10. Since the typical lifetime of an aerosol in the MBL is usually assumed to be about 3 days, the surface deposition for particles smaller than about 1 to 2 μm can be neglected. For larger particles the neglect of gravitational settling within the body of the MBL, as we have done in this case, is not valid. Inclusion of gravitational settling will be addressed in the next section.

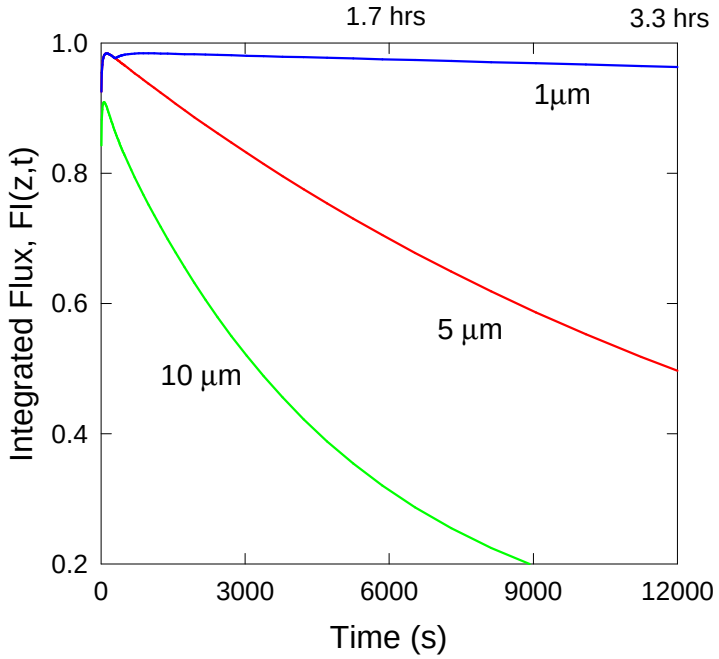

Figure 27. Decay with time of the integrated flux from a single puff for particle radius of 1, 5 and 10 μm. z=2 m.

Before leaving this case mention should be made of the effect of varying K. Figure 28 shows the concentration profile for K=1, 2, and 5 m^2 s^{-1} 60 seconds after a unit puff. The larger the value of K the more rapid is the upward mixing and dilution near the surface. Since the surface deposition is proportional to the concentration the surface deposition during the initial dispersion decreases with increasing value of K (the opposite as in the case for conventional deposition with flux downward from above). However the particles dispersed to higher altitudes require longer to redeposit, increasing deposition at longer times. The integrated diffusion flux near the surface shown in Figure 23 will always be near unity shortly after the puff and eventually decay to zero. For example, the time integrated flux shown in Figure 23 decreases more rapidly with time over about the first 3000 seconds, but has about the same value at the end time (12000s) as shown in the figure when K is decreased from 5 to 1 m^2 s^{-1}. Consequently the change in the integrated flux from a series of puffs shown in Figure 25 is nearly unchanged when K is changed from 5 to 1 m^2 s^{-1}. There was a very small decrease in the curve for Δt=10 s (red curve) because the earliest puffs were still in the state of more rapid surface deposition (still far from equilibrium). The above observation is important because it indicates that while the value of K may be important in establishing the rate of change for a single puff, it does not play a major role in determining the long term value for a series of puffs, ***provided the gravitational settling term is neglected in the differential equation*** (small particles). As we will see when gravitational settling is included K(z) is important in suspending large particles and determining the gravitationally induced vertical gradient.

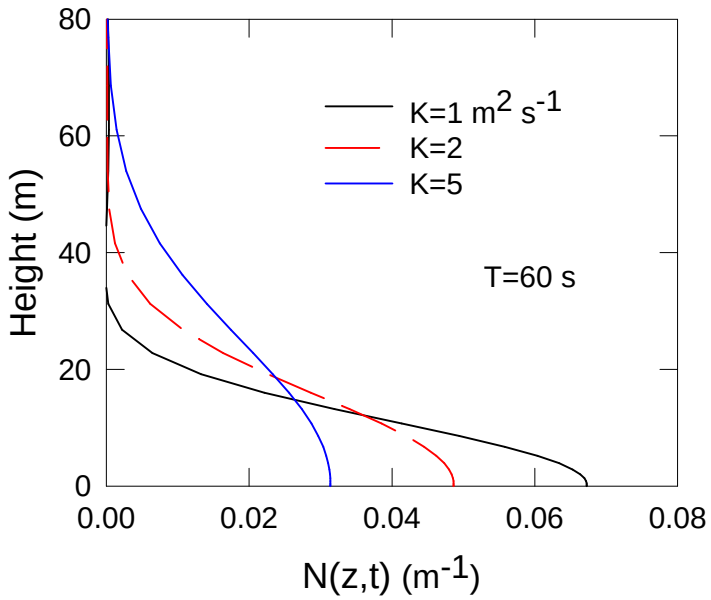

Figure 28. Concentration profile for single puff at 60 s for K=1, 2, and 5 m^2 s^{-1}.

The analysis given above assumes that the loss of particles is only due to surface deposition. Additional loss of particles will occur as a result of detrainment of the particles to the free troposphere at the top of the MBL, dilution due to subsidence, and loss by precipitation scavenging. These processes can have a large effect on the time constant for achieving equilibrium, especially at small radii where the deposition velocity is small. A more rigorous

treatment of the filling time constant and the effects of entrainment, subsidence and precipitation scavenging can be found in *Hoppel et al.* [2002, Eqs. (21), (24) and (26)].

III. Puff plumes with gravitational settling of particles (Cases 5, 6 and 7)

When the gravitational settling is included an additional flux term occurs, and the differential equation for the z component can be written as

$$\frac{\partial N}{\partial t} = \frac{\partial}{\partial z}\left(K(z)\frac{\partial N}{\partial z} \right) + \frac{\partial}{\partial z}\left(v_g N \right) \tag{31}$$

III. a. Surface boundary condition. A number of investigators [*Godson*, 1958; *Smith*, 1962] suggest that the appropriate surface boundary conditions for Eq. (31) can be written as

$$\left[K(z)\frac{dN}{dz} + v_g N \right]_{z=0} = v_d N(0,t) \tag{32}$$

where v_d is called the deposition velocity. We believe a more general expression for the boundary condition at the surface is that the net flux at any time is the difference in the gradient flux and the gravitational settling flux

$$\left[K(z)\frac{dN}{dz} + v_g N \right]_{z=0} = F_{net}(0,t) \tag{33}$$

The net flux at the surface is some function of time, but not limited to the same time dependence as the concentration. There is no reason to suspect that, in general, the time dependencies of the concentration and concentration gradient will be the same, as implied by Eq. (32). Eq. (32) would obviously be valid for the steady state. In the case where $K(z)=kz^n$ ($n>0$), $K(0)=0$ and v_d must be v_g. However when $v_g=0$, the only flux to the surface is the gradient flux and it is legitimate to impose the boundary condition

$$\left[K(z)\frac{dN}{dz} \right]_{z=0} = v_d N(0,t) \tag{34}$$

This forces the gradient to have the same time dependence as the concentration at the surface, and was the boundary condition used in Case 4 [Eq. (27)], and for the totally reflective case the surface gradient is zero. For the totally absorbing case the boundary condition was not a boundary condition on the flux, but rather the surface concentration was set equal to zero, leaving the gradient flux to be determined by the solution. {Note. We could let the surface be at some height $z=d$ or $K(z)$ have some residual at z=0 (i.e. $K(z)=kz+D$) to account for other surface-loss processes, but that would require a different solution (boundary conditions) than the one we are discussing.}

For the case when v_g *is not zero* a surface boundary condition is more difficult to specify, but we do not accept the convention given by Eq. (32) as the most general case. As will be apparent in what follows the net flux can be downward while the turbulent /gradient flux is upward opposing the gravitational settling. In other cases, such as total absorption at the surface, the gradient flux is downward reinforcing the gravitational settling. For Case 6 below, the solution for a linear eddy diffusion coefficient derived by *Rounds* [1955] is accepted and is stated by later authors to be the solution for the flux boundary condition given by Eq. (32) when $v_g=v_d$. However, for a linear diffusion coefficient which goes to zero at the surface, both Eqs. (32) and (33) require that v_g must equal v_d at the surface. As we will see, the time dependence of the concentration and concentration gradient are not the same. It may well be that Eq. (32), in general, over specifies the allowable boundary conditions by limiting both the concentration and gradient. For parabolic differential equations with open boundary conditions, specifying both the gradient and concentration over determines the solution (*Morse and Feshbach*, 1953, p. 706).

Case 5. Surface puff with constant K, $v_g>0$.

In the prior three cases we have neglected the gravitational settling of the particle. Any loss of particles at the surface due to settling, in the prior case, was simulated by a deposition velocity, but no gravitational effects within the body of the boundary layer were included. For larger particles the downward gravitationally induced flux is important as is the gravitationally induced vertical concentration gradients. The diffusion equation, similar to Eq. (2), for constant K and constant settling velocity v_g is

$$\frac{\partial n}{\partial t} = K_x \frac{\partial^2 n}{\partial x^2} + K_y \frac{\partial^2 n}{\partial y^2} + K_z \frac{\partial^2 n}{\partial z^2} + v_g \frac{\partial n}{\partial z} \tag{35}$$

where the horizontal wind speed is taken to be constant and the observer is moving with the mean wind speed (horizontal advection terms are zero). If the following substitution is made for *n* in Eq. (35)

$$n(x,y,z,t) = w(x,y,z,t) Exp\left\{ -\left(\frac{v_g z}{2K_z} \right) - \frac{v_g^2 t}{4K_z} \right\} \tag{36}$$

(*Frank and Mises* [1943]), Eq. (35) becomes

$$\frac{\partial w}{\partial t} = K_x \frac{\partial^2 w}{\partial^2 x} + K_y \frac{\partial^2 w}{\partial^2 y} + K_z \frac{\partial^2 w}{\partial^2 z} \tag{37}$$

This is the same as Equation (2) for which solutions have already been found in Cases 1 and 4. As in the prior cases we can separate out the horizontal dispersion and consider only the vertical dispersion

$$N(z,t) = w(z,t)Exp\left\{-\left(\frac{v_g z}{2K_z}\right) - \frac{v_g^2 t}{4K_z}\right\} \tag{38}$$

where, as before, *N(z,t)* is the total number of particles in a layer dz (particles per unit length obtained by integrating over the x-y plane).

In Eq. (38) *w(z,t)* can be the solution provided by Eq. (4) for the reflecting or totally absorbing surface, or Eq. (25) for a partially absorbing surface. In the limit as v_g goes to zero, the solution will the same as before and satisfy the original BCs. Each of the solutions for *w(z,t)* will give different surface boundary conditions for N(0,t) than for *w(z,t).*

For a reflecting surface discussed earlier in Case 1 the gradient of the concentration, $\partial w(z,t)/\partial z$, was zero at the surface. The reflective BC on the gradient of *w(z,t)* leads to the following BC on the surface gradient of *N(z,t).*

$$\left(\frac{\partial N(z,t)}{\partial z}\right)_{z=0}^{refl} = -\left(\frac{v_g}{2K_z}\right) w(0,t)Exp\left(\frac{-v_g^2 t}{4K_z}\right) = -\left(\frac{v_g}{2K_z}\right) N(0,t) \tag{39}$$

The surface gradient is no longer zero because the gradient is now being advected downward by gravitational settling.

In terms of deposition velocity referenced to the surface concentration, this BC implies that

$$v_d = \frac{-K_z\left(\frac{\partial N(z,t)}{\partial z}\right)_{z=0}^{refl} - v_g N(0,t)}{N(0,t)} = \frac{v_g}{2} - v_g = -\frac{v_g}{2} \tag{40}$$

The gradient flux at the surface is upward and equal to half the downward gravitational flux. The upward gradient flux at the surface is the result of constant K_z at the surface and necessary if there is a gravitationally induced gradient in particle concentration. The $+v_g/2$ part of the deposition velocity in Eq. (40) is the non-gravitational part of the deposition velocity and is analogous to the Brownian diffusion deposition in the case when K(z) goes to zero at the surface – only here the "diffusion" deposition is unreasonably large and the gradient is in a direction to oppose deposition not encourage it. If K_z went to zero at the surface, as it does in the atmosphere, then we would expect the deposition velocity referenced to the surface concentration to be just the settling velocity as given for the equilibrium case by *Hoppel et al.* [2005].

The above procedure of deriving the surface boundary condition by *assuming* the reflecting case when $v_g=0$ does not follow the usual convention of imposing a boundary condition and looking for the solution which satisfies that boundary condition. The difficulty in specifying the boundary condition is undoubtedly related to the boundary conditions allowable by a parabolic D.E. equation. We cannot specify independently both the concentration and the gradient. In the case with no gravitational settling, we specified only the concentration or the

gradient or, as in Eq. (27), a relationship between the two. Here we have specified the gradient as zero in the limit as v_g goes to zero. Once that choice has been made our options have been exhausted. In the next section where *K(z)* goes linearly to zero at the surface, only the gravitational flux is specified at the surface and we need not specify the gradient. This is probably the reason that those (*Rounds* [1955] and *Smith* [1962]) who have presented a general solution to the plume equation when $K(z)=kz^n$ and $v_g>0$ do not develop the case for $n=0$ even though it is logically the first step.

For simplicity we consider the case of the reflecting surface with source at the surface $h=0$, such that the equation for $w(z,t)$ is found from Eq. (4) as

$$w(z,t) = \frac{1}{\sqrt{pK_z t}} \exp\left(\frac{-z^2}{4K_z t}\right) \tag{41}$$

and (after completing the squares in the exponent) we find

$$N(z,t) = \frac{1}{\sqrt{pK_z t}} \exp\left(\frac{-\left(z+v_g t\right)^2}{4K_z t}\right) \tag{42}$$

where v_g is now positive downward.

The vertical gradient of N is just

$$\frac{\partial N(z,t)}{\partial z} = -\frac{2\left(z+v_g t\right)}{4K_z t} N(z,t) \tag{43}$$

The diffusion flux at the surface is

$$F_{diff}(0,t) = -K_z\left(\frac{\partial N}{\partial z}\right)_{z=0} = \frac{v_g}{2} N(0,t) \tag{44}$$

The total deposition flux is

$$F_{dep}(0,t) = -K_z\left(\frac{\partial N}{\partial z}\right)_{z=0} - v_g N(0,t) = \left(\frac{v_g}{2} - v_g\right) N(0,t) \tag{45}$$

As found in the more general case [Eq. (40)], the diffusion flux opposes the gravitational force and decreases the deposition velocity from v_g to $v_g/2$ when the deposition velocity is referenced to the concentration at the surface.

The concentration and vertical gradient are shown in Figures 29 and 30 as functions of height at 20, 40, 100, and 200 s for $K_z=1$ m^2 s^{-1} and $v_g=0.0125$ m s^{-1}, a fall velocity which corresponds to a unit density particles with radius of about 10 μm. The total flux

$$F(z,t) = -K_z\left(\frac{\partial N(z,t)}{\partial z}\right) - v_g N(z,t) \qquad (46)$$

crosses zero and is positive very near the surface. The gradient flux is always upward; it is the gravitational flux that causes the flux to be downward at the surface. (Only the gradient – negative of the gradient flux – is shown in Figure 30).

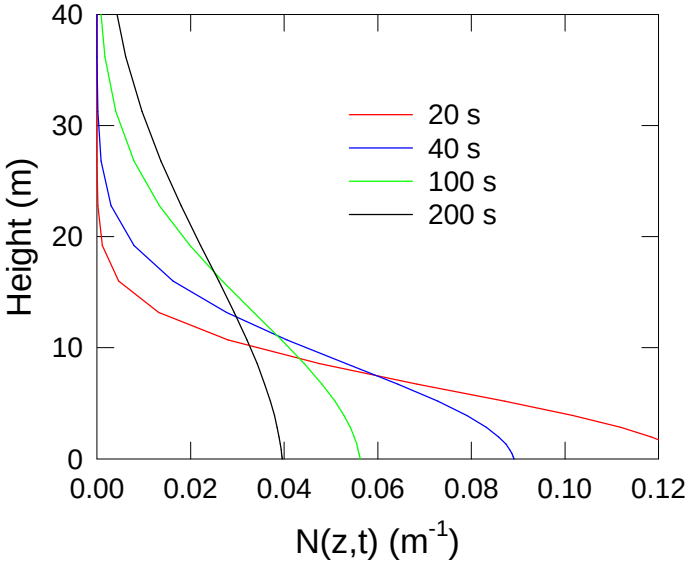

Figure 29. Vertical profile of concentration at 20, 40, 1000 and 200 seconds for $K_z=1$ m^2 s^{-1} and $v_g=0.0125$ m s^{-1}.

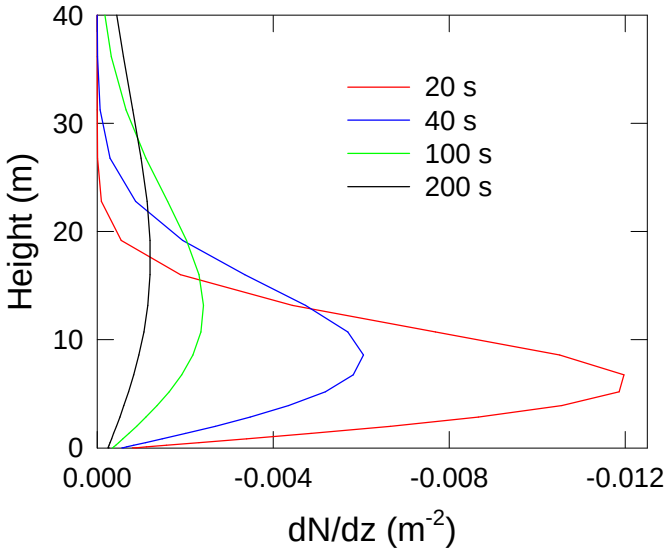

Figure 30. The concentration gradient as function of height at 20, 40, 100 and 200 seconds for $K_z=1$ m^2 s^{-1} and $v_g=0.0125$ m s^{-1}.

The height at which the net flux changes direction, is shown in Figure 31 as a function of time. For a single puff it takes about 10 minutes for the flux to be downward at all heights below 7 meters.

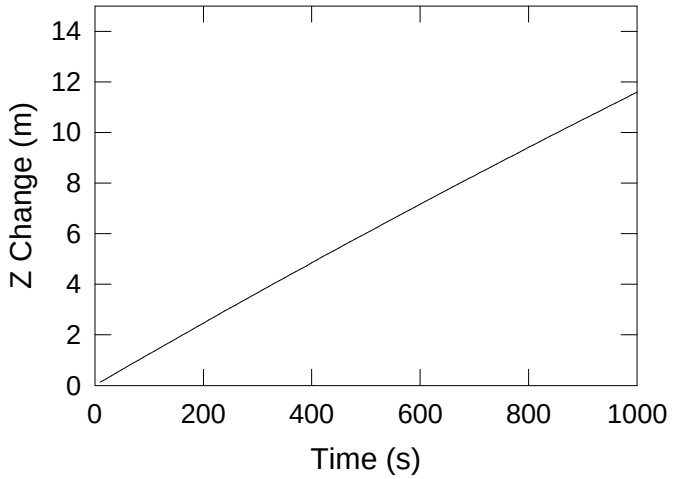

Figure 31. Height at which the flux changes from downward to upward as a function of time for $K_z=1$ m^2 s^{-1} and $v_g=0.0125$ m s^{-1}.

Integration of the flux evaluated *at the surface* from time zero to time t, gives the error function. So that the total integrated flux at time t is

$$FI(0,t) = 1 - \int_0^t F_{dep}(0,t)dt = 1 + Err\left(\sqrt{\frac{v_g^2 t}{4K_z}}\right) - 2Err\left(\sqrt{\frac{v_g^2 t}{4K_z}}\right) = 1 - Err\left(\sqrt{\frac{v_g^2 t}{4K_z}}\right) \quad (47)$$

where we have written out the two error function terms to indicate that the first error term relates to the upward "gravitationally-induced" gradient flux and the second accounts for the gravitational settling term. *FI(0,t),* the number of particles above the surface, is initially unity and goes to zero when all the particles are re-deposited and is shown by the dashed light blue line in Figure 32. Also at z=0

$$FI_{dep}(0,t) = -\frac{v_g}{2} NI(0,t) \quad (48)$$

where $NI(0,t)$ is the time integrated value of the surface concentration.

The above analysis is for the flux at z=0. The fluxes can be evaluated at any height at which we wish to calculate the upward and downward fluxes. In some cases it may be of interest to consider the fluxes at the midpoint of the bottom cell of a numerical model. The net integrated flux at z=2 m, found by numerical integration of Eq. (46) is shown in Figure 32 by the solid line for values of the parameters given above. The fact that integrated flux does not reach unity is due to the gravitational settling of particles so that they do not reach the 2 m level. Also shown by dotted lines are the integrated gradient flux and integrated gravitational flux (these are, of course, mathematical terms not real fluxes). The gradient flux opposes the gravitational flux even

during the dissipation phase. The fact that the integrated gravitational and diffusive fluxes are greater than unity results from the fact that the particles are, in effect, being re-suspended by the upward diffusive force at the surface. We have expanded the time scale by using a logarithmic scale to show that all particles eventually fall out; in this case (open system) that requires over a day. However in reality many additional white caps will be encountered during that time period. The integrated depositional flux, found by using a deposition velocity $v_g/2$, is the difference between the integrated flux (particles above z) and the total number provided by the puff as indicated by the arrow in Figure 32.

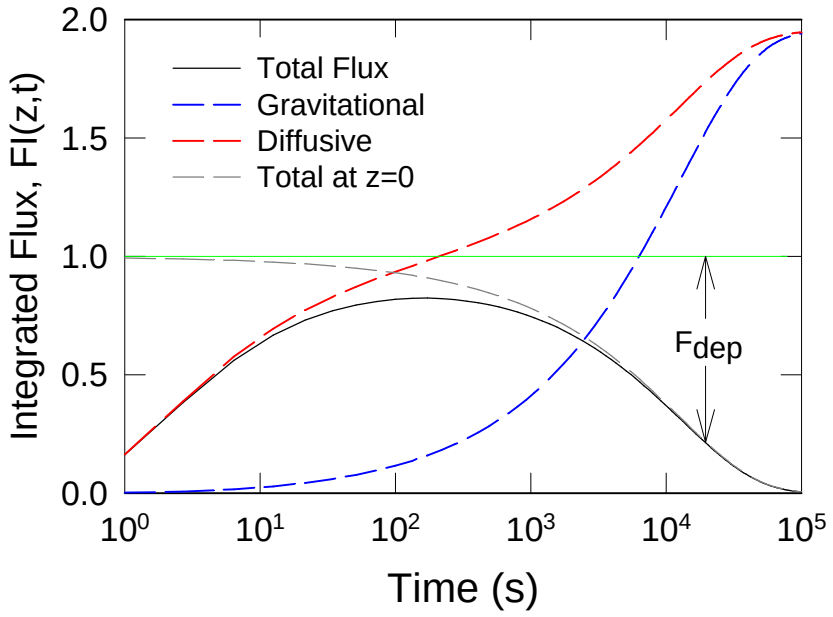

Figure 32. Time integrated flux at *z=2* m from time zero to time t for v_g=0.0125 m s^{-1} is shown by the black line and by the grey dashed line for *z=0*. Red and blue dotted lines are the integrated gradient and gravitational fluxes at z=2 m.

The integrated values of net flux calculated from Equation (48) summed over 500 puffs separated by time intervals of 20, 40 and 100 seconds is shown in Figure 33. The integrated net flux in Figure 33 is shown as a function of the number of puffs not as function of time. The difference in the total integrated flux at the end point is due to the loss between puffs, the longer the interval between puffs the greater is the loss. (Since these are unit puffs a line with slope of one (dashed line) would represent no loss.) The integrated flux for 10 s and 100 s puff separation is about 55% and 22% that for the case where there is no loss. The total time for 500 puffs separated by 20 s is 5000 s (~2.8 h) whereas the total time for 500 puffs separated by 100 s is 50,000 s (~14 h). The results shown are a strong function of the particle size, and we emphasize that the results shown here are for a particle of radius of about 10 μm radius and unit density. When the curves become horizontal equilibrium has been achieved and the downward gravitational flux is just equal to the upward flux provided by the additional puff.

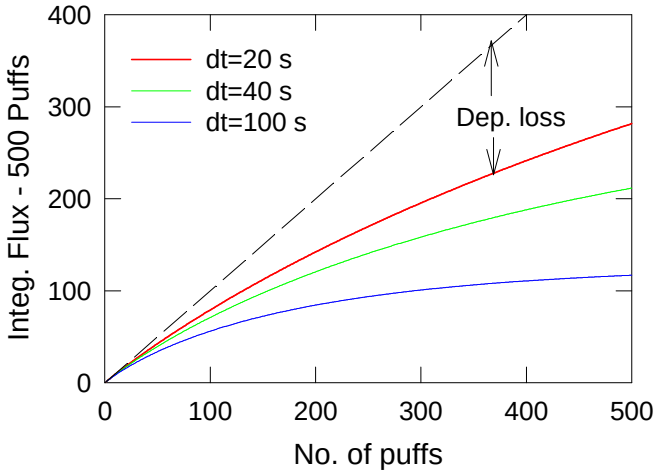

Figure 33. Time integrated flux from 500 puffs separated by 20, 40, and 100 seconds at z=0.

The average net flux at any point is the slope of the integrated flux plotted as a *function of time* (not of m as plotted in Figure 33). The average net flux (between puffs m and m+1) is shown in Figure 34 as a function of the number of puffs. The decrease in the flux as the time interval increases is a result of the lower frequency of puffs and the surface loss between puffs. The average (total) flux goes to zero at long times as equilibrium between the upward gradient flux is balanced by the downward gravitational flux (steady state). This is much different than the Case 4 where the settling velocity was simulated by including it in the deposition velocity but not included in the differential equation. In both cases the total flux goes to zero at long times (indicating equilibrium). *In this case the total flux goes to zero because the upward gradient flux equals the downward gravitational flux. In the former case the flux went to zero because the gradient flux approached zero.*

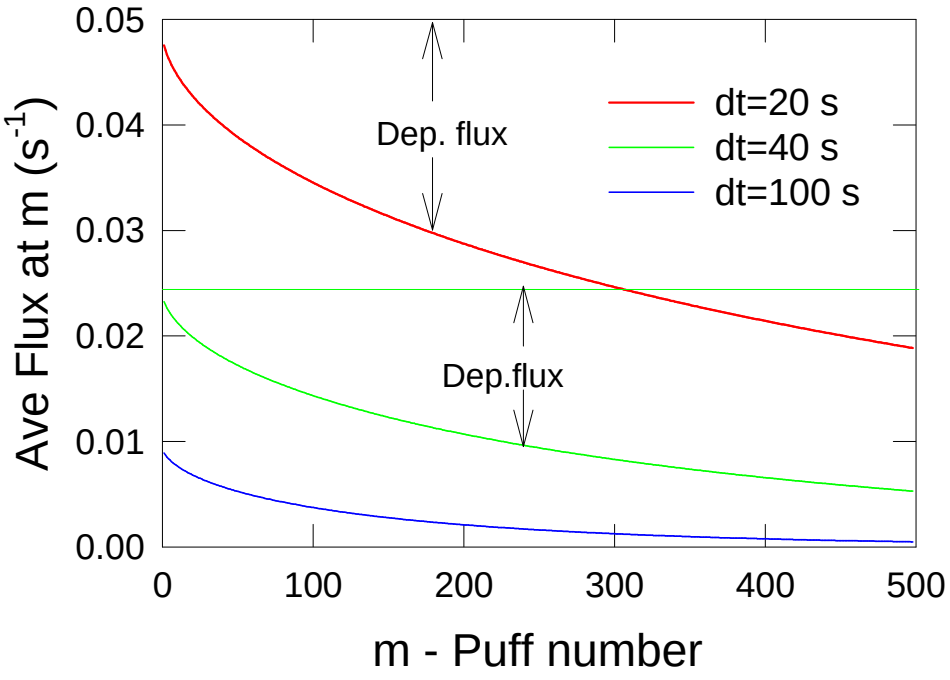

Figure 34. Average net flux as a function of the number of puffs for puff intervals of 20, 40, and 100 seconds. The horizontal lines are the average flux if there were no surface deposition for puff intervals of 20 and 40 seconds.

The curves in Figures 33 and 34 may be better understood in terms of the definitions given in Table 1, which may be written here as

$$FIS(0, M\Delta t) = M - \sum_{m=1}^{M} \left(FI_{dep}(0, m\Delta t) \right) \tag{49}$$

and

$$SI(0, M\Delta t) = \frac{1}{\Delta t} - \frac{FI_{dep}(0, M\Delta t)}{\Delta t} = S_{puff} - \frac{v_g}{2} \frac{NI(0, M\Delta t)}{\Delta t} \tag{50}$$

where S_{puff} is just the source strength of a unit puff and at equilibrium SI goes to zero and the source strength is obtained from the average concentration *NI/Dt* between puffs M-1 and M (or at time MΔt).

Figure 35 shows the vertical concentration profile after 50, 200, 400, and 800 puffs where the puff separation is 40 seconds. The time for 400 and 800 puffs is about 16,000 s (4.4 hrs) and 32,000 s (8.8 hrs) respectively, where the concentrations are about at their equilibrium value, where the upward gradient flux and downward gravitational fluxes are equal. The time constant for a well-mixed column of height H to come to equilibrium is estimated in to be about $t = H / v_g = 100 / 0.0125 = 8000 s$, somewhat less (but same order of magnitude) as that found

here. Also shown is the steady-state profile for a uniform surface source, arbitrarily normalized to 4 at the surface.

$$N_{ss} = 4.0 Exp\left(\frac{-v_g z}{K}\right) \tag{51}$$

During the filling process the profiles are in a quasi steady state where the shape of the vertical profile remains nearly constant during the transient filling process.

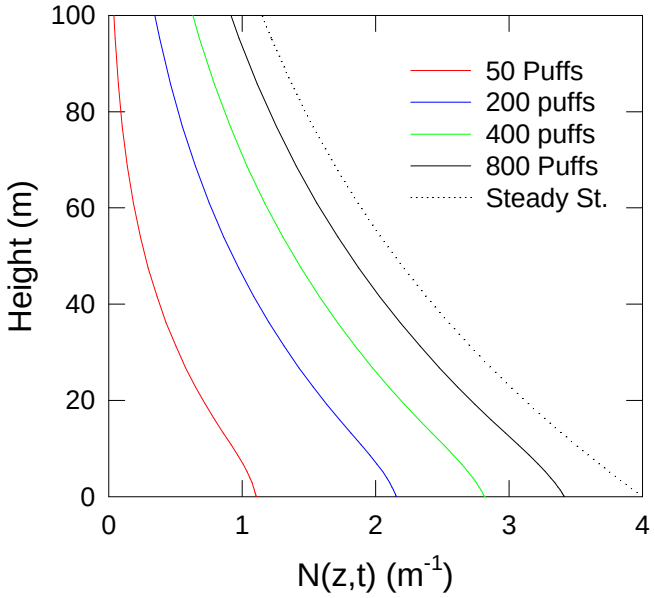

Figure 35. Concentration as a function of height after 50, 200, 400, and 800 puffs separated by 40 s. Corresponding end times of 2000, 8000, 16,000 and 32,000 s (4.5 hour). Also shown is the shape of the steady-state profile normalize to a concentration of 4 at the surface.

Unlike Cases 1 and 2 where the only allowable flux is a gradient flux, here the total integrated flux can be divided into two opposing fluxes. The blue curve in Figure 36 gives the integrated upward flux (solid blue line) and the dashed blue line the downward gravitational flux for puff intervals of 100 seconds. The difference in the two curves corresponds to the bottom curve of Figure 33; the net flux. Similarly, the red curves correspond to puff intervals of 10 seconds and the difference gives the upper curve of Figure 33. The magnitude of the curves are considerably larger than for the net flux shown in Figure 33. This is consistent with the integrated flux for a single puff shown in Figure 32.

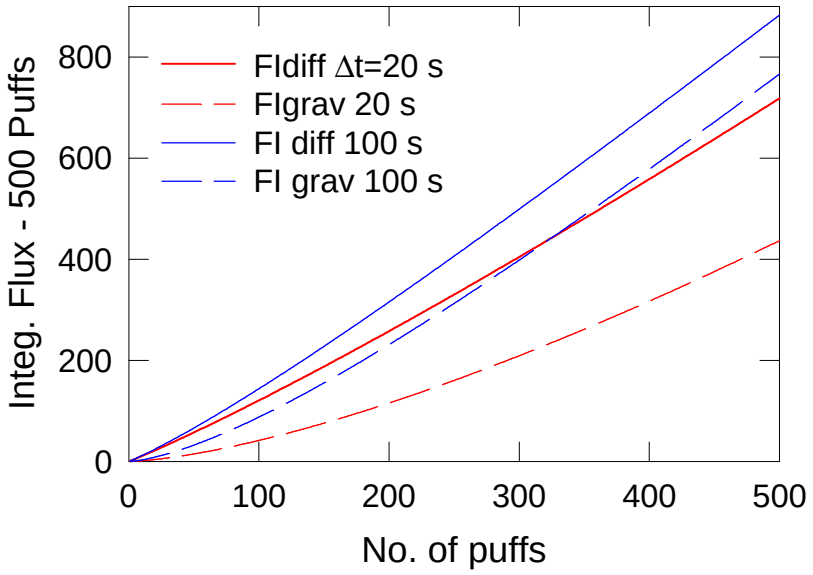

Figure 36. Integrated upward flux (solid lines) at the surface for 20 s (red) and 100 s (blue) puff separations. The dashed lines are the corresponding downward gravitational fluxes (at z=0).

In large-scale numerical models where the source of particles and deposition are calculated explicitly within the model, it is appropriate to *input the average upward flux as the source* at some average height of the lowest cell and let the model calculate the gravitational (surface) deposition and exchange with the cells above. Figure 37 shows the time average upward flux (source) as a function of the number of puffs for puff separations of 20, 40, 100 and 200 seconds (time derivative of the solid curves in Figure 36). The upward flux is nearly constant after about 40 to 60 minutes. The upward diffusion (source) flux includes the effect of a "re-suspension" diffusive force which opposes the gravitational deposition. A measurement of the diffusive flux would include this effect which reduces the effective deposition velocity by $v_g/2$. The corresponding loss from that cell due to downward flux would then be v_g (not $v_g/2$) and the average net flux (Figure 34) goes to zero as equilibrium is approached. On the other hand if there was a measurement of the average diffusion flux and the concentration, the average source strength of the puffs themselves could be calculated at any point in time by subtracting $N(0,t) \cdot v_g / 2$ from the diffusion flux. For example, the difference in the solid red curve and the red dotted line in Figure 37 is $N(0,t) \cdot v_g / 2$. Here the factor $v_g/2$ is related to the fact that $v_g/2$ is the non-gravitational part of the deposition velocity. The horizontal red dotted line (at 0.05 is the effective source strength of the puff (unit puff per 20 second). This is true at any point in time during the approach to equilibrium. After equilibrium has been achieved, only the concentration is required to obtain the source $N(0,\infty) \cdot v_g / 2$, where here the factor $v_g/2$ is related to the fact that $v_g/2$ is the gravitational part of the deposition velocity. The analysis here is all for a height of $z=0$ and no adjustment is made for gradients which may exist between the surface and the center of the lowest cell in a model. We emphasize this is different than the usual case where

K(z) goes to zero at the surface and the deposition velocity is v_g as in *Hoppel et al.* [2002, 2005].

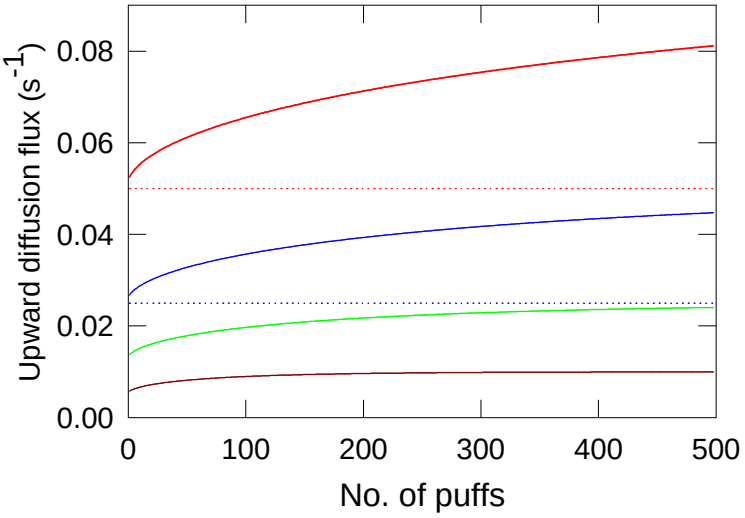

Figure 37. Average upward diffusive flux at the surface (excluding gravitational flux) as function of the number of puffs with puff intervals of 20, 40, 100, and 200 seconds. Dotted lines are the source resulting from the sum of the puffs.

If it is assumed that the surface source is uniform, the differential equation for the steady state can be written as

$$K\frac{dN(z)}{dz} = -v_g N(z) \qquad (52)$$

This equation implies that, at equilibrium the deposition velocity is v_g, and the solution can be written as

$$N(z) = N(0)Exp(\frac{-v_g}{K}z) \qquad (53)$$

By contrast, if we have a sufficiently long series of puffs such that there is an equilibrium, *in an average sense*, between the source of particles from the series of puffs and the gravitational fall out, the net deposition velocity is $v_g/2$ not v_g. As illustrated in Figure 35 the shape of the vertical profile is that given by of the equilibrium profile (and not that given by Eq. (53) with v_g replaced by $v_g/2$.) This paradoxical behavior is difficult to understand. However for a puff or series of puffs no equilibrium solution exists; i.e., an unbounded region can never be filled. It is interesting to note that the effective deposition velocity for the case where there is both gravitational settling and diffusive transport to a surface from an infinite region above the surface, initially uniformly filled with particles is also $v_g/2$ (*Fuchs* [1964], pp. 197-198). In this regard Fuch's states: "…deposition consists of a diffusive deposition which occurs in the absence of settling and half the sedimentation which would occur in the absence of diffusion.

This example shows clearly that serious errors may result …… by simply summing the individual effects of each."

Since the diffusion at the surface gives rise to a non-gravitational component of the deposition velocity it is tempting to liken it to the non-gravitational part of the deposition velocity for the conventional case of deposition when the source is from above, where there is both a gravitational and non-gravitational component, v_a, resulting from Brownian diffusion and impaction at the surface expressed as

$$F_{dep} = \left(- v_a - v_g \right) N_0 \tag{54}$$

This is not a good analogy because here $v_a = - v_g/2$. The negative deposition velocity is actually a force which suspends the particles, not a deposition force. However there is an important similarity, in that, the effect of the non-gravitational boundary flux at the surface is carried in the diffusion flux above the surface.

In summary, this case where the turbulent diffusion coefficient is assumed to be constant with altitude gives rise to a large 're-suspension force' at the surface for large particles which does not exist in the atmosphere. This boundary condition effects the diffusive flux throughout the MBL and would predict a larger diffusive flux than actually exists.

Case 6. Puff plume with gravitational settling of particles; *K(z)=cz*, source at *z=h*

Solutions to the turbulent diffusion equation with gravitational settling and turbulent mixing increasing with height as some power of *z* are discussed by *Rounds* [1955], *Godson* [1958], and *Smith* [1962]. While the solutions given are for a continuous line source, the solution for a puff plume can be obtained by considering the downwind coordinate as the time coordinate, as discussed earlier. Of particular interest is the linearly increasing eddy mixing coefficients given by $K(z)=cz$. For neutrally stable conditions $c = ku_*$ where κ is von Karman's constant and u_* is the wind-dependent friction velocity. In this case the only deposition at the surface is that due to gravitational settling. Equation (33) {and, for this case, also Eq. (32)} requires the surface deposition velocity to be v_g. The boundary condition at the surface (z=0) is then

$$\underset{z \to 0}{Limit} \left[c\, z \left(\frac{\partial N}{\partial z} \right) \right] = 0 \tag{55}$$

for any finite value of the surface gradient.

The solution to Eq. (31) with this boundary condition is given by *Rounds* [1955] (Also Case v of *Smith* [1962]). After assuming the wind profile is constant with height and converting the downwind coordinate to a time coordinate, Rounds solution can be written as

$$N(t,z) = \left(\frac{1}{ct} \right) \left(\frac{h}{z} \right)^{\frac{u}{2}} Exp\left[\frac{-(z+h))}{ct} \right] I_u \left(\frac{2\sqrt{hz}}{ct} \right) \tag{56}$$

where $\nu = v_g / c$, h is the height at which the puff is injected at $t=0$, and $I_u(y)$ is the modified Bessel function of order ν. For particles smaller than 20 μm and wind speeds less than the order of 10 m s^{-1}, the order of the Bessel function, ν, will be a small fraction. As in the prior cases, the lateral and longitudinal dispersion about the centroid is taken to be Gaussian ($K_{x,y}$=constant). The concentration as a function of height is shown by the solid lines in Figure 38 for time of 20, 50 and 100 seconds; χ=0.16 m s^{-1}, v_g=1.25x10^{-2} m s^{-1} and ν=0.079, corresponding roughly to 10 m s^{-1} wind speed and 10 μm radius particles. The source height is taken to be h=0.2 m.

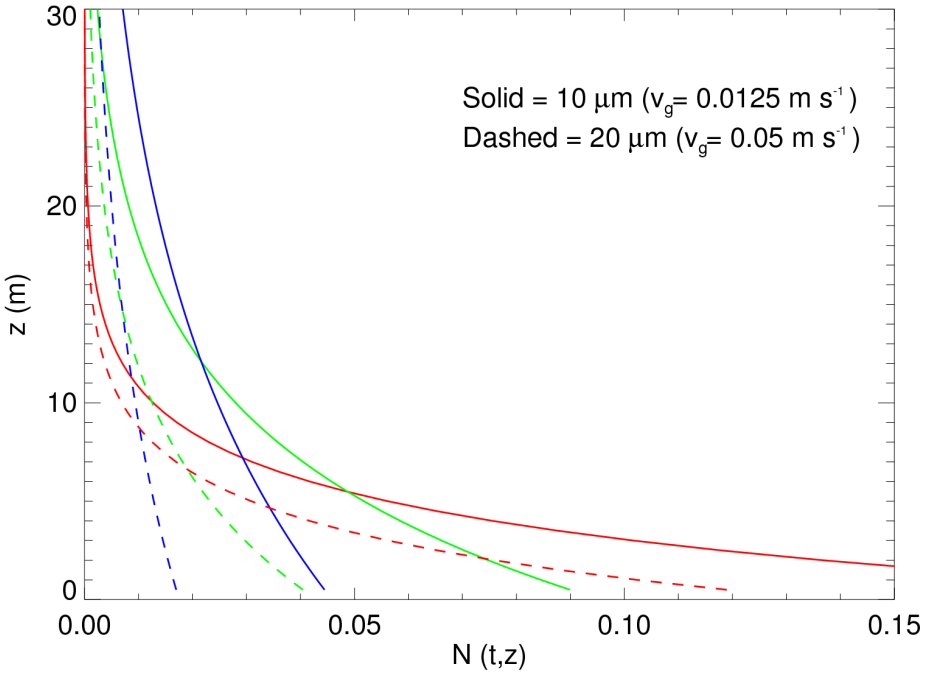

Figure 38. Solid curves are concentration as a function of height at times of 20, 50 and 100 seconds for 10 μm radius particles; dashed lines are for 20 μm radius particles.

The solid lines of Figure 38 can be compared to Figure 29 for constant K (and h=0). Here the particle concentrations are initially greater near the surface because of the lower turbulent mixing near the surface but once the particles reach higher altitudes they are rapidly mixed to even higher altitudes because of the linearly increasing value of the turbulent mixing coefficient. The dashed lines give the concentration profiles for 20 μm radius particles (v_g=0.05 cm s^{-1}) under the same conditions and illustrates the effect of more severe gravitational settling on the concentration profile.

At the surface the deposition flux is only due to the gravitational settling and can be expressed as

$$F_d(0,t) = v_g N(t,0) = \frac{v_g Exp\left(\frac{-h}{ct}\right)}{c\,t\,\Gamma\left(\frac{v_g}{c}+1\right)}\left(\frac{h}{ct}\right)^{\frac{v_g}{k}} \qquad (57)$$

Equation (57) can be integrated to give the accumulated deposition from time t=0 to t=τ when z=0

$$FI_d(t) = \int_0^t F_d(t)dt = \frac{\Gamma\left(\frac{v_g}{c}, \frac{h}{ct}\right)}{\Gamma\left(\frac{v_g}{c}\right)} \qquad (58)$$

where $\Gamma(x, y)$ is the incomplete gamma function and $\Gamma(x)$ is the complete gamma function. Since $\Gamma(x,0) = \Gamma(x)$, all particles eventually get re-deposited on the surface but because mixing increases indefinitely with height, the time to complete the deposition become unrealistically long. In the real atmosphere the MBL is capped at some height. The net integrated source from t=0 to t=τ must include the initial unit puff source and is given by $FI(0,t) = 1 - FI_d(t)$. $FI(0,t)$ is shown by the solid lines in Figure 39 for particles of about 4 μm (red), 10 (blue), and 20 μm (black) injected at 0.2 m and where χ=0.16 (corresponding to about 10 m s^{-1} wind speed). As pointed out earlier the curves give the fraction of the particles which remain suspended at time τ. For comparison, the dashed lines show the net flux for a constant K=1 m^2 s^{-1}. The initial deposition for the linear case is greater because the upward mixing at the injection height is much less than for a constant K. However at longer times, particles mixed to very high altitudes by the linearly increasing eddy mixing take much longer to be re-deposited and the curves for K=constant eventually cross over those for the linear case.

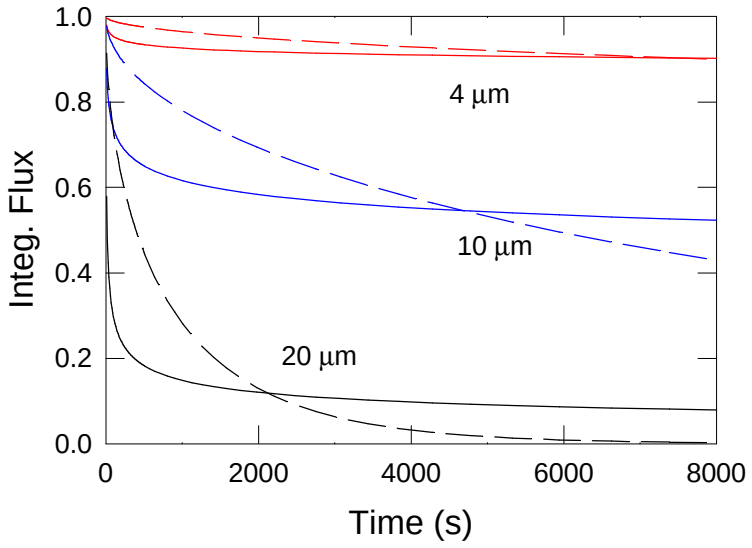

Figure 39. Net integrated flux, *FI(z,t)*, as a function of time for a single puff. Solid lines are for linear K(z)=χz, for particle radii of 4 μm (red), 10 μm (blue) and 20 μm. Dashed lines are for K=1 m^2 s^{-1}.

The net integrated surface source flux given above is an approximation because the puff is introduced at the a height $z=h$, and the deposition is at z=0. In fact, a surface puff source is incompatible with a K(z) which goes to zero at the surface, because there is no mechanism by which particles at the surface can be mixed upward from z=0. The net flux at heights above the surface will consist of both a gradient flux and gravitational flux and any upward gradient flux will act as the source at the given height. After considerable algebra the net flux through a plane at height z is found to be

$$-F(t,z) = cz\left(\frac{\partial N}{\partial z}\right) + v_g N = \left\{\frac{z}{t}\left[\left(\frac{h}{z}\right)^{\frac{1}{2}} \frac{I_{u+1}(y)}{I_u(y)} - 1\right] + v_g\right\} N(t,z) \qquad (59)$$

where $y = \dfrac{2\sqrt{hz}}{ct}$.

The flux as a function of time at 2 m height for a source at a height of 0.2 m is shown in Figure 40 by the solid black line for 10 μm radius particles; the solid green and red lines show the gradient and gravitational components of the flux. There is a strong upward gradient pulse during the first 20 seconds or so. At longer times the gravitational component dominates. The dashed lines are for 20 μm radius particles and illustrates the loss resulting from increased gravitational settling.

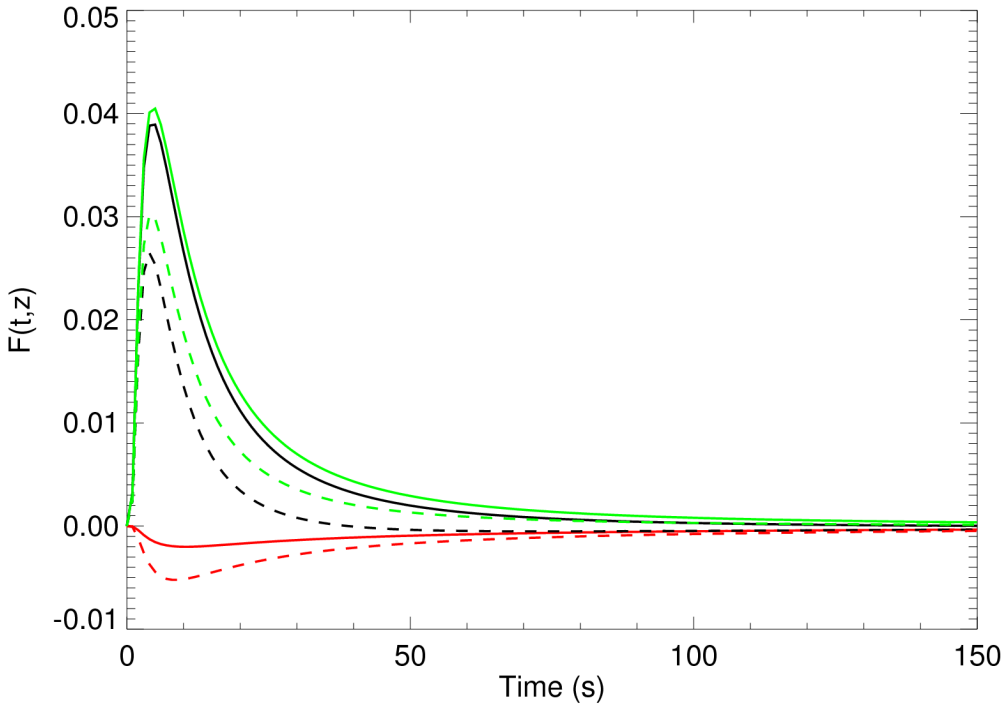

Figure 40. The black curve is the flux at 2 meters due to a single puff introduced at 0.2 meters. The green line is the upward gradient flux and the red line is the downward gravitational

flux. Solid lines are for 10 μm radius particles and dashed lines are for 20 μm radius particles.

Figure 41 gives the integration of the flux through the plane at 2 m shown in Figure 40 over a greatly expanded time span for 10 μm radius particles. The integrated total flux (black curve) is initially dominated by the upward gradient flux (shown in green) and reaches a maximum at about 100 seconds, after which, there is a slow decrease driven by gravitational settling. Beyond several hundred seconds the curves are similar to those shown in Figure 39 on a linear plot. The maximum integrated flux reaches a value of about 0.7, indicating that about 70% of the 10 μm particles penetrate the 2 m level before settling back to the surface. Contrasting Figure 41 with 32 shows that the initial pulse at 2 m is delayed because of the much smaller mixing coefficient below about 5 m for the linear case. However, particles that are dispersed to higher altitudes take an inordinate amount of time to be re-deposited because of the extremely large mixing coefficients encountered at higher altitudes. The total flux will eventually go to zero indicating that an equilibrium can exist for a series of puffs where the gravitational fallout between puffs will equal the input from the additional puff. (Since this is an open system equilibrium will never totally be achieved.) The integrated diffusive flux reaches its asymptotic value much sooner than does the integrated gravitational flux. This is also seen for constant K in Figure 32.

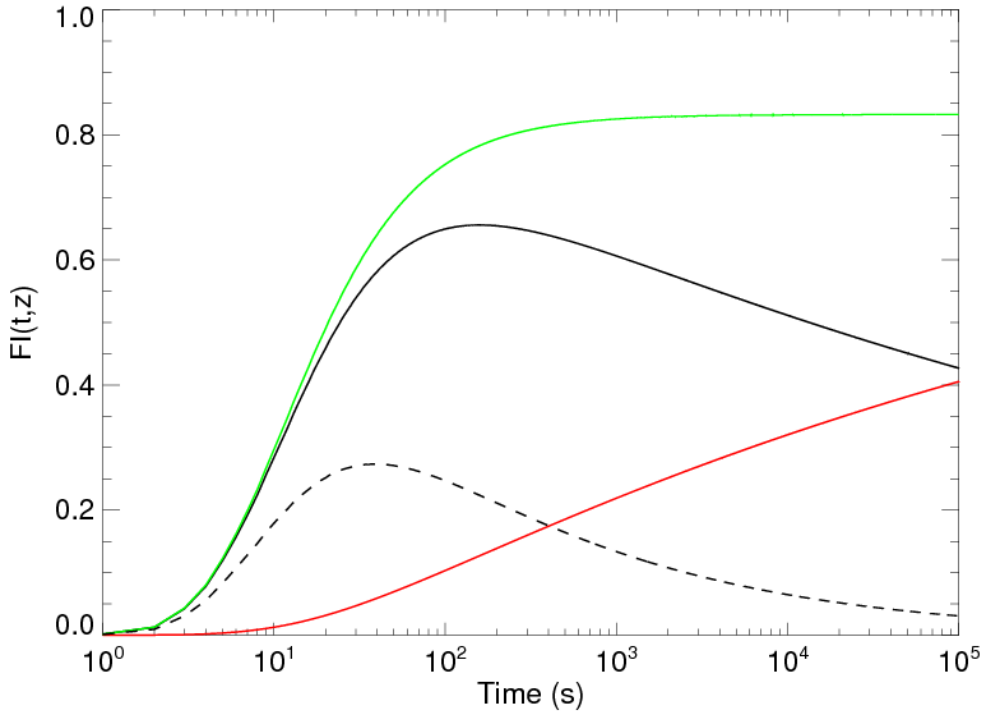

Figure 41. The integrated flux (integration of the Flux shown in Figure 40) from time zero to time t for 10 μm radius particles for a single puff at 2 meters. The solid black curve is the total integrated flux and the green and red are the integrated gradient and gravitational flux respectively. The black curve can be interpreted as the fraction of particles above 2 meters. Compare to Figure 32 for constant K. The dashed black line is for particles of 20 μm radius.

Lastly we need to consider the effects of many puffs on the integrated flux penetrating a plane at which we wish to define as the height of the source function. Figure 42 illustrates the increasing concentration as a function of height for a series of 25, 100, and 400 puffs separated by 40 seconds. Solid lines are for 10 μm radius particles and dashed lines are for 20 μm radius particles and illustrates the effect of size on loss and on the vertical profile of the concentration.

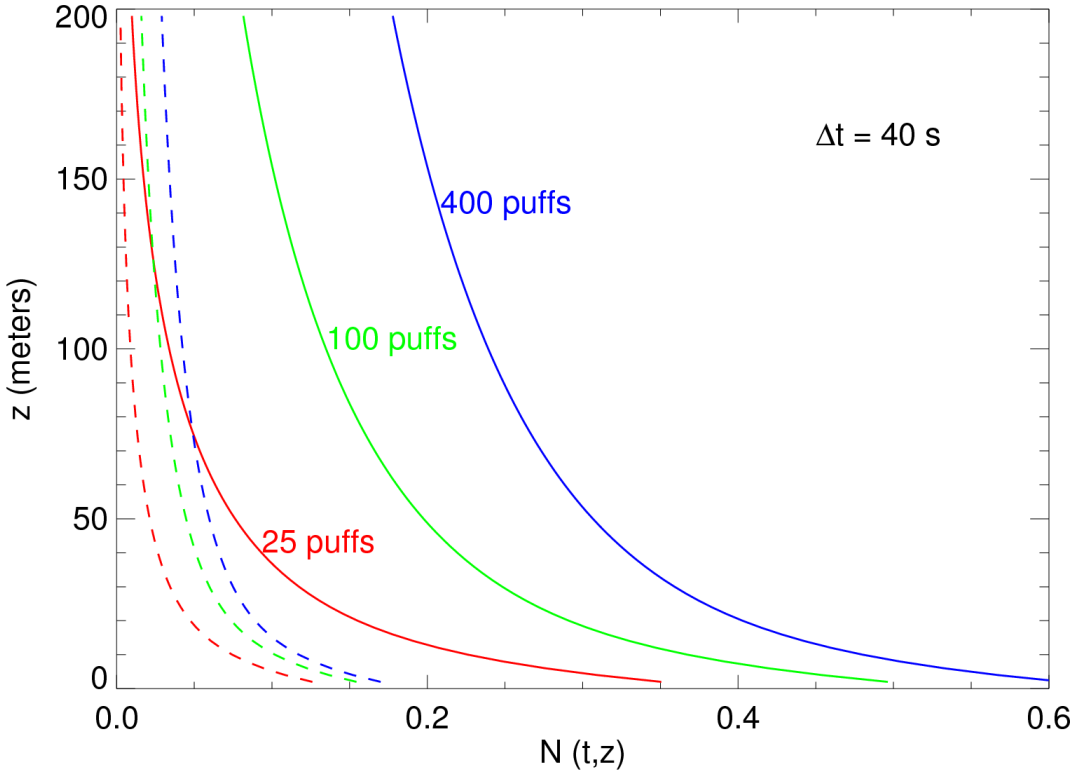

Figure 42. Profile of concentration resulting from 25, 100 and 400 puffs separated by 40 seconds. Solid lines are for 10 μm radius particles and dashed lines are for 20 μm radius particles.

The integrated flux (as before) is given by

$$FIS(z,M\Delta t)=\sum_{n=1}^{M} FI(z,n\Delta t)=\sum_{n=1}^{M}\int_{0}^{t=n\Delta t} F(z,t)dt \qquad (60)$$

where the integral is what is shown in Figure 41. Figure 43 shows *FIS(z,MDt)* for a series of 500 puffs separated by 10 (red), 20, 50 and 100 seconds as a function of the number of puffs (total time is *Dt* times the number of puffs). The loss is greater when the time between puffs is greater. Figure 43 can be compared to Figure 33 for constant K(z). The loss is greater in Figure 44 especially at shorter time periods; the different in the two figures is explained by the different

K(z) employed in the two cases as mentioned above. The broken lines give the gradient and gravitational components for Δt=100 s and the difference is just the net curve for Δt=100 s.

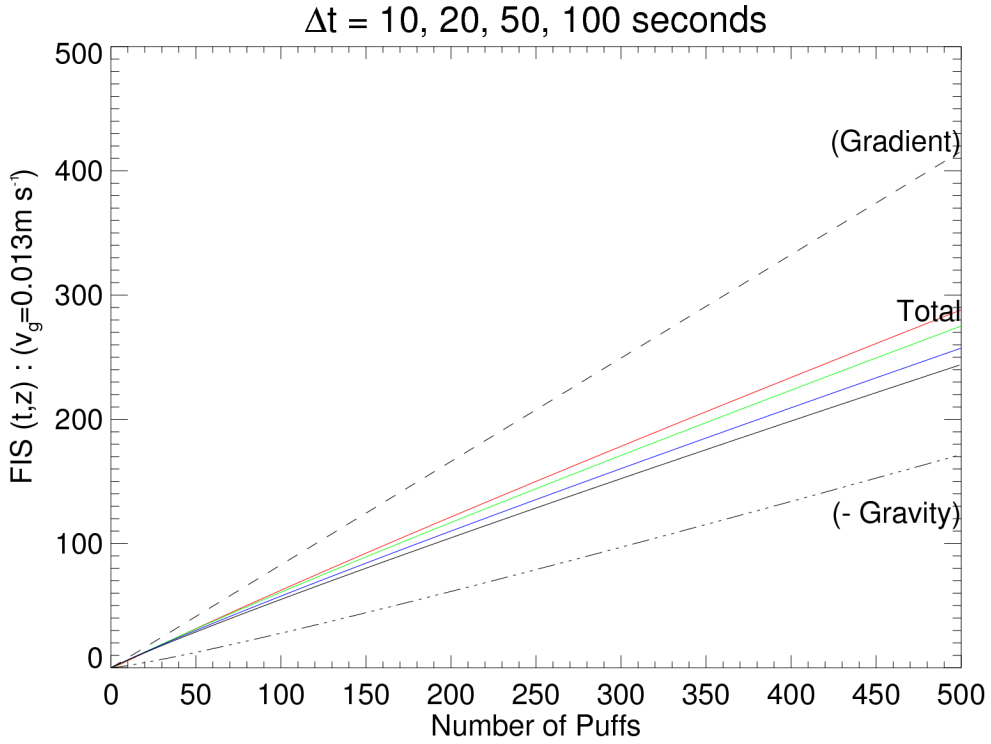

Figure 43. Sum of the integrated puffs as a function of the number of puffs for *Dt* = 10, 20, 50 and 100 s. The solid lines are the net flux and the broken lines for the gradient and gravitational components for *Dt=100 s*.

The time derivative [Eq. (10)] of the curves in Figure 43 is the average flux. Figure 44 gives the average net flux at 2 m as a function of the number of puffs. The average net flux will continue to decrease with time until equilibrium is achieved. The unreasonable slow decrease seen in Figure 44 is a result of the linearly increasing diffusivity with height in the unbounded region above the surface. The horizontal line shows the puff source flux. Since some of the particles never reach 2 m and since at longer times the particles above are being redeposited, the number of particles above 2 m (integrated net flux) is smaller than the number introduced by the puffs.

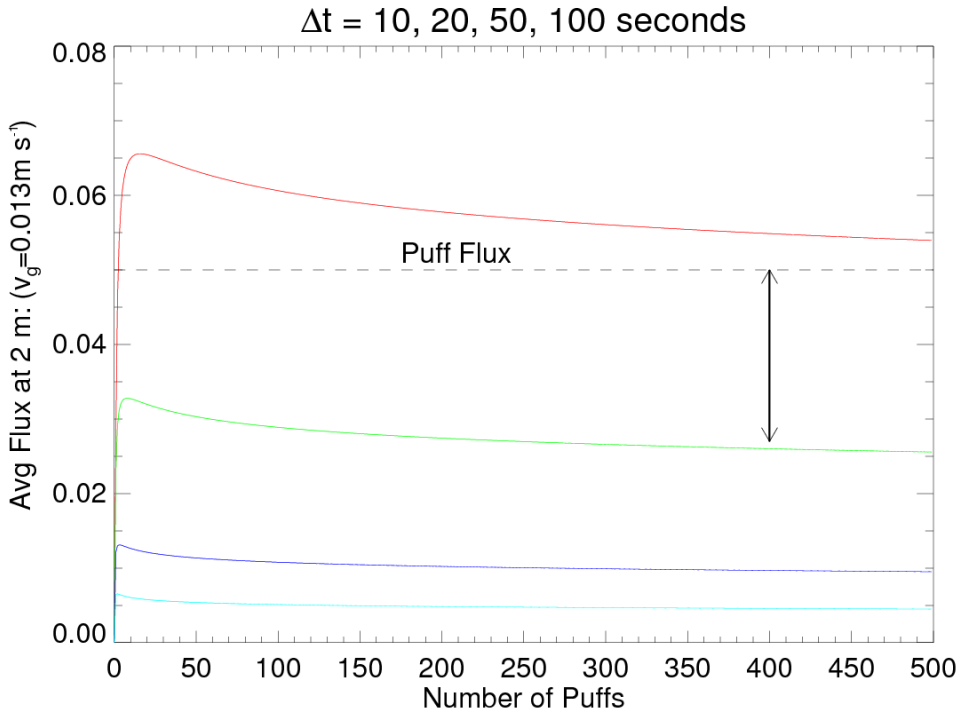

Figure 44. The average net flux (s^{-1}) at 2 m as a function of the number of puffs for puff separations of 10, 20, 50, and 100 s.

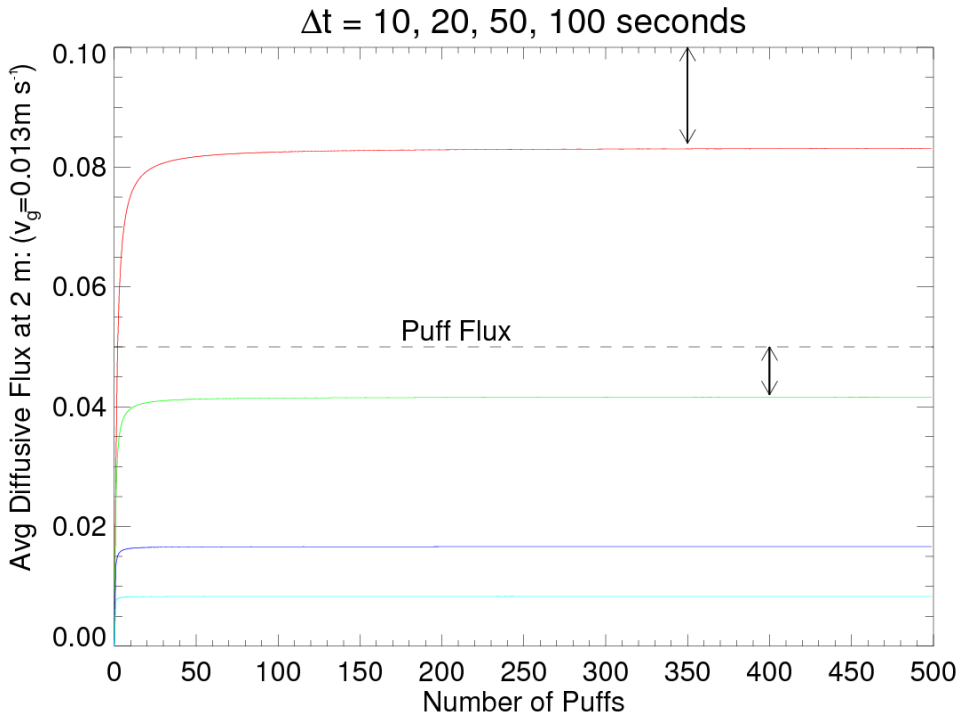

Figure 45. The average diffusive flux (s^{-1}) at 2 m as a function of the number of puffs for puff separations of 10, 20, 50, and 100 s.

Figure 45 is the average gradient flux at 2 m from a series of puffs at 0.2 m. The upward diffusive flux reaches a constant value rather quickly as indicated in Figure 41 for a single puff. The upward flux leads to a filling of the (infinite) region above 2 m as shown in Figure 42. Eventually the concentration will build up to the point where the average downward gravitational flux will equal the upward flux and an equilibrium will be achieved (in this case of an open system this would take an infinite amount of time). The upward gradient flux can be considered the source at 2 m; however, it is less than the puff source at 0.2 m. If we had a numerical model with the center of the lowest cell at 2 m, it would be appropriate to use the gradient source at the center as the surface source for the lowest height of the model and calculate the removal flux as the concentration at 2 m times v_g. If we knew the puff source we would have to lower the source at 2 m by about 17% as shown in Figure 45. This amount can be obtained from Figure 45.

We have not considered the important case where we have both gravitational settling and a non-gravitational deposition (such as impaction loss) at the surface. However Case 5, where the constant diffusivity at the surface gives rise to a non-gravitational flux at the surface, indicates that the relationship between the puff source flux and gradient flux is more involved than in either case separately.

Case 7. Puff plume with gravitational settling; *K(z)=cz*, MBL capped at *z=H*, and source at *z=h*.

During the preparation of this report it became clear that the prior two cases were too limited to give a reasonable representation of a puff plume in the MBL when gravitational settling was dominant. In Case 5 the constant diffusivity down to the surface gives rise to a large re-suspension force which does not exist in the MBL, where the turbulent diffusivity is very small at the surface. In Case 6, the unbounded domain in the vertical direction, coupled with a linearly increasing eddy diffusivity, mixes particles to great heights resulting in unreasonably long times for the particles mixed to higher altitudes to settle out. In the present case, we have capped the MBL so that there is no flux of particles through the top of the MBL at *z=H*.

The six prior cases were extensions of cases found in the literature. The analytical solution for this case has not, to our knowledge, appeared in the literature. The problem is identical to that of the prior case except here the MBL is capped and total flux at *z=H* is forced by the boundary conditions to be zero. The solution is now an eigenvalue problem and the solution is in terms of an infinite series of eigenfunctions – in this case, Bessel functions.

In the derivation that follows, the plume is introduced at a height *z=h*, the boundary layer extends to height *z=H* and the eddy diffusivity *K(z)* increases linearly throughout the boundary layer, as in previous cases:

$$K(z) = k u_* z = c z$$

As discussed in Section II.1, we consider only the concentration of particles N(z,t) in a layer dz after integrating over the horizontal plane. The differential equation can then be written as

$$\frac{\partial N(z,t)}{\partial t} = -\frac{\partial F(z,t)}{\partial z} \tag{61}$$

where

$$F(z,t) = -c\, z \frac{\partial N}{\partial t} - v_g N(z,t) \tag{62}$$

and v_g is the gravitational settling velocity and taken to be a positive number. Combining (61) and (62) gives

$$\frac{1}{c}\frac{\partial N}{\partial t} = z\frac{\partial^2 N}{\partial z^2} + (1+2n)\frac{\partial N}{\partial z} \qquad \text{where } n = \frac{v_g}{c} \tag{63}$$

If we make a change of variable $z = x^2$ Equation (63) becomes

$$\frac{4}{c}\frac{\partial N}{\partial t} = \frac{\partial^2 N}{\partial x^2} + \frac{(1+n)}{x}\frac{\partial N}{\partial x} \tag{64}$$

The following substitution can be made to separate the variables

$$N(x,t) = \frac{x^{-n}}{H^{\frac{-n}{2}}} X(x)T(t) \tag{65}$$

If the separation constant is chosen to be $-s^2/H$, then the solution for the time dependent part *T(t)* is

$$T(t) = T_0 Exp\left(\frac{-c\,s^2 t}{4H}\right) \tag{66}$$

The equation for *X(x)* is

$$x^2\frac{d^2X}{dx^2} + x\frac{dX}{dx} + \left(\frac{s^2}{H}x^2 - n^2\right)X = 0 \tag{67}$$

This is Bessel's equation for which the solution is

$$X(x) = c_1 J_n(s\,y) + c_2 J_{-n}(s\,y) \tag{68}$$

where we have set $y^2 = \frac{x^2}{H}\left(= \frac{z}{H}\right)$

and where J_n is the Bessel function. J_n and J_{-n} are linearly independent solutions provided ν is not an integer. If ν is and integer then J_{-n} must be replaced by Y_n, another Bessel (Weber) function.

The complete solution can then be written as

$$N(x,t) = y^{-n}\ c_1 J_n(s\ y)\, Exp\left(\frac{-c\,s^{2}t}{4H}\right) \tag{69}$$

where we have set c_2=0 because J_{-n} blows up at z=0 and T_0 has been incorporated into the constants.

The diffusion flux is given by

$$F_{diff}(z,t) = -c\,z\frac{\partial N}{\partial z} = -\frac{c}{2}\,y\frac{dN}{dy} \tag{70}$$

We can use the following relationship

$$\frac{\partial}{\partial x}\left[x^{-n} J_n(s\ x)\right] = x^{-n} J_n^{'}(s\ x) - n\ x^{-n-1} J_n(s\ x) = -x^{-n}\, s J_{n+1}(s\ x) \tag{71}$$

to evaluate (70), where the last step uses the recursion relationship for the derivative $J_n^{'}(s\ x)$ found in mathematical handbooks such as Abramowitz and Stegun (1964).

$$F_{diff}(y,t) = \frac{c}{2}\, y^{-n+1}\ s\ J_{n+1}(s\ y)\cdot Exp\left(\frac{-c\,s^{2}t}{4H}\right) \tag{72}$$

Since J_{n+1} goes to zero at z=0 the diffusion flux goes to zero and only the gravitational flux remains by which particles are deposited on the surface.

If we wanted the diffusion flux to go to zero at *z=H*, we would need to find the values of σ at which $J_{n+1}(s\ y) = 0$. These values, s_i^{n+1}, would determine the eigenfunction $J_n(s_i y)$ appropriate for the series solution. This would be the case for a problem with no fall velocity. Here we need to set the total flux to zero at *z=H*. The total flux is

$$F_{tot}(x,t) = \left[\frac{c}{2}\, y^{-n+1}\ s\ J_{n+1}(s\ y) - v_g y^{-n} J_n(s\ y)\right]\cdot T(t) \tag{73}$$

If the total flux is to be zero at z=H (x=1) at all times, then σ must satisfy the following equation

$$f(x) = xJ_{n+1}(x) - 2n\,J_n(x) = 0 \tag{74}$$

The roots of (74) determine the eigenvalues, σ_i , and the solution is given by the series

$$N(y,t) = y^{-n} \sum_{i=1}^{\infty} c_i J_n(s_i y)\, Exp\left(\frac{-c s_i^2 t}{4H}\right) \tag{75}$$

We have now to determine the c_i's from the initial conditions at *t=0*. We can represent our initial condition as a delta function source at height h at time *t=0*; i.e., $N_0\, d\,(z\text{-}h)$ at *t=0*. Rearranging (75), multiplying both sides by $y^{n+1} \cdot J_n(s_j y)$ and integrating over the interval *0<z<H* (or *0<y<1*) yields

$$\int_0^1 y^{n+1} N_0 d(y - y_0) J_n(s_j y) dy = \sum c_i \int_0^1 y \cdot J_n(s_i y) \cdot J_n(s_j y) dy \tag{76}$$

The orthogonality of the Bessel functions depends on the boundary conditions and the interval. The following relationship can be obtained from Abramowitz and Stegun (1964)

$$\int_0^1 y J_n(s_m y) \cdot J_n(s_n y) dy = \frac{1}{2s_n}\left(\frac{a^2}{b^2} + s_n^2 - n^2\right)(J_n(s_n))^2 \qquad \text{for } m=n \tag{77}$$

For $m \neq n$ the integral is zero. The constants a and b are determined by the boundary condition at *z=h* (*y=1*).

$$aJ_n(x) + bxJ_n'(x) = 0 \tag{78}$$

The boundary condition at y=1 is obtained from the bracketed expression in Eq. (73) in terms of the derivative of the Bessel function as

$$-\frac{c}{2}\left[nJ_n(s_i y) + y s_i J_n'(s_i y)\right] = 0 \tag{73b}$$

It is clear from (73b) that in our case, *a= n* and *b=1 (at y=1).* Therefore Eq. (76) yields

$$c_i = \frac{2y_0^{n+1} N_0 J_n(s_i y_0)}{J_n^2(s_i)} \tag{79}$$

and

$$\frac{N(y,t)}{N_0} = 2y_0\left(\frac{y}{y_0}\right)^{-n}\sum_{i=1}^{\infty}\frac{J_n(s_i y_0)\cdot J_n(s_i y)}{\left[J_n^2(s_i)\right]}\cdot Exp\left(\frac{-cs_i^2 t}{4H}\right) \tag{80}$$

or, in terms of the variable z

$$\frac{N(z,t)}{N_0} = 2\left(\frac{h}{H}\right)^{0.5}\left(\frac{z}{h}\right)^{-\frac{n}{2}}\sum_{i=1}^{\infty}\frac{J_n\left(s_i\sqrt{\frac{h}{H}}\right)\cdot J_n\left(s_i\sqrt{\frac{z}{H}}\right)}{\left[J_n^2(s_i)\right]}\cdot Exp\left(\frac{-cs_i^2 t}{4H}\right) \tag{81}$$

where N_0 is a normalization constant determined by the magnitude of the puff.

The diffusion flux can be obtained by differentiation of (81) or (more easily) from Eq. (72).

$$\frac{F_{diff}(y,t)}{N_0} = y_0 c\left(\frac{y^{1-n}}{y_0^{-n}}\right)\sum_{i=1}^{\infty}\frac{s_i J_n(s_i y_0)\cdot J_{n+1}(s_i y)}{\left[J_n^2(s_i)\right]}\cdot Exp\left(\frac{-cs_i^2 t}{4H}\right) \tag{82}$$

The gravitational flux is just

$$F_{grav} = v_g N(z,t) \tag{83}$$

The integrated diffusion and gravitational fluxes from time t=0 to time τ are, respectively,

$$\int_0^t F_{diff}(y,t)\cdot dt = 4y_0 N_0 H\left(\frac{y^{1-n}}{y_0^{-n}}\right)\sum_{i=1}^{\infty}\frac{s_i^{-1}J_n(s_i y_0)\cdot J_{n+1}(s_i y)}{\left[J_n^2(s_i)\right]}\cdot\left[1-Exp\left(\frac{-cs_i^2 t}{4H}\right)\right] \tag{84}$$

$$\int_0^t F_{grav}(y,t)\cdot dt = 8y_0 v_g N_0\frac{H}{c}\left(\frac{y}{y_0}\right)^{-n}\sum_{i=1}^{\infty}\frac{s_i^{-2}J_n(s_i y_0)\cdot J_n(s_i y)}{\left[J_n^2(s_i)\right]}\cdot\left[1-Exp\left(\frac{-cs_i^2 t}{4H}\right)\right] \tag{85}$$

To be consistent with our prior cases the normalization constant, N_o, must be chosen to give a unit puff (normalized to one particle per puff). This can be done by integrating Equation (81) or (82) from the surface to the top of the boundary layer at times short enough that no particles have been lost to the surface and choosing N_o such that the vertically integrated number is unity. Carrying out the integration at time 0.01 s yields values of $1/N_o$ of 8.3 and 6.2 respectively, for 10 and 20 μm radius particles for a source height of 0.2 meters. The normalization constant, when determined by the procedure above (where we have used a delta function in concentration rather than a delta function of the flux) depends both upon v_g and the source height, h. Alternatively, the normalization constant can also be obtained by calculating the total gravitational deposition over all time and choosing N_o such that the total integrated deposition is unity. It was verified that both procedures give the same values of the normalization constant.

The concentration, N/N_o, as calculated from equation 81 for a unit puff and particle radii of 10 and 20 μm is presented in Figure 46 as a function of height for a source height h = 0.2 m, a capping inversion H = 100 m, at 20, 50, and 100 seconds, and is comparable to Figure 38 (Case 5, the uncapped solution).

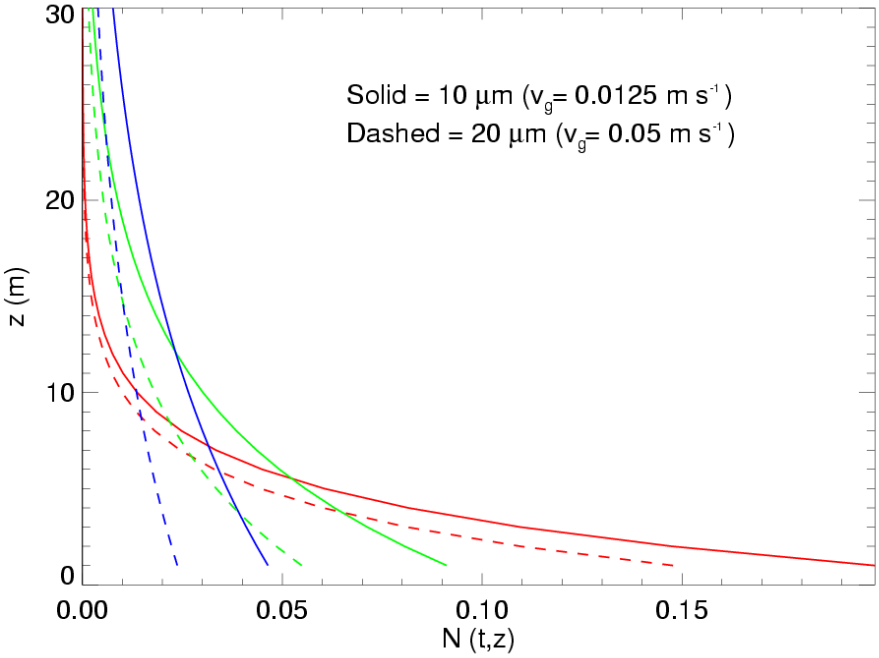

Figure 46. N for a single puff plume with gravitational settling of particles and a capped boundary layer (100 m) at 20, 50, and 100 seconds as calculated from equation 80, as corrected by N_o as calculated by integrating N/N_o at time = 0.01 s. Solid lines are for 10 μm particles, dashed lines for 20 μm particles.

Comparing Figure 46 with Figure 38 shows the vertical profiles of N near the surface to be almost identical for this case and Case 5 (uncapped BL), as could be expected for the relatively short time intervals of 20, 50, and 100 seconds. Figure 49 plots values for FI, the total integrated flux, for the same case (h = 0.2) at a level of 2 m, and is comparable to Figure 41 for Case 6. The 2 cases appear similar initially, with peak values of ~0.7 near 100 s, but over time the capped case presented here shows that all particles are seen to settle out in times on the order of 2 to 8 hours (10 and 20 μm particles, respectively). Since the total flux does go to zero, equilibrium is achieved for a series of puffs in the order of hours in the capped MBL, whereas in the uncapped MBL (Figure 41) it required days for equilibrium to be reached! Figure 41 suggest that for 10 μm radius particles, equilibrium may never be achieved in an atmosphere where the turbulent mixing increases linearly with height.

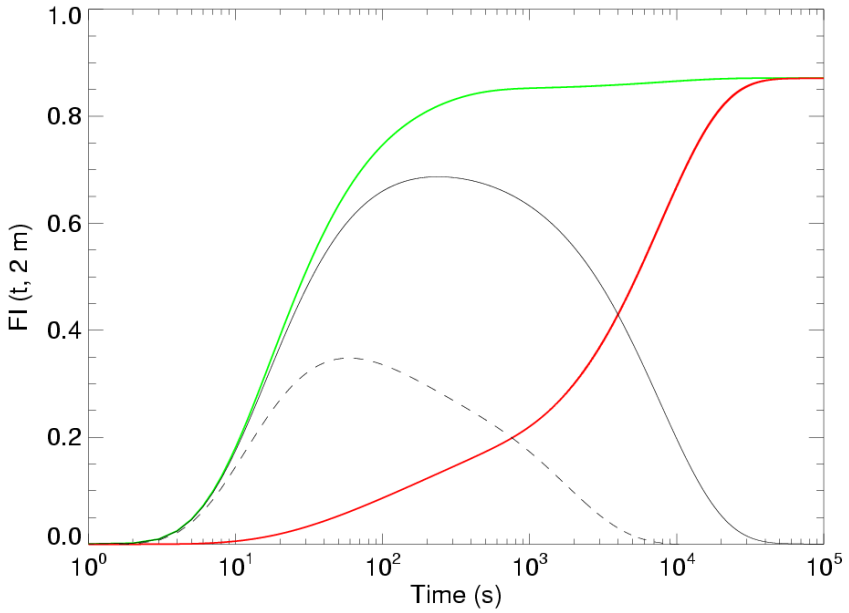

Figure 47. Integrated flux for a single puff as a function of time for 10 μm (solid lines) and 20 μm particles. The integrated fluxes (black lines) can be interpreted as reaching 0 at time of ~30000 s / 8 hours (10 um) and 7000 s/2 hours (20 um). Compared to Figure 41, where the total flux (black) approaches zero over much longer times, here having the boundary layer capped at 100 m produces a much faster decrease with eventual removal of all particles

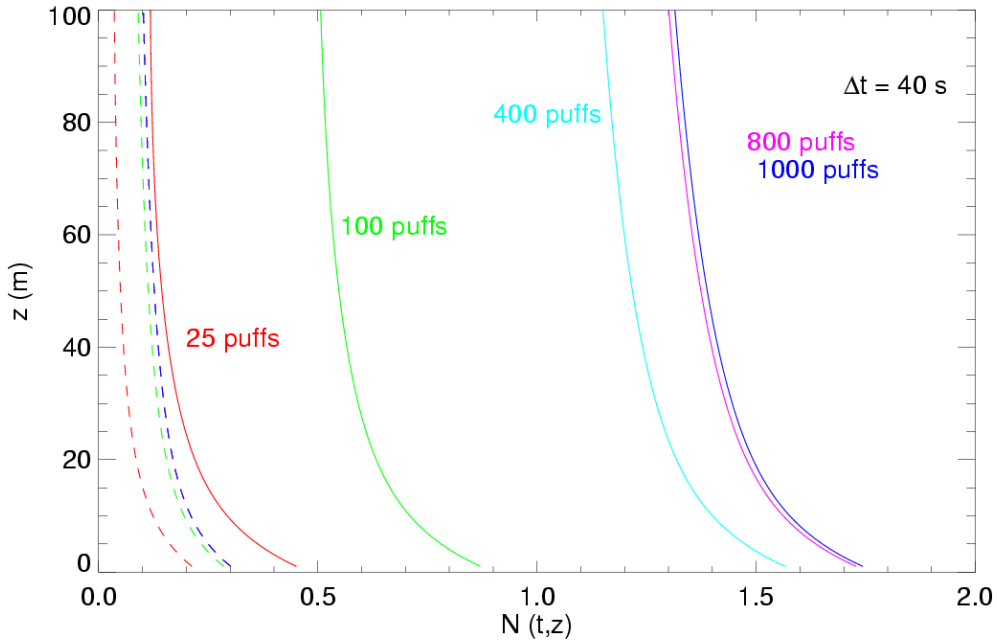

Figure 48. Concentration profiles for 25, 100, 400, 800, and 1000 puffs, separated by 40 seconds. Solid lines are for 10 μm radius particles and dashed lines are for 20 μm particles. The dashed lines for 400 and 800 puffs are overlain by the 1000 puff (blue) line.

Figure 48 details the concentration profiles for a series of 25, 100, 400, 800, and 1000 puffs occurring regularly at 40 second intervals, and is comparable to Figure 42 for case 6. It appears that sometime between 800 and 1000 puffs (8-9 hours) a steady state is reached for 10 μm particles (solid lines), where the flux of new particles is balanced by the gravitational loss at the surface (as seen by the constant vertical concentration profile), and after only 100 puffs for the larger 20 μm particles. Figure 49 shows the sum of the integrated fluxes from a series of puffs (i.e., the total number of particles) at a height of 2 m for 1 to 500 puffs with a Δt of 10, 20, 50, and 100 seconds for 10 μm particles. The dashed lines give the gradient and gravitational components of the flux for Δt = 100 s.

Figures 50 and 51 show the average diffusive and net fluxes, respectively, for this series of puffs. Unlike the case 6 results, here for a puff separation of 100 s, the integrated flux nearly levels off at ~300 puffs, indicating equilibrium, which is also indicated in Figure 51 where the average net flux approaches zero. Figures 49 – 51 are plotted as the number of puffs. To view as a function of time the horizontal axis must be adjusted to account for the different time intervals.

The average diffusive fluxes depicted in Figure 50 can be considered the source flux to use as inputs to numerical models that separately calculate deposition via gravitational settling.

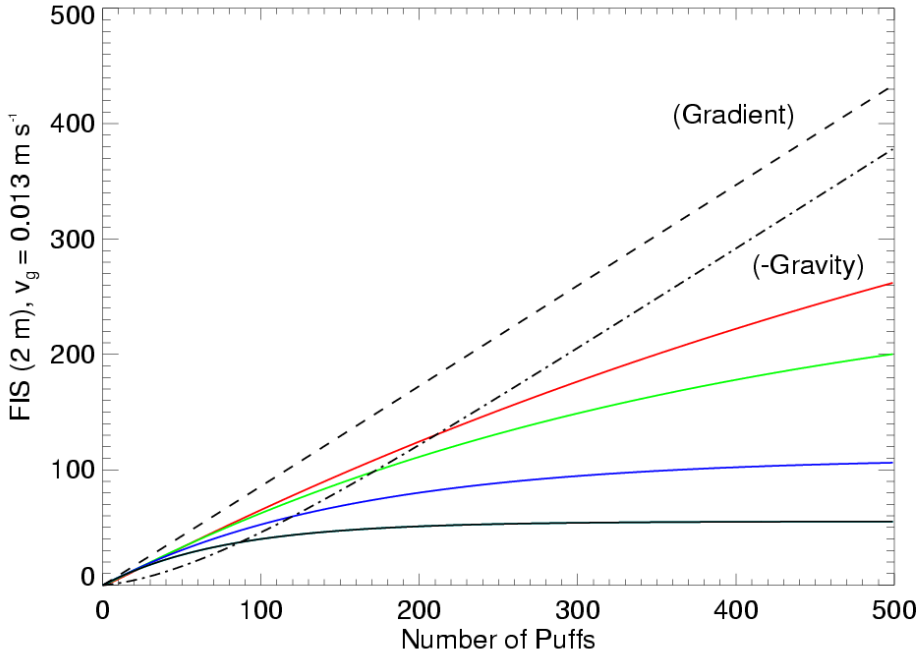

Figure 49. FIS, the sum of integrated puffs for 1 to 500 puffs for Δt of 10 (red), 20 (green), 50 (blue), and 100 (black) seconds at a height of 2 m for a source height of 0.2 m for Case 7.

As seen in Figure 45 for case 6, this flux is less than the flux at the source at 0.2 meters (shown in the dashed lines) due to surface loss before mixing up to 2 m, and the values are very similar to those in Case 6. As stated previously, the flux values shown in Figure 50 would be appropriate source fluxes for a numerical model with the center of the lowest cell at 2 m.

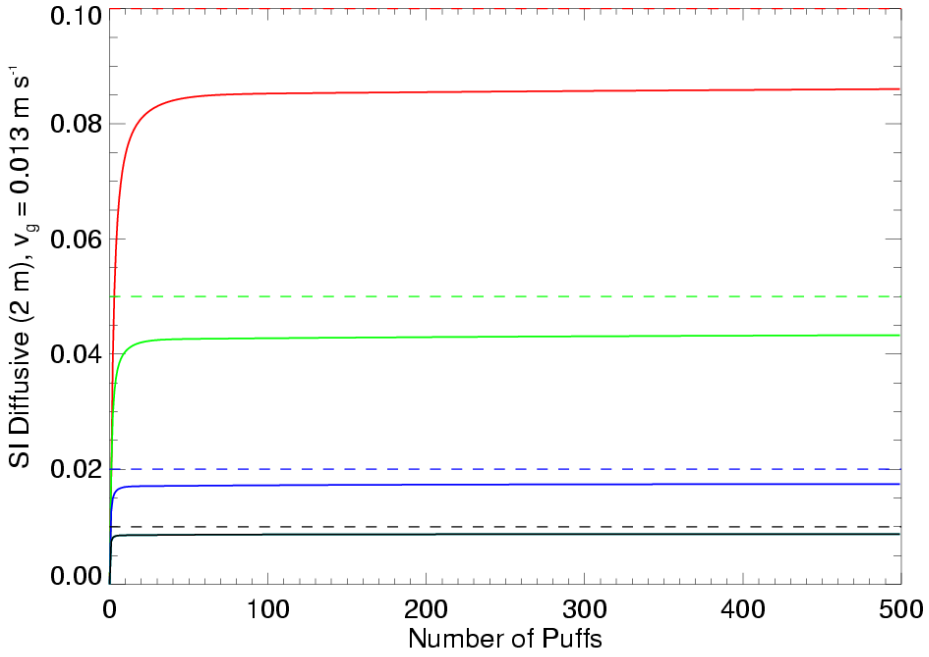

Figure 50. Average diffusive flux, SI, at 2 m as a function of number of puffs and puff separation of 10 (red), 20 (green), 50 (blue), and 100 (black) seconds for Case 7. Dashed lines indicate the source flux at the source height of h = 0.2 m.

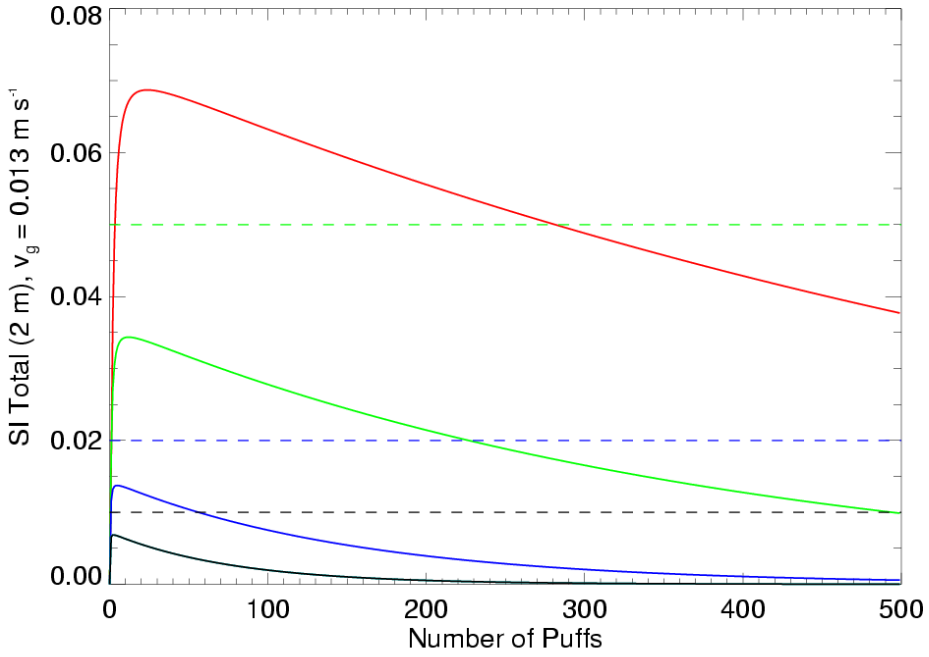

Figure 51. Average net flux, SI, at 2 m as a function of number of puffs and for puff separations of 10 (red), 20 (green), 50 (blue), and 100 (black) seconds for Case 6. Dashed lines indicate the source flux at the source height of h = 0.2 m.

IV. Summary and Interpretation of the puff cases

IV. A. Summary of puff plume cases

1. Totally reflecting surface. For the case of a reflecting surface the upward flux of particles from a series of whitecaps is just the sum of the fluxes due to the individual whitecaps. The average source flux can then be obtained by time averaging the individual puffs. Even though the concentration of particles keeps increasing with time, a quasi steady state can be defined during the filling process. Since the deposition loss of submicron particles is small during their lifetimes in the atmosphere, the reflecting surface approximation is valid for many applications where the calculation of the concentration of particles in the MBL is desired. These small particles are removed by precipitation scavenging events, detrainment into the free troposphere, or diluted by subsidence. If the flux per whitecap or unit of white cap area is known from subsidiary measurements over the ocean or from laboratory measurements, that information can be applied to the MBL (as discussed further in Section V). The source flux can also be measured directly by correlation techniques with no appreciable correction for surface deposition. Figure 10 shows the constant source flux, after an initial transient. The source flux is proportional to the white cap frequency. If the vertical domain is capped, the measured source function will be a function of height, *z*, since the volume to be filled above *z* decreases with height (Figure 19). The actual profile of $K(z)$ is not very important - regardless of the profile in the surface layer the particles rapidly become well mixed (Figure 17).

2. Case of the totally or partially absorbing surface and no gravitational settling term in the differential equation. In this case where loss occurs through processes which occur only at the surface, the only mechanism of transferring particles above the surface is via the gradient flux. For a single puff there is an initial upward flux near the surface, which disperses particles upward, followed by a period where the gradient reverses direction and the particle flux is downward at the surface thereafter. We have shown that if there is a continuous series of puffs, the *average* flux will be upward at every altitude above the source. However this average flux will decrease with time as the MBL fills. The increased concentration increases the surface deposition flux, which will eventually equal the source flux. The average upward source flux is entirely a gradient flux and includes all source and deposition effects occurring at the surface. Initially the gradient flux will be upward and equal to the puff source strength as in the case of a totally reflecting surface. As the concentration in the MBL builds up the gradient above the source weakens, decreasing the upward flux, and the gradient below the source strengthens driving more of the newly injected particles back to the surface. During this transient phase the ratio of the newly injected particles diffusing upward to those diffusing back to the surface continues to decrease, but the sum of the upward diffusive flux and the downward deposition flux is equal to the puff source flux (Figures 25 and 26). Correlation measurements of the flux (via wind speed and concentration fluctuations) over the ocean measure the gradient flux and therefore would correspond to the average diffusive flux as we have calculated here; i.e., include the effects of surface loss. This correlation flux will also be changing with time and will eventually go to zero (for capped MBL). This final equilibrium state may never be reached if other removal mechanisms become important over the lifetime of the particle. Indeed, the only time equilibrium is expected to be reached in the MBL are for particles where the gravitational

flux plays a dominant role, as discussed next. While this case is appropriate for the deposition of many gaseous / scalar contaminants, it is of very limited applicability to particle deposition.

3. Including gravitational settling in the diffusion equation (cases 5 - 7). For particles where the deposition due to gravitational settling is an important loss mechanism, the gravitational settling term should be included in the differential equation as in Equation (31). Only in this case can we obtain equilibrium between the upward (gradient) flux and the downward gravitational flux. Only in this case do we have a deposition flux which is not contained in the gradient flux. In Case 5, for simplicity, it was assumed that the turbulent diffusivity was constant with height, giving rise to an unrealistically large diffusive effect at the surface that contributed to the deposition velocity (reducing the deposition velocity for a surface source). In the more realistic Case 7, the turbulent diffusivity goes to zero at the surface and the correct deposition for a surface source is just v_g, as shown for the equilibrium case in *Hoppel et al* [2002, 2005], and very nearly v_g in the steady-state (filling) case (*Hoppel et al*. [2005]). If there are additional losses at the surface, in addition to gravitational settling, these must be reflected in the gradient flux. The reason for this is, of course, that there is no other mechanism to transmit surface effects to the interior of the MBL.

Table 2. Summary of cases

Case	DE includes gravitational settling (v_g)	K(z)	Lower boundary condition	Upper boundary
1a	No	Constant	$F_o=0$ Total reflection	Unbounded
1b	No	Constant	$n(0)=0$ Total absorption	Unbounded
2	No	$K(z)=kz$ (Linear)	$F_o=0$ Total reflection	Unbounded
3	No	$K(z)=kz\left(1-\frac{z}{H}\right)$	$F_o=0$ Total reflection	Reflective at z=H Top of BL
4	No	Constant	Dep. velocity, v_d limited $F_0=K\left(\frac{dn}{dz}\right)_{z=0}=v_d N_0$	Reflective at z=H Top of BL
5	Yes	Constant	$K\left(\frac{dn}{dz}\right)_{z=0}=-\frac{v_g}{2}N_0$	Unbounded
6	Yes	K(z)=kz (Linear)	$F_0=v_g N_0$	Unbounded
7	Yes	K(z)=kz (Linear)	$F_0=v_g N_0$	Reflective at z=H Top of BL

All the cases have limitations. The most realistic cases are Case 4 for small particles (and Case 3 in the limit of negligible surface deposition), and Case 7 for large particles. For small particles the particles become well mixed throughout the BL so that the concentration profile is only weakly dependent on the mixing coefficients, *K(z)*, and the height of the BL becomes important in confining the particles to the BL. For Case 4, unlike Case 1b, the loss to the surface can be limited by specifying the deposition velocity, even though K remains constant down to the surface. The small particle case is similar to the description required by trace gases. By contrast, large particles require that the gravitational settling be included in the differential equation. If the particles are large enough they will fall out before reaching the top of the BL and the profile of mixing is important in determining the gravitationally induced gradient. Case 6 is unrealistic in that it predicts an unreasonably long time to reach equilibrium – a result of the linearly increasing diffusivity coupled with unbounded vertical domain. In Case 7, the MBL is capped and gives a more reasonable estimate of equilibrium and the time to reach equilibrium.

Case 5 added settling velocity to the perfectly reflecting case. There we showed that any solution for a constant *K* and a gravitational settling velocity could be transformed to a solution which included a constant settling velocity v_g. We developed Case 4 which included a non-gravitational deposition velocity v_a (actually called v_d in Case 4) and a capped MBL, *such that it also included gravitational settling*. We do not have time to present that case here. Suffice it to note that since *K* is constant down to the surface this case suffers from the same defect as Case 5; namely there is a large gravitationally induced gradient term at the surface. The deposition velocity becomes $v_d=v_a+v_g/2$ rather than $v_g/2$ as in Case 5 [Eq. (45)].

IV. B. An interpretation of the flux resulting from a series of puff plumes

The net integrated source from a series of puffs, discussed in last sections and shown in Figures 10, 14, 19, 26, 34, 37, 44 (45 for the source flux), and 51 (50 for the source flux) is the average flux at a given time and at a specific height z, from a series of puffs integrated over the entire x-y plane from all the prior plumes, in various degrees of decay. {In going from Eq. (3) to Eq. (4) we have integrated over the x-y plane and kept only the vertical variation for a given puff.} To translate the prior results to source per unit area, more needs to be specified about the horizontal distribution of white caps and exactly what our puff plumes represent. Real white caps occupy a finite area, and grow and decay over a number of seconds. Our unit puff plumes occur as a delta function in time and space. To relate our puff plumes to quantitative values, the unit source strength must be given a magnitude that represents the source associated with a whitecap of specified spatial and temporal extent. For example, the strength of the puff could be normalized to the source strength per square meter of whitecap during its several second lifetime. To illustrate the connection of the calculations in the last section to average surface fluxes we will here assume that the white cap frequency, *f*, (number of white caps per m^2 per second) is known, rather than the more usual specification of fraction, *W*, of the ocean surface covered with white caps.

For the purpose of visualization, a horizontal grid with the x-direction orientated in the direction of the wind is constructed as shown in Figure 52. The grid spacing in the direction of the wind is $Dx=uDt$ and the y-grid spacing is Dy. Now consider the symmetric case where (white

cap) puffs occur at the midpoint of each fixed grid cell at a rate such that an advecting rectangular column, whose base has the area of a grid cell, receives a puff when the midpoint of the column passes over the center of a grid cell. The cell length in the x-direction is thus $Dx=uDt$ where u is the mean wind speed and Dt is the time between puffs as used in calculations given in the prior sections. The average source flux calculated in the prior sections is thus the flux passing through a horizontal plane at a given height z within the advecting column. Initially the puff will be contained within the cell boundary, so that the average flux within the cell boundary is the flux per area of the cell. As the puff disperses, the horizontal boundary of the puff will extend beyond the boundary of the cell and the flux will be too large if the area of the cell is used as the normalizing area. However for the symmetric case shown, the excess flux that is outside the boundary of the cell in which the given puff occurs is just the amount that enters the cell from puffs occurring in adjacent cells. As an example, consider the case where the whitecap frequency is $f=10^{-4}$ m^{-2} s^{-1}, a wind speed of 10 m s^{-1}, with puffs occurring every 10 seconds; then $Dx=uDt=100$ m, resulting in Dy=10 m ($f\Delta t\Delta x\Delta y=1$). We have chosen the grid size such that one puff occurs on average every 10 seconds in the advecting column. The flux SI(z,t) calculated in the prior sections for a series of puffs would then be the flux per area associated with the area of the cell, $A_g=\Delta x\Delta y=(f\Delta t)^{-1}$ (which is 1000 m^2 in the example). Eventually, the unit puff must be scaled in accordance with the strength of the white cap. The flux per m^2 within the grid is given by

$$S(z,t)=\frac{SI(z,t)}{A_g}=f\,SI(z,t)\Delta t \tag{86}$$

where Dt is the time between puffs and SI, as before, is the time averaged total flux (s^{-1}) resulting from a series of puffs separated by time Dt. $SI(z,t)Dt$ is the number of particles crossing the horizontal plane within one cell and $S(z,t)$ is the number per unit area per unit time. {The Dt in Eq. (86) and the Dt used to calculate S must be the same.} Since every cell is the same, this flux, S, is also the large area flux. In the case of no surface deposition, SI is inversely proportional to Dt so that S depends only on f and not on the Dt (except as SI depends on Dt).

While the probability of the highly symmetric case illustrated above is infinitesimal, it is one realization of a nearly infinite number of realizations, which corresponds to the given value of whitecap frequency. It is not unreasonable to postulate that the average of all realizations that give a single whitecap frequency will behave similarly with respect to overlapping plumes, as does the symmetric realization.

The above analysis can only be expressed in terms of white cap coverage, W, if additional information on the size and duration of the white cap is known. Whitecaps are assumed to form over an initial area A_{wc} and then decay with an exponential time constant τ (*Monahan et al*., 1986), so that the average white water coverage over an arbitrary time interval Δt is just

$$A_{ave}=\frac{A_{wc}t}{\Delta t}\left[1-\exp\left(\frac{-\Delta t}{t}\right)\right]\cong\frac{A_{wc}t}{\Delta t} \tag{87}$$

where the approximation holds if $Dt >> t$. From experimental observations an appropriate value for τ is about 3.5 seconds (*Monahan et al*., 1986)

$$W = \frac{A_{ave}}{A_g} = \frac{A_{wc} t}{\Delta t (f \Delta t)^{-1}} = (A_{wc} t) f \tag{88}$$

f is the white cap frequency (number per unit area per unit time). In the example of the prior paragraph, the white cap coverage for a white cap area of 1 m^2 would be 0.035%.

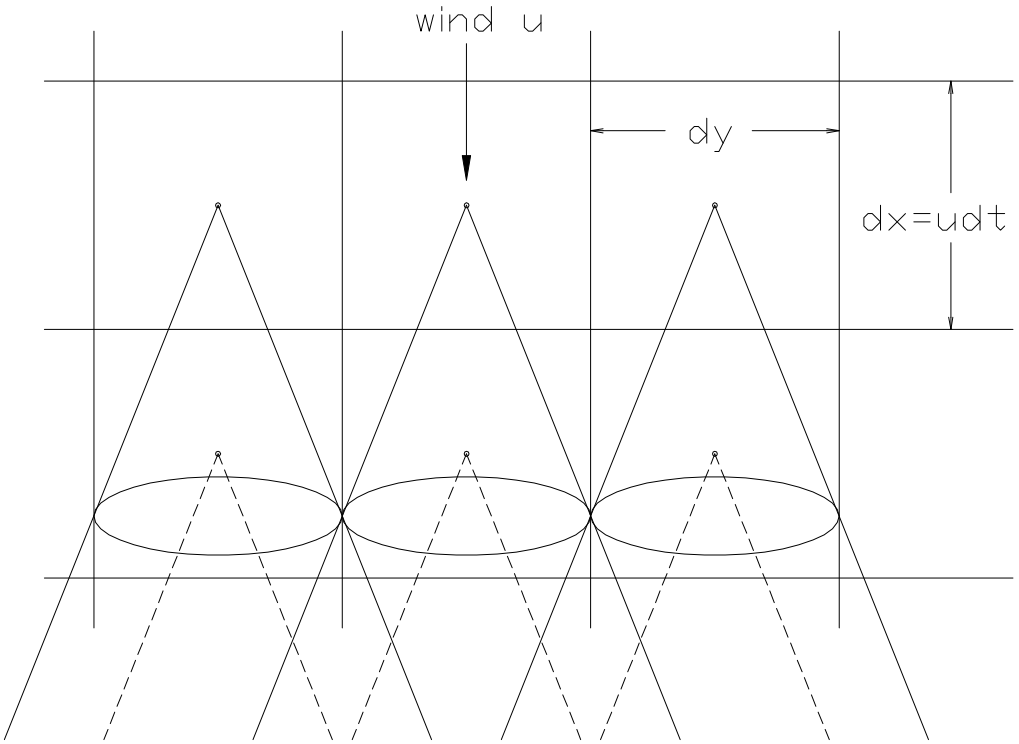

Figure 52. Moving columns with base the same as the fixed grid advect with the wind. Moving columns encounter puffs when they pass over the center of the fixed grids.

The importance of the above illustration is not in the numerical implementation, but in illustrating that the consequences seen in the series-of-plumes analysis are applicable to the source function formulation.

The net flux (in units of s^{-1} m^{-2}) is then given by Eq. (86), which can be expressed as

$$S(z, M\Delta t) = \frac{SI(z, M\Delta t)}{A_g} = f\, SI(z, M\Delta t)\Delta t = f\, FI(z, M\Delta t). \tag{89}$$

For a reflecting surface, after a significantly long period of time S will be the source function and, for puffs of unit strength, is just equal to the white cap frequency. To be useful we must have experimental data to assign a magnitude to the puff. This will be discussed later. For an absorbing surface, after a sufficiently long period of time the net flux will go to zero indicating

the system has reached a steady state. For the case when v_g=0, this requires that the gradient in concentration be zero above the source. (Below the source there would be a constant gradient driving the newly formed particles to the surface.) As we have seen in Case 4 where v_g=0 and small deposition velocity, the time to reach equilibrium for small particles is much longer than the lifetime of the particle and the source approaches that of a reflecting surface, $FI(z,\infty)=1$. In the case of large particles (Case 5-7) where v_g is included in the differential equation, equilibrium is reached where the upward diffusion flux is balanced by downward gravitational flux. $FI(z,\infty)$ can be divided into two parts, an upward diffusion flux and a downward gravitational flux, as in Figures 50 and 51. The total $FI(z,\infty)$ will eventually go to zero indicating equilibrium has been achieved, at which point the upward diffusion flux is balanced by a downward gravitational flux. In the latter case, when parameterizing the surface source in numerical models, it is useful to consider the upward gradient flux as the source in the lowest cell of the model and the model calculates the gravitational deposition. In the latter case only the upward flux would be used in Eq. (89) to calculate the source as in Figure 50.

In terms of the white cap coverage the source function for unit puffs can be written as

$$S(z,M\Delta t)=\frac{W\cdot SI(z,M\Delta t)\cdot\Delta t}{A_{wc}t}=\left(\frac{W}{A_{wc}t}\right)FI(z,M\Delta t) \tag{90}$$

Here, if the flux is associated with the flux per unit area of white cap, then $A_{wc}=1$. $FI(z,t)$ is a function which adjusts the flux for the loss resulting from surface deposition and the height at which you need to apply the flux. Application of these equations when experimental data on the source strength is known is discussed in Section V.

V. Implications of the above analysis to the surface source and deposition in large-scale numerical models

The horizontal grid size used in high-resolution mesoscale and global models range from several to hundreds of kilometers. Atmospheric processes that occur on the scale less than a kilometer cannot be resolved by these models, yet processes occurring on the scale of meters have a major effect on large-scale meteorological simulations. Since the meteorological models cannot resolve these smaller scale influences, the small-scale processes must be parameterized in the meteorological models. Examples of small-scale phenomena that must be parameterized are cloud formation, precipitation, and effects related to the BL turbulence, such as momentum, moisture and heat transport in the BL. When aerosols are added to large-scale models, similar parameterizations are required, such as turbulent transport of particles in the BL, surface deposition, precipitation scavenging and exchange between the BL and the FT. In order to supply realistic parameterizations, it is necessary to solve the small-scale transport problem and then parameterize the effect for use in large-scale models. Hence micrometeorologists study the BL dynamics to understand the mechanisms of momentum, moisture and heat transport, and derive parameterizations that simulate these effects in meteorological models. Likewise, production of sea-salt aerosol generated by highly localized and intermittent whitecaps and subsequent dispersion and deposition must be parameterized to obtain a SSASF and deposition velocity appropriate for the large scale averages required by meteorological models.

Before proceeding with the Sections V and VI, it is helpful to review key elements of the derivation of the turbulent diffusion equation used in the prior analysis and used in numerical models.

V.1. The turbulent diffusion equation

The conservation equation for a given particle species of concentration $n(\vec{x},t)$ is just

$$\frac{\partial n}{\partial t} + \nabla \bullet \vec{J} = Ss - R \tag{91}$$

where the flux is

$$\vec{J} = (\vec{v} + \vec{v}_S)n - v_g n\hat{z} - D\nabla n \tag{92}$$

$\vec{v}$ is the fluid velocity, v_g is the gravitational settling velocity and $\vec{v}_s$ is the "slip" velocity, which accounts for any motion of the particle relative to the fluid, in addition to the gravitational fall velocity; e.g., inertial effects on the particle resulting from acceleration in the turbulent eddies. *D* is the ordinary diffusion coefficient and *Ss* and *R* represent any volume sources and sinks, if present. The over arrow indicates vector quantities and $\hat{z}$ is a unit vector in the z-direction.

Following the standard procedures which can be found in most micrometeorological textbooks, the variables are represented by a time-average value (in brackets) plus a fluctuation component denoted by primes

$$n = < n > + n'$$

$$\vec{v} = < \vec{v} > + \vec{v}' \qquad (93)$$

$$\vec{v}_s = < \vec{v}_s > + \vec{v}'_s = \vec{v}'_s$$

where the average slip velocity is taken to be zero. Substituting (93) into (92) and taking the time average yields

$$\frac{\partial \langle n \rangle}{\partial t} + \nabla \bullet \left\langle \vec{J} \right\rangle = \langle Ss \rangle - \langle R \rangle \qquad (94)$$

and

$$\left\langle \vec{J} \right\rangle = \left\langle \vec{v}' n' \right\rangle + \left\langle \vec{v} \right\rangle \langle n \rangle - v_g \langle n \rangle \hat{z} + \left\langle \vec{v}_s' n' \right\rangle \qquad (95)$$

The Brownian diffusion term can be neglected except in the molecular sub-layer very near the surface where it can be included in the deposition velocity. The last term, which represents the flux due to the correlation of the slip velocity with the particle concentration can be important for large particles where the aerosol trajectory can deviate from the fluid velocity due to inertial effects. Here we confine our attention to particles that are sufficiently small that inertial induced fluxes are negligible.

First order closure is obtained by assuming the turbulent (eddy) diffusion approximation holds and is given by

$$\left\langle \vec{v}' n' \right\rangle = -K(x, y, z) \nabla < n > \qquad (96)$$

Closure allows the correlation term to be written in terms of the average (bulk) variables without solving for the fluctuating components. The brackets are thenceforth omitted with the understanding that all variables are the average values, averaged over sufficient time such that the averages include the effect of the turbulent fluctuations of all scales important in the BL, such that the time average of the prime quantities is zero. The turbulent diffusion equation is now Eq. (91) where the flux density is given by

$$\vec{J} = \vec{v} n - K(x, y, z) \nabla n - v_g n \qquad (97)$$

The solution for a puff plume is the solution to the diffusion equation with R=0 and

$$Ss = S_0 d(\vec{x} - \vec{x}_0, t - t_0) \tag{98}$$

where the puff occurs at time t_o and position $\vec{x}_0$. In keeping with the assumption in the above statistical averaging, the puff plume calculated from the turbulent diffusion equation does not represent any single puff plume but the average of a large ensemble of puff plumes.

If we wish to view the dispersion of the particles in a coordinate system moving with the wind velocity $\vec{v}$,

$$\frac{Dn}{Dt} = \frac{\partial n}{\partial t} + \nabla \bullet n\vec{v} = \nabla \bullet \left(K(x,y,z)\nabla n + v_g n\right) + S - R \tag{99}$$

where *Dn/Dt* is the change in the coordinate system moving with the wind. In our prior analysis we assumed that K_x and K_y were constants so that the x and y profile of the plume is Gaussian. Integration over the x-y plane gives the number of particles N (per unit length) in a layer dz. (See Equations (3) and (4).)

$$N(z,t) = \int_{-\infty}^{\infty}\int_{-\infty}^{\infty} n(x,y,z,t)dxdy \tag{100}$$

and

$$\frac{DN}{Dt} = \frac{d}{dz}\left[K(z)\frac{\partial N}{\partial z}\right] + \frac{\partial}{\partial z}\left(v_g N\right) \tag{101}$$

The solution of this equation for a unit puff at time t_0 and position z_0, $Ss = d(z-z_0, t-t_0)$, is the Green's function solution for a given set of boundary conditions.

V.2. Large scale model requirements

The general dynamic equation for aerosols used in large-scale models include terms for coagulation, condensational growth, etc. (see *Fitzgerald et al.* (1998)), in addition to the advection and turbulent mixing of aerosol particles treated here. In larger-scale models, aerosol particles are advected and mixed according to wind fields and turbulent mixing coefficients generated within the model, and the particles fall at a rate determined by their equilibrium size at the relative humidity determined by the model (*Fitzgerald et al.* (1998) and *Caffrey et al.* (2006)). The resolution of aerosol properties is thus limited to the spatial and temporal resolution of the large-scale model. The limitations imposed by the lack of resolution of large-scale models are not severe for some aerosol-modeling applications. Concentrations of highly dispersed small particles may not vary significantly over the grid size and time step of the large-scale model far from localized point sources (such as industrial and combustion sources). However, for large particles the gravitationally induced vertical gradients may be too large to be resolved by the vertical cell spacing of large-scale models and fallout of large particles may be significant over a single horizontal grid spacing. Near localized sources or intermittent sources, horizontal inhomogeneities can be very pronounced. Since the horizontal concentration

variations cannot be resolved they must be replaced by an appropriate average value assumed to be horizontally homogeneous over the horizontal grid spacing. Unlike industrial and combustion sources, whitecaps are more or less uniformly distributed, in the statistical sense, over the ocean surface on a horizontal scale comparable to that of the grid spacing of large-scale models. Inherent in the derivation of a parameterization is the assumption that the effect of small-scale processes are statistical in nature with averages which are nearly constant over the spatial and temporal scales of the large-scale model and that the slowly-varying, longer-term trends in the variables are resolved by the model.

The problem then is to determine how best to average the flux from the intermittent and sparse whitecap events to generate a SSASF and deposition velocity that can be applied uniformly over the grid used in large-scale models. This study uses puff plumes to represent the intermittency and small-scale features of the aerosol plume from a whitecap. The differential equation used to represent the plume is the same as that used to represent vertical mixing in the large-scale model. However in the plume we have assumed a certain form of the mixing coefficients to obtain an analytical solution, whereas in a numerical model these coefficients are generated internally and not limited to a specified functional form. Numerical models, however, do assume the coefficients are constant over a vertical cell and horizontal grid used in the finite difference approximation to the differential equation. We have used the puff plumes to represent the sub-grid intermittent whitecap production of aerosol to show:

(1) that the effect of whitecaps can be averaged to give an average source flux which can be applied to the large scale problem (existence of a SSASF)

(2) that for no surface deposition the average flux is just the average of all the individual puffs

(3) that this average, near the surface, is approximately constant during the quasi steady-state as well as for a true steady state (which is never obtained in the boundary layer for small particles)

(4) that in the case that the gravitational settling term can be neglected above the surface but surface deposition is important, the vertical gradient will be small in the surface layer. The upward gradient flux plus the surface deposition flux is equal to the source flux. Even though the source remains constant, the ratio of the gradient flux to the deposition flux will change during the transient state.

(5) For large particles where the gravitational settling is the only important component of the deposition flux, vertical gradients near the surface will be important and the source into the lowest cell must be adjusted (decreased) to reflect loss below the mean height of the cell. The upward gradient flux will be constant as the gravitational flux increases. When the downward gravitational flux equals the upward gradient flux, equilibrium is achieved. Removal to the surface will just be the concentration in the cell times v_g.

(6) The case where both gravitational and non-gravitational deposition are important there must be a correction for the effect of the non-gravitational deposition carried by the gradient flux in addition to a decrease resulting from the gravitationally induced vertical gradient.

While we have analyzed the concentration of particles for a series of puffs over time periods long compared to the time step in the model and at heights greater than the lowest vertical cell in order to obtain the average fluxes near the surface, it is not necessary that our puff solutions represent the real atmosphere over the entire domain. The purpose of a parameterization is to provide a good approximation for the source and deposition at some reference height in the lowest cell and then the numerical model calculates the variables over time and spatial scales resolved by the numerical model.

VI. Implications for experimental determination of the SSASF

To obtain an actual SSASF, experimental measurements must be made to relate white cap aerosol production to the whitecap frequency or whitecap coverage. The most common measurements from which the SSASF is derived are: (1) laboratory or field measurements of the aerosol production per unit area of whitecap, (2) direct correlation measurements of $\left\langle \vec{v}'n' \right\rangle$ from fluctuation measurements of concentration and vertical velocity, (3) the equilibrium method for large particles) where the gravitational flux (determined by measuring the concentration) must equal the upward flux; i.e., SSASF., and (4) the build up of aerosol concentration in air passing over white caps.

VI. 1 Measurements of aerosol generation by individual white caps

Laboratory measurements of sea-salt aerosol production purport to measure the number of particles formed per unit area of whitecap, which we here define as P (m^{-2}). All particles are assumed to be counted without any loss to deposition. The area of the white cap is characterized by an initial area A_{wc} with an exponential decay with time constant τ. In Eq. (90) the puff plume is normalized such that the total flux of particles from a single puff is unity. The (calibrated) flux per unit area is just source function

$$SF(0,\Delta t) = P \cdot A_{wc} \cdot S(0,t) = \frac{W}{t} P \cdot FI(0,t) \tag{102}$$

We have set z=0 under the assumption that the measurement of P is representative of the surface production rate. Equation 102 is for particles of a discrete radius, r. A differential source flux can be defined in terms of the number of particles per unit radius interval, dr, in which case Eq. 102 becomes

$$\frac{d[SF(0,\Delta t)]}{dr} = \frac{dP}{dr} \cdot A_{wc} \cdot S(0, M\Delta t) = \frac{W}{t}\frac{dP}{dr} \cdot FI(0, M\Delta t) \tag{103}$$

dP/dr corresponds to the quantity *dE/dr* obtained experimentally by *Monahan et al*. [1986] and Eq. (103) is just the expression given by *Monahan et al*. [1986], except for the additional term, *FI(z,MDt)*, in Eq. (103). *FI(z,MDt)* accounts for the fall out of particles between white caps and adjusts for the height at which one wishes to apply the source function. As shown earlier, for small particles with negligible deposition velocity, *FI(z,MDt)* is unity near the surface, after some time period as shown in Figure 7 (see also Figure 19 for capped MBL). In the case where there is significant surface deposition and *FI(z,MDt)* is less than one, a correction must be made for deposition of the particles formed earlier. In the extreme case when *FI(z,MDt)=0*, there is no net flux above the source because equilibrium has been achieved. For this equilibrium condition, two cases can be distinguished:

(1) When the gravitational settling is negligible compared to surface deposition due to processes other than gravity, this requires that the average gradient above the source approach zero

(the MBL is full, i.e. reached equilibrium) and all new particles are driven to ground by the large gradient below the source. This equilibrium is never reached in the marine boundary layer.

(2) For the case where gravitational deposition is large compared to surface deposition resulting from other processes, the net flux [*FI(z,MDt)*] is zero, not because the gradient flux is zero but because the upward diffusive flux (source flux) is just balanced by a gravitational deposition flux. The only equilibrium case of importance in the MBL is probably the latter; i.e., for large sea-salt particles where gravitational settling flux balances the production flux. As discussed earlier, for modeling large sea-salt particles it is then useful to define the source only as the upward diffusion flux (as in Figure 45 and 50) and let the model calculate the downward gravitational flux.

The validity of the assumption that the laboratory measurement of *P* measures the production rate accurately without loss to the walls or surface and that the laboratory generated white water is representative of real ocean conditions with regard to particle production is not addressed here.

VI. 2. Direct measurements of the flux using eddy correlation methods.

Under the assumption of first order closure as described in Eq. (96), the measured correlation flux is just the diffusion flux. Therefore the spatial and temporal behavior of the diffusion flux calculated and displayed in the prior analyses corresponds to the measured correlation flux. It is also clear from Figures 8, 12 and 40 that most of the eddy correlation flux will occur in bursts very near the white cap, and the instrumentation must be able to resolve these puffs if the correct average diffusion flux is to be resolved. The puffs shown are for "average" puff plumes, and for some plumes the bursts can be expected to be much shorter than those shown. It should also be emphasized that the correlation measurement must be specific for sea-salt aerosol; this may be a problem if there are other species that cannot be distinguished by the measurement method. From the proceeding analysis it is clear that the diffusion flux and eddy correlation flux contain the effect of surface deposition due to all processes except gravitational deposition. Our discussion can be divided into three regimes: (1) when particle deposition is negligible during the life time of the particles, (2) when particles are so large that only gravitational deposition is important, and (3) when both gravitational settling and deposition due to other processes are important.

(1) When particle deposition is negligible during the lifetime of the particle, *FI(z,MDt)* becomes unity indicating that particles continue to build up in the MBL and a quasi steady-state filling of the MBL exists. Plume Case 3 best represents this situation. The average eddy correlation flux is constant with time and is the source flux. For a capped MBL there will be a height dependence of the eddy flux as indicated in Figure 19. A rough estimate of the particle radius, for which deposition can be neglected, can be obtained from the lifetime, H/v_d , of the particle due to deposition, which must be longer than the lifetime of the particle in the MBL due to other processes; primarily, precipitation scavenging and free troposphere exchange. Taking the height of the MBL as 1000 m and the deposition velocity referenced to the surface concentration, we find that particle deposition should be negligible during a nominal lifetime of 3 days if the

particle is smaller than about 1 μm and the wind speed is less than about 25 m s^{-1}. At higher wind speeds the 1 μm radius limit cited here might have to be lowered.

(2) In the other extreme, for large sea-salt particles, the gravitational flux must be included in the D.E. and dominates the deposition velocity (at r>20 μm). In this case the net *FI(z,MDt)* goes to zero at times much shorter than the aerosol lifetime due to other loss mechanisms, and the equilibrium is the result of the balancing of the upward eddy correlation flux by the downward gravitational flux, which are both constant with time. This is illustrated in Figure 47. The eddy correlation flux can then be considered as the average source flux, but it will decrease with height because of the significant gravitationally induced gradient. In practice, once equilibrium is reached it is much easier to determine the flux by measuring the concentration which together with v_g gives the gravitational flux, which is just equal and opposite the gradient flux.

The time for the steady state to be achieved for various profiles of the diffusion coefficient can be estimated from Figure 47 for linearly increasing K. A more detailed discussion with an analytical expression for the time to reach equilibrium can be found in Hoppel et al. [2002] together with the result of numerical modeling, which establishes the time to reach equilibrium in a 500 m MBL for 5 and 10 μm radius particles to be about 30 and 5 hours, respectively, in reasonable agreement with the results shown in Figure 47 for 10 μm particles when the difference in MBL heights is considered. The time about doubles for a MBL height of 1000 m for a 5 μm particle, whereas for larger particles, the time becomes less sensitive to the height of the MBL since gravitational forces confines the particles to lower levels of the MBL. The validity of the assumption that the concentration is in equilibrium between production and gravitational fall out will obviously depend on the particle size and how fast meteorological conditions (including sea surface whitecap coverage) are changing; an assumption which must be verified for a specific experiment.

If the only deposition flux is that due to v_g (requires r >15 μm for wind speeds of about 25 m s^{-1}), then the diffusive source flux reaches its equilibrium value much faster than the system as a whole. The slow response of the gravitational flux caused by the slow build up of the concentration is responsible for the slow system response. Figures 47 and 50 clearly show that the upward diffusive (source) flux reaches a constant value in a relatively short time so that the eddy correlation measurement will indicate the source strength even though the system has not yet reached equilibrium. For particles with radius greater than about 20 μm, the deposition velocity can be assumed to be entirely that due to v_g. Since the critical radius cited here depends on the impaction component of the deposition velocity, the critical radius depends on the strength of turbulence, which in turn is a function of wind speed.

(3) A big advantage of the above two cases is that ignorance of the non-gravitational deposition velocity does not effect the result and the diffusive (correlation) flux is the source flux (at the measured height). In the intermediate cases (*1<r<20* μm) where surface processes contribute significantly to the deposition flux, the gradient flux will be changing with time, even when the surface conditions remain constant. Here the MBL will usually be in a transient state where the gradient flux is changing with time and the filling time is comparable to the lifetime of the aerosol. Under the assumption that deposition mechanisms other than gravitational settling dominate surface deposition, there will be an initial quasi steady state filling where surface loss

is negligible. As the concentration builds up, surface deposition increases. This increase in concentration decreases the net upward flux. The loss at the surface, if it can be accurately calculated, plus the upward gradient flux at the surface will equal the "surface source". If the filling process were to continue to completion then the gradient flux would go to zero and the deposition flux at the surface would equal the source. If the measured eddy correlation flux were small, it would be difficult to determine whether or not equilibrium had been achieved or there was no source. This asymptotic behavior is different than in the second situation above where the deposition is due to the gravitational settling and just equal and opposite the diffusion flux. The scenario just described is for pure non-gravitational deposition; in general, there will be both a non-gravitational and gravitational component and the situation is more complicated. In Section VII we will see that if we can represent the transient case as a family of steady-state cases (quasi steady-state process) where we measure both the gradient and concentration, then the source function can be calculated from the measured flux and concentration.

VI. 3 Equilibrium method for determining source function for large particles.

The justification for the equilibrium method is the same as that given in item 2 under VI. 2 where we have shown that for large particles, where gravitational settling dominates the deposition, the gradient flux at a given height is the source function applicable to that height. Since the gravitational flux at any height is just equal and opposite the gradient flux (definition of equilibrium)

$$F(z) = -v_g N(z) = -K(z)\left(\frac{dN}{dz}\right) = SF(z) \qquad (104)$$

Hence, the source function can be obtained by measuring either the concentration or the eddy flux. Unlike v_a, the gravitational settling velocity, v_g, is well known and does not depend on meterolological and ocean surface conditions. The concentration of aerosol particles of a given size is a much easier measurement under ambient conditions than is the eddy correlation measurement. Therefore, if it can be established that the aerosol particles of a given (large size) are in equilibrium, the equilibrium method is probably the most reliable method of determining the source function.

VI. 4. Defining the Sea-salt aerosol source function (SSASF)

The mechanisms by which sea-salt aerosol are formed and injected into the MBL are varied and complicated. The mechanisms are as diverse as bursting bubbles at the ocean surface to spume aerosol blown off the crest of a wave. It is difficult to characterize the height at which the particle is injected. The diverse mechanisms are discussed elsewhere (*Lewis and Schwartz* [2004]), but it is easy to appreciate the difficulty in characterizing and defining the source strength and its effective height. Some of the particles, depending on size and method of injection, will return immediately to the sea surface while still over white water. If the source function is defined as the total number injected exclusive of deposition, then the fraction re-deposited must be calculated and subtracted from the source. The source strength can also be defined as the upward flux out of the shallow surface layer (micro layer) in which generation and deposition occurs. Both methods have advantages under different circumstances. In the puff

analysis given in the prior sections, it has been assumed that the particles have been generated at a height near the surface, $z=h$; the surface deposition then had to be calculated from an ill defined deposition velocity. *Hoppel et al.* [2005] argue that the only relevant source is the upward diffusive flux out of the micro layer ($z<d$) and defines the source as

$$S_d = \left[K(z)\left(\frac{dN}{dz} \right) \right]_{z=d} \tag{105}$$

From the proceeding sections we see this definition works well for small particles where surface deposition is negligible during the lifetime of the particles (determined by other processes). This definition also works well for large particles where, at equilibrium, the upward diffusive flux is the source flux just balancing the downward gravitational flux. The gradient flux also works as the source flux even when the steady state has not been achieved if deposition is the result only of gravitational deposition (Figure 43 and related discussion). Based upon steady-state arguments, Hoppel et al. (2005) argued {Eq. (8) and related discussion in *Hoppel et al*. [2005]} that the upward flux S_δ is always the preferred way to define the source function since it avoided the uncertainties involved in determining the non-gravitational deposition velocity. Their argument was based on a stationary micro layer (for given meteorological and ocean conditions). The argument given by *Hoppel et al.* [2005] is valid at all sizes if a true steady state exists, and this has been the assumption in most prior analyses. However, as we have discussed above, during transient conditions (e.g.; filling of the MBL) the concentration is changing with time. This is seen in Figure 26 and is important at intermediate radii ($1 < r < 20$ μm) where (1) the non-gravitational component of the deposition velocity is important and (2) particle loss due to deposition during the particle lifetime is important. Under these transient conditions (important in the intermediate size range), the definition (Eq. 105) may not be the best definition of the SSASF. During transient filling, we need additional information as discussed in the Case 4 section, and again in Section VII.

VII. The quasi steady state solution

The quasi steady state is defined by *Hoppel et al.* (2002, 2005) as a transient state where the shape of the vertical aerosol profile remains constant during the transient period; i.e., the ratio of the concentrations at any two altitudes is constant. The quasi steady state would be expected if the turbulent mixing throughout the MBL is fast compared to the temporal change of the concentration. The quasi steady state is discussed in detail in *Hoppel et al.* (2002) where it is shown both analytically and by numerical modeling to hold in the MBL.

The results cited in the above paragraph were in the context of a uniform surface source as opposed to the intermittent puff analysis given in earlier sections. However we have seen in the prior sections that the average profile obtained by summing over a series of puffs gives the same vertical shape as the equilibrium profile. This was shown in Figure 35 for constant K-profile and in Figure 42, near the surface, for the linear K profile. Since the Figures 35 and 42 are for open system cases, we would not expect the quasi steady state to hold far above the surface. For small particles there is no vertical gradient and the MBL can be considered well-mixed at all times.

We have also seen that when non-gravitational deposition is the only important deposition mechanism then the gradient flux changes during transient conditions; but, in such a way that the gradient flux plus the deposition flux equals the total source flux (see Case 4 discussion). We emphasis that this is not the case with pure gravitational deposition where the gradient component remains constant and the total deposition flux goes to zero as the gravitational flux increases to exactly counter the diffusion flux (see Figures 41-45 and 50-51).

The above observations suggest that in order to define the transient system both the gradient flux and concentration must be allowed to change in a manner which is consistent with the constant source and surface boundary conditions. In the following analysis we assume that a steady state (but non-equilibrium) exists where a constant source, S, near the surface is supplying particles at a constant rate at height, h. The deposition flux results from both gravitational and non-gravitational deposition. The partitioning between the upward gradient flux and deposition flux is determined by the current concentration, which is a free variable that will change slowly with time. Changing the concentration gives a family of steady-state curves each of which lies on a time trajectory describing the transient behavior.

The following analysis includes analyses contained in unpublished communications with *Chris Fairall* in 2004 and material found in *Hoppel et al.* (2005). Subsequently (February 2007) the authors of this report had access to and submitted comments on an early version of a manuscript in preparation (*DeLeeuw et al*. (2007)). At the time of submission of this report the final version of that manuscript was not yet available, but it is expected that there is much overlap between that manuscript and the analysis given here. In the above referenced manuscript the relevant parts of the manuscript were the work of *Chris Fairall*, one of several authors.

The one-dimensional steady-state equation for the aerosol concentration n(z) when the eddy diffusivity is given by $K(z) = k\ u_* z = c\ z$ (κ and u_* are von Karman's constant and the friction velocity) is

$$c\,z\frac{dn}{dz}+v_g n=-F_\infty \tag{106}$$

where F_∞ is the steady-state flux above the source. In principle the fact that F_∞ is nonzero requires a removal mechanism at the top of the MBL. Here we assume that the removal mechanism is the upward flux into the MBL and, within the concept of the quasi steady state, can be a slowly varying function of time.

The solution in terms of the concentration at the height of the source, $z=h$ is

$$n(z)=-\frac{F_\infty}{v_g}\left[1-\left(\frac{z}{h}\right)^{\frac{-v_g}{c}}\right]+n_h\left(\frac{z}{h}\right)^{-\frac{v_g}{c}} \tag{107}$$

It is convenient to define a reference height z_r which may be the height at which a measurement is made or the mid-point of the lowest cell in a numerical model where we wish to evaluate the fluxes. The concentration at the reference height is given by

$$n_r=\frac{F_\infty}{v_g}\left(f_{hr}-1\right)+n_h f_{hr} \tag{108}$$

where $f_{ab}=\left(\frac{b}{a}\right)^{-\left(\frac{v_g}{c}\right)}$ (109)

solving for n_h

$$n_h=f_{hr}^{-1}n_r+\frac{F_\infty}{v_g}\left(f_{hr}^{-1}-1\right) \tag{110}$$

If we inject a source of particles S at z=h conservation of flux requires

$$F_\infty+v_{dh}n_h=S \tag{111}$$

where v_{dh} is the deposition velocity for particles at a height h.

The deposition velocity given by *Hoppel et al*. (2002, 2005) can be written as

$$v_{dh}=\frac{v_g+v_d}{1+\frac{v_a}{v_g}(1-f_{dh})} \tag{112}$$

where v_a is the non-gravitational part of the deposition velocity and δ is the height of the micro layer. A more rigorous expression for v_{dh} can be found in (*DeLeeuw et al*. (2007)).

Solving Eq. (111) for n_h gives

$$n_h = \frac{S(1-f_{hr}) + v_g n_r}{f_{hr} v_g + (1-f_{hr}) v_{dh}} \tag{113}$$

which can be used to eliminate n_h .

The <u>net</u> flux above (F_∞) and below (F_0) the source are then found to be

$$F_\infty = \frac{f_{hr} S - v_{dh} n_r}{f_{rh} + \frac{v_{dh}}{v_g}(1-f_{rh})} \tag{114}$$

$$F_0 = \frac{-(1-f_{hr})\frac{v_{dh}}{v_g} S - v_{dh} n_r}{f_{rh} + \frac{v_{dh}}{v_g}(1-f_{rh})} \tag{115}$$

where

$$v_{dh} = \frac{v_g + v_a}{1 + \frac{v_a}{v_g}(1-f_{dh})} \tag{116}$$

Equations (114) and (115) sum to S as required, and are equations (44) and (43) in *Hoppel et al.* (2005). It is clear that the fraction (F/S) going upwards or downward is determined by the n_r . The "solution" above is not a unique solution but a family of solutions. Each solution is a steady-state solution with different flux rates, $F_\infty(n_r)$ into the domain above the source. Under the quasi steady state assumption each of solutions above will lie on a time trajectory of states during a transitory period. If initially the MBL is particle free n_r=0 will give the initial flux and equilibrium will be obtained when n_r reaches a value where $F_\infty(n_r) = 0$. If we define a column of base dA extending from the source at h to the top of the MBL denoted by z=H with only exchange of particles at the base, then the time dependence of the total number of particles, N_t in the column is

$$\frac{dN_t}{dt} = F_\infty dA \tag{117}$$

$$\text{where} \quad N_t = dA\int_h^H n(z)dz \propto dA \cdot H \cdot n_r \tag{118}$$

The last step uses the proportionality of N_t to the concentration at any given height with time implied by the quasi steady state assumption. Using Eq. (114) for F_∞, we can write

$$dA \cdot H \frac{dn_r}{dt} \propto \left(f_{hr} S - v_{dh} n_h \right) dA \tag{119}$$

where we have used Eq. (111) for F_∞ and have also assumed that H>>h. Integration gives

$$n_r(t) \propto \frac{f_{hr} S}{v_{dh}} \left(1 - Exp\left(\frac{-t}{t} \right) \right) \tag{120}$$

where $t = \frac{H}{v_{dh}}$

When t>>τ steady state is obtained and is, as expected, $f_{hr} S = v_{dh} n_h$ and $F_\infty = 0$. In the limit of large particles Eq. (116) $v_{dh} \approx v_g$, and in the limit of small particles $v_{dh} = v_a / \left[1 + \frac{v_a}{c} \ln\left(\frac{h}{d} \right) \right] \approx v_a$. For a 500 m MBL and 1 μm radius particles τ is about 20 days; whereas for 20 μm radius particles τ is less than 3 hours.

A more rigorous version of the time constant given in Hoppel et. al (2002) can be used

$$t = \frac{h}{v_{dh}} \frac{\left[\left(\frac{H}{h} \right)^{1 - \frac{v_g}{c}} - 1 \right]}{1 - \frac{v_g}{c}} \tag{121}$$

This expression is given in Eq. (21) of Hoppel et al. (2002) and plotted as a function of radius in Figure 5 in Hoppel et al. (2002). The time constant (equation 121) is the same as above in the small particle limit, but in the large particle limit it is independent of H because very large particles never reach the height H.

At equilibrium Eq. (111) gives

$$S = f_{hr}^{-1} v_{dh} n_r = f_{hr}^{-1} v_g n_r \tag{122}$$

The last term is for large particles. For small particles this equilibrium is never achieved. If n_r is increased above that given by the equilibrium value, $F_\infty = 0$, then F_∞ becomes negative indicating that there is some source above which is overriding the (opposing) surface source and driving particles to the surface. Here we interpret F_∞ as the transient filling flux. However it is clear that higher in the MBL the (transient) filling flux decreases with height as some of the upward flux is siphoned off to fill the intermediate region of the MBL as discussed earlier in connection with Figure 19. For small particles the net flux will almost always be such as to "fill" not "empty" the MBL because removal processes such as precipitation events, entrainment, and dilution by large-scale vertical motions occur at a faster rate than does deposition.

Equation (114) is for the net flux the difference of the upward and downward flux. We now get the expressions for the upward and downward fluxes. We first express *n(z)* in terms of S and n_r

$$n(z) = \frac{-f_{hr}S + v_{dh}n_r + \left[S + \left(v_g - v_{dh}\right)n_r\right]\left(\frac{z}{h}\right)^{\frac{-v_g}{c}}}{f_{hr}v_g + \left(1 - f_{hr}\right)v_{dh}} \tag{123}$$

We can now calculate the upward diffusion flux

$$F_{diff}(z) = -cz\left(\frac{dn}{dz}\right) = \frac{S + \left(v_g - v_{dh}\right)n_r}{f_{rh} + \left(\frac{v_{dh}}{v_g}\right)\left(1 - f_{hr}\right)}\left(\frac{z}{h}\right)^{\frac{-v_g}{c}} = \left(\overline{w'n'}\right) \tag{124}$$

This gives the eddy correlation flux at any height. The downward flux is just given by $v_g n(z)$ where *n(z)* is Eq. (123). With a little algebra it can be seen that even though both the upward flux and the downward flux depend on z, the net flux is constant with height as required by the steady state assumption used throughout the analysis. The following identity is satisfied by the above equations

$$F_{diff}(z) - v_g n(z) = F_\infty \qquad \text{where } F_\infty \text{ is as given in Eq. (114).} \tag{125}$$

We can solve for S in Eq. (124)

$$S = F_{diff}\left[f_{hr} + \frac{v_{dh}}{v_g}\left(1 - f_{hr}\right)\right]\left(\frac{z}{h}\right)^{\frac{-v_g}{c}} + \left(v_{dh} - v_g\right)n_r \tag{126}$$

In (124) and (126) the eddy flux measurement, F_{diff}, does not have to be at the reference height. If we do take *z* to be at the reference height we find

$$S = F_{diff}\left[1 + \frac{v_{dh}}{v_g}\left(f_{hr}^{-1} - 1\right)\right] + \left(v_{dh} - v_g\right)n_r \tag{127}$$

For large particles $v_{dh} \approx v_g$, and

$$S_{big} = F_{diff}\, f_{hr}^{-1} \tag{128}$$

We can therefore measure the large particle source by either measuring the eddy correlation (upward flux) or the concentration at a reference height (downward flux)

$$F_{diff} = -v_g n_r = S f_{hr}^{+1} \tag{129}$$

For small particles, $v_g << v_a$,

$$S_{small} \approx F_{diff} + \frac{v_a n_r}{1 - \frac{v_a}{c}\ln\left(\frac{h}{d}\right)} \approx F_{diff} + v_a n_r \tag{130}$$

where the last expression follows if $c >> v_a$, which will generally be the case except possibly for calm winds. We note that in the small particle limit where only the non-gravitational deposition is important, the non-gravitational part of the deposition modifies the diffusion flux. This is consistent with what was found in the puff analysis given earlier; n_r will be increasing with time, causing a decrease in F_{diff} as the MBL 'fills'.

It is clear from Eq. (127) (and also Eq. (126)) that the source S can be calculated from a measurement of the diffusive flux and concentration at the reference height provided an accurate value of the deposition velocity is known. For large particles only one measurement is required. For particles where v_g is negligible, both the diffusive flux and concentration is required (Eq. (130)). However, in practice, for particles with $r < 1$ μm only the flux is required because the concentration term (deposition) is negligible (over the life span of a particle).

Application of the prior results to calculating the source to, and loss from, the lowest cell in a numerical model can best be implemented by introducing and removing particles at some representative average height into the cell, here defined as the reference height. The upward flux at the reference height is just the diffusion flux obtained from Eq. (127)

$$F_{diff} = \frac{S - (v_{dh} - v_g) n_r}{1 + \frac{v_{dh}}{v_g}\left(f_{rh}^{-1} - 1\right)} \tag{131}$$

where n_r at z_r is known from the prior time step of the calculation. For small and large particles Eq. (131) reduces to Eq. (130) and Eq. (129) respectively. The (downward) removal from the lowest cell is then just $n_r v_g$. One might wonder why the apparent deposition velocity here is just v_g. The reason is that the effect of the non-gravitational deposition is already included in the reduced source flux given by Eq. (131). The expressions could be recast, into an equivalent set of equations using the two terms of Eq. (114), but then the deposition velocity would appear in both the effective source term and in a deposition term. We prefer this formulation because these are the actual upward and downward components of the flux at the reference point in the cell, the same components of the flux which appear in the differential equation, and the same as used in calculating the exchange between cells above the surface. As we saw in the puff analysis the effect of the non-gravitational deposition velocity is transmitted by the upward diffusive flux.

References

Abramowitz, Milton, and Irene A. Stegun (1964) *Handbook of Mathematical Functions.* National Bureau of Standards. Applied Mathematics Series 55. 1046 pp.

Andreas, E.L., (2002) A Review of the sea spray generation function. *Atmos. Ocean Interaction, 1*, 1-46.

Caffrey, P. F., W. A. Hoppel, and J. J. Shi (2006), A one-dimensional sectional aerosol model integrated with mesoscale meteorological data to study marine boundary layer aerosol dynamics, *J. Geophys. Res.*, 111, D24201, doi:10.1029/2006JD007237.

DeLeeuw et al. (2007) In press

Fitzgerald, J.W., W.A. Hoppel, and F. Gelbard (1998), A one-dimensional sectional model to simulate multicomponent aerosol dynamics in the marine boundary layer. I. Model description. J. *Geophys. Res., 103*, 16085-16102.

Frank, P. and R. von Mises (1943) *Differential- and Integralgleichungen der Mechanik und Physik*, 2nd Edition, Vol. II, Chapter 14, Mary Rosenberg, New York.

Fuchs, N.A. (1964) *The Mechanics of Aerosols*. Pergamon Press, New York, 408 pp.

Godson, W.L. (1958) The diffusion of particulate matter from an elevated source. *Archiv feur Meteorologie and Geophysik, Serie A., 10a*, 305-327.

Hanson, Jeffrey L., and O.M. Phillips (1999). Wind sea growth and dissipation in the open ocean. *J. of Phys. Oceanography, 29*, 1633-1648.

Hoppel W.A., G.M. Frick, and J.W. Fitzgerald (2002) Surface source function for sea-salt aerosol and aerosol dry deposition to the ocean surface. *J. Geophy. Res. 107(D19)*, ACC, 7:1-17, dio:10.1029/2001JD002014.

Hoppel, W. A., P. F. Caffrey, and G. M. Frick (2005), Particle deposition on water: Surface source versus upwind source, *J. Geophys. Res.*, 110, D10206, doi:10.1029/2004JD005148.

Huang, C.H. (1979) The theory of dispersion in turbulent shear flow. *Atmos. Environ., 13*, 453-463.

Lewis, E.R. and S.E. Schwartz (2004) *Sea Salt Aerosol Production: mechanisms, methods, measurements and models. Geophys. Monogr. Ser., vol. 152*, AGU, Washington D.C.

Monahan, E.C., D.E. Spiel, and K.L. Davidson (1986) A model of marine aerosol generation via whitecaps and wave disruption, in *Oceanic Whitecaps and Their Role in Air-Sea*

Processes, edited by E.C. Monahan and G MacNiocaill, pp. 167-174, D. Reidel, Norwell, Mass.

Morse, Philip M., and Herman Feshbach (1953) *Methods of Theoretical Physics,* Vol 1, McGraw-Hill, New York.

Nieuwstadt, F.T.M. (1980) An analytic solution of the time-dependent one-dimensional diffusion equation in the atmospheric boundary layer. *Atmos. Environ*., *14*, 1361-1364.

Rounds, Wellington, Jr. (1955) Solutions of the two-dimensional diffusion equation. *Trans. Am. Geophys. Union*, *36*, No.2, 395-405.

Seinfeld, John H. (1986) *Atmospheric Chemistry and Physics*. John Wiley and Sons, Inc, New York, 1326 pp.

Seinfeld, John H., and Spyros N. Pandis (1998) *Atmospheric Chemistry and Physics of Air Pollution*. John Wiley and Sons, Inc, New York, 738 pp.

Smith, F.B. (1962) The problem of deposition in atmospheric diffusion of particulate matter. *J. of Atmos. Sci.*, *19*,429-434.

Wu, Jin (1986) *Whitecaps, Bubbles, and Spray* in *Oceanic Whitecaps and Their Role in Air-Sea Processes*, edited by E.C. Monahan and G MacNiocaill, pp. 113-124, D. Reidel, Norwell, Mass.

Wu, Jin (1992) Bubble flux and marine aerosol spectra under various wind velocities. *J. Geophys. Res. 97*, 2327-2333.